

H α emitters from the Southern Photometric Local Universe Survey (S-PLUS)

L. A. Gutiérrez-Soto,¹* R. Lopes de Oliveira²

¹Departamento de Astronomia, IAG, Universidade de São Paulo, Rua do Matão, 1226, 05509-900, São Paulo, Brazil

²Departamento de Física, Universidade Federal de Sergipe, Av. Marechal Rondon, S/N, 49000-000 São Cristóvão, SE, Brazil

Accepted XXX. Received YYY; in original form ZZZ

ABSTRACT

In the way to map 9000 deg² of the Southern hemisphere, the S-PLUS project is also surveying the sky in a proxy of a myriad of astrophysical processes: the H α transition. Here we explore such a capability from its DR3 to make H α emitters in evidence from the ($r - J0660$) versus ($r - i$) color-color diagram and distinguish the red from the blue ones by exploring the ($r - i$) and ($g - z$) diagram. Our catalog is composed of 9,200 objects that exhibit excess in the narrow $J0660$ band which is consistent with H α in emission. Unsupervised, clustering machine learning approach revealed two distinct populations: one with an intense blue continuum and another with a red one. The hierarchical clustering algorithm was compared with the HDBSCAN. By adopting a “soft” clustering approach, we assigned the probability of each emitter belonging to a given population, blue or red clusters. We use synthetic and observed (SDSS) spectra to emphasize the potential of color-color diagrams to distinguish several classes of emission line emitters that include planetary nebulae, H II regions, young stellar objects, symbiotic stellar systems, cataclysmic variables, blue compact galaxies, star-forming galaxies, and quasars, and trace the way to reveal new ones with S-PLUS data.

Key words: surveys – stars: emission-line, Be – novae, cataclysmic variables – galaxies: dwarf – quasars: emission lines

1 INTRODUCTION

The existence of an ionizing radiation field can lead to Balmer hydrogen emission lines. From the presence of the H Balmer lines in the optical spectra of some sources it is well known the possible presence of ionized gas. Many important astronomical objects involve the physics of photo-ionized gases and the interpretation of the emission-line spectra. Emission line objects as the H II regions allow us to study the star formation history of the far reaches of our Galaxy and of distant galaxies. Planetary nebulae let us to see the remaining envelope of dying stars. Star-burst galaxies and QSOs are one the most luminous objects and hence the most distant that can be observed. Their spectra can reveal details about of the first generation of star and the formation of heavy elements in the young universe. On the other hand, emission lines can also infer the presence or lack the accretion discs (Schwope et al. 2000; Ratti et al. 2012), the properties of single or double picked line can allow us to infer geometrical characteristics (Horne & Marsh 1986), the nature of donor stars in binary system (Steeghs & Casares 2002; van Spaandonk et al. 2010; Casares 2015) and the compact objects as black holes (Casares 2016).

Emission lines are also associated with stars in very early-type and/or very late evolutionary stage which are short phase. As already mentioned are also associated with binaries that experiencing mass transfer. These group of emission line stars includes young stellar (YSOs) and Herbig-Haro (HH) objects, post-asymptotic and some asymptotic giant branch (AGB), some red giant stars (RGB), Wolf-

Rayet (WR) stars, supernova remnants, classical Be stars, active late-type dwarfs, interacting binary system like symbiotic stars (SySt) and cataclysmic variables (CV). Most of these class of object are in-homogeneous and some contains many few identified members, for instance at the moment around 323 symbiotic system have been identified from which 257 belong to the Galaxy and ~66 are extra-galactic objects (Akras et al. 019a). The same occurs with PNe from which around 3500 of them are been cataloged (Parker et al. 2016), this current number of PNe represents only about 15-30% of the estimated total of Galactic PNe (Frew, 2008; Jacoby et al., 2010) showing that a small fraction of the PNe have been cataloged. Many galaxies, in addition to harbor Planetary nebulae and H II regions, show characteristic nebular in their spectra. In most of these objects, the gas is photoionized by hot stars in the nucleus, which is thus much like giant H II region, or perhaps many H II regions. The galactic nucleus with very strongest emission lines of this type are often called blue compact galaxies, extragalactic H II regions, star forming or starburst galaxies (Osterbrock & Ferland 2006). There are also spiral galaxies that present emission lines.

In the past H α surveys with modest spatial resolutions have been used to identified extended nebular emission to study supernova remnants, galaxy groups and star forming regions (Davies, Elliott & Meaburn 1976). More recently, higher resolution surveys such as the INT Photometric H α survey (IPHAS; Drew et al. 2005; Barentsen et al. 2014) have focused in the study of compact emission line sources on the Galactic plane, typically with objects in different stage of stellar evolution. The Anglo-Australian Observatory UKS chmidt Telescope Supercosmos H α Survey (Parker et al. 2005) is another H α survey of the Southern Galactic Plane and Magellanic

* E-mail: gsoto.angel@gmail.com

Cloud which has covered to $b \sim 10\text{--}13^\circ$ (verificar esto). Currently ongoing is the VST Photometric $\text{H}\alpha$ Survey of the Southern Galactic Plane and Bulge (VPHAS+; Drew et al. 2014) that will cover the Galactic bulge and plane in five filters.

Like VPHAS+, others ongoing surveys that are used to study the population of emission line objects are the The Javalambre Photometric Local Universe Survey (J-PLUS¹, Cenarro et al. 2018) and the Southern-Photometric Local Universe Survey (S-PLUS², Mendes de Oliveira et al. 2019) are providing observations of the Galactic halo covering both northern and southern celestial hemispheres in a systematic way with twin telescopes using the same set of multi-band filters. In addition to the $\text{H}\alpha$ filter, which is already vastly applied to systematically searching for $\text{H}\alpha$ emitters the telescopes offer 11 more filters. And more ambitious yet the JPAS survey that will the same area of J-PLUS in 56 narrow-band filters.

Traditionally, color-color diagrams based in $\text{H}\alpha$ filter are been used to identify $\text{H}\alpha$ emitters. The analysis the color-color diagram ($r - \text{H}\alpha$) versus ($r - i$) has resulted on the discovered of new emission line objects, for instance Witham et al. (2006, 2007) used the ($r - \text{H}\alpha$) versus ($r - i$) colour-colour diagram to find for new CV. On the other hand, Vink et al. (2008) reported the discovery of YSOs by using this same colour criteria. In this sense using this methology a variety of classes of objects are been identified, which include symbiotic stars (Corradi et al. 2008; Corradi & Giannanco 2010; Corradi et al. 2011), early type emission line stars (Drew et al. 2008) and planetary nebulae (Viironen et al. 2009; Sabin et al. 2010). Recently, by using this same color diagram were also identified compact PN candidates in VPHAS+ catalog (Akras et al. 2019). And the same diagram in conjunction with new ones shows to be very efficient to find for PN candidates (Gutiérrez-Soto et al. 2020). In general terms, Witham et al. (2006) presented a methodology and first results in looking for emission line sources in narrow-band surveys.

In this era of big data on astronomy, machine learning techniques are becoming in important statistical tools for the analysis and find meaning from massive data sets. Particularly, unsupervised machine approaches have showed a promised in various applications, especially in automatic classification task. Including object classification and selection, using galaxies with active galactic nuclei as example (Geach 2012), morphological analysis of galaxies (Martin et al. 2020), classification of variable stars, relying only on the similarity among light curves. (Valenzuela & Pichara 2018). Using unsupervised machine learning can be very advantageous because they do not require a labeled data training sets. Unlike of supervised methods like Random Forest algorithm. Instead, unsupervised techniques are generally based in the data itself to identify patrons, e. g. cluster of similar objects, in some pre-defined feature space where the data are defined.

In this work, we used S-PLUS observations of the southern hemisphere to search for objects with an excess of $\text{H}\alpha$ using automatic methods based on the ($r - \text{H}\alpha$) versus ($r - i$) color-color diagram. We have also used color criteria based in ($g - r$) and ($z - g$) in conjunction to unsupervised machine learning techniques to split the final list in those with blue and red continuum. The paper is organized as follows...



Figure 1. Transmission curves of the S-PLUS filters set. The narrow-band filter J0660 detects the $\text{H}\alpha$ emission line. Over-plotted are different classes of emission line objects, from upper to down PN, SySt...

2 OBSERVATIONS: THE S-PLUS PROJECT

We are implemented data from S-PLUS DR3 (ref) to carried out our study. S-PLUS is 12-band optical photometric survey, which are formed by seven narrow-band ($J0378$, $J0395$, $J0410$, $J0430$, $J0515$, $J0660$ and $J0861$) and five broad-band like SDSS filters (u , g , r , i and z , Fukugita et al. 1996). The narrow-band set include the filter $J0660$ which detect the $\text{H}\alpha$ emission line. For more detailed about the configuration of S-PLUS filter set see Figure 1 shows the Javalambre filter system (Marín-Franch et al. 2012) overlapping are the optical spectra of several class of emission line objects on which it is possible to see that the $\text{H}\alpha$ line falls into the $J0660$ filter, except for the QSOs.

The actual data release contains about 60 millions of objects covering a total area of $\sim 8000 \text{ deg}^2$, at high Galactic latitudes ($> 30 \text{ deg}$) using a dedicated 0.83m robotic telescope, the T80-South (T80S), located at Cerro Tololo, Chile. S-PLUS will cover an additional $1,300 \text{ deg}^2$ of the Galactic plane and bulge to enable Galactic studies. In this work, we focus on the aspects that are of particular interest to the second data release of the S-PLUS main survey. Additional information about S-PLUS can be found in Mendes de Oliveira et al. (2019).

3 METHODOLOGY

We first constructed a sub-sample from all S-PLUS DR3 from which we applied an iterative and automatic technique to select objects with an excess of $\text{H}\alpha$ emission line. Once the objects were selected we also make a separation of them into two groups those with red and blue continuum by using optical colors in conjunction with unsupervised machine learning statistical tools. These procedures are described below:

3.1 Initial selection sample

The first step in our selection procedure consist in the following criteria to guarantee the quality of the observations of the objects:

- (i) The sources must have detection in the filters: r , i and $J0660$. To assure that we select object must have error minor or equal to 0.2 in each of three filters.
- (ii) Must have an r magnitude until $r = 21$.

3.2 Finding the main stellar locus and selecting the $\text{H}\alpha$ emitters

Once the initial cut were made, we proceed to select the objects with an excess of $\text{H}\alpha$ which is represent with a relatively high value of the

¹ <https://www.j-plus.es>

² <http://www.splus.iag.usp.br>

J0660 filter in comparison with r-band filter. For that we first divided our sub-sample in four magnitude bins using the r -band magnitudes. The bins have the follow distribution:

- (i) objects with magnitude in the r -band $r < 16$
- (ii) objects with magnitude in the r -band $16 \leq r < 18$
- (iii) objects with magnitude in the r -band $18 \leq r < 20$
- (iv) objects with magnitude in the r -band $20 \leq r < 21$

To select the emission lines we used the same method created and implemented by [Witham et al. \(2008\)](#) its possible to do that because the S-PLUS has similar filters that the IPHAS project, which are r , J0660 and i . This technique was used by [Scaringi et al. \(2013\)](#) to identify blue objects with excess of H α and after that [Wevers et al. \(2017\)](#) also applied this methodology to create catalogue of candidate H α emission showing an high effectiveness. In this order of ideas we attempted this methodology in S-PLUS.

We first generated the $(r - J0660)$ versus $(r - i)$ color-color diagram for each magnitude bins. We then carried a out an initial straight line fit to all objects in each magnitude bin. This initial fit is an attempt to find the loci of main-sequence and giant stars. We implemented a iterative σ -clipping technique to find the best-fitting of the main stellar locus. In this order of ideas, we made four interactive σ -clipped. Once we have found the appropriate fitting for each magnitude bin, we identified those objects significantly above of this final fit as likely sources with a excesses of H α . Objects with a significant contribution of H α meet the condition:

$$(r - J0660)_{\text{obs}} - (r - J0660)_{\text{fit}} \geq C \times \sqrt{\sigma_s^2 - \sigma_{\text{phot}}^2} \quad (1)$$

where σ_s is the root mean squared value of the residuals around the fit and σ_{phot} is the error on the observed $(r - J0660)$ colour index. C is a constant which has the value 4 following [Wevers et al. \(2017\)](#). The fits are carried out with the aid of the python library `astropy.modeling`³.

Figure 2 illustrates the procedure used to selected the H α emitters in S-PLUS DR3 for each magnitude bin. The continuous black lines represent the initial fit and the dashed lines indicate the 4- σ clipping fit lines. The dotted lines are the cut selection criteria for the H α emitters – the 4- σ above of the final fit-. Note that theses cut lines are only an approximations because to trace them, it is only considered the residual around the fit. The actual selection criteria used here also include the photometric uncertainties in $r - J0660$ for each individual data source as shows on the Equation 1.

After the algorithm was applied to all data, we visually inspectioned the resulting list by seeing the S-spectra and corresponding colored image. The figure 3 shows an example of how looks like a S-spectra⁴ of sources in magnitude unities selected with methods explained above. This object clearly exhibits strong H α emitter.

Fig 4 exhibits the distribution of the emission on the $r - J0660$ versus $r - i$ color-color plane. At this point we can say that the algorithm implemented works well in selected objects with a excess in emission on the J0660 filter. It is possible to affirm that, because the identified objects are located above of the loci of the main and giant stars. The S-PLUS synthetic photometry of the stellar locus is represent by the contours in the diagram and was obtained by using the filter transmission profiles, shown in Fig. 1, and the library of stellar spectral energy distributions of [Pickles \(1998\)](#). This synthetic

magnitudes were defined in the AB magnitude system ([Oke & Gunn 1983](#)). The wide distribution of fonts across the colors ($r - J060$) and ($r - i$) indicates that several types of objects were selected. For instance, higher values on the $r - J060$ color of some sources could be indicating that they are H II regions or/and blue compact galaxies and PNe. On the hand, the $r - i$ color indicates the rendered sources such as SySt and young stellar objects or source with strong blue continuum as cataclysm variables.

Fig. 5 displays the distribution of all emitters in Galactic la ic latitude and longitude. The density map regions represent the spatial positions of the objects on the sky. The surface density of J0660-excess objects is highest near the Galactic plane.

Once, we felt confident of our sample of H α emission lines sources, we proceeded to classify the objects into two big groups; one group containing those objects with a strong blue continuum and another with an intense emission of the continuum on the blue part of the spectrum.

3.3 Unsupervised machine learning/clustering techniques

In this work we are using unsupervised machine learning approaches to divided our sample in two groups: one represent the blue sources and the another one are the red sources. The blue are those that have strong emission of the continuum on the part blue of the spectra and the another with strong emission continuum of the red one. For that task, was implemented two clustering techniques; hierarchical clustering and Hierarchical density-based cluster selection based on the $(g - r)$ and $(z - g)$ colors.

3.3.1 $(g - r)$ versus $(z - g)$ color-color diagram

In order to find the best color-color diagram to separating the final sample of emission line objects into two color types, we first attempted constructed color-color diagrams by using the S-PLUS simulated photometry of several classes of emission line objects⁵. The $(g - r)$ versus $(z - g)$ color-color diagram is displayed on the Fig. 6. The SySt span a wide range on the $(z - g)$ color, from approximately -0.5 to 6.0. This wide range on the color may refer to the different type spectral of the cold stellar component of the binary system. All the YSOs and many SySt are located on the top-left on the diagram indicating a reddening effect of the circumstellar disk for many SySt (for example for those symbiotic with a Mira star) and YSOs. On the other hand, the PNe, HII regions, CVs, QSOs and emission line galaxies are located on the lower-right region in the diagram. This indicates blue continuum present in each classes of theses objects, mainly by the presence of the high excitation star, for instance, white dwarf in planetary nebulae and cataclysm variable stars and massive young stars in H II regions and the starburst galaxies. Although some SySt are located in the region where appear the blue sources, this color-color diagram seems to separate very well two color types, blue from red sources.

We constructed the $(g - r)$ versus $(z - g)$ color-color diagram using the photometry of our final list of H α emitters, which is presented in Fig. 7. As was we expected two-color population is showed in the diagram perceptible in the level of the color of the density region on which yellow areas represent a higher concentration of points. This is re-forced by the bi-modal shape of the $(g - r)$ and $(z - g)$ color

³ <https://docs.astropy.org/en/stable/modeling/index.html>

⁴ S-spectra signify the S-PLUS emission in flux or magnitude unities of an object in all twelve bands.

⁵ It is important to note that there are other classes of objects with emission lines that have not been included, because our main objective is to separate between two types of these objects by their photometric colors.

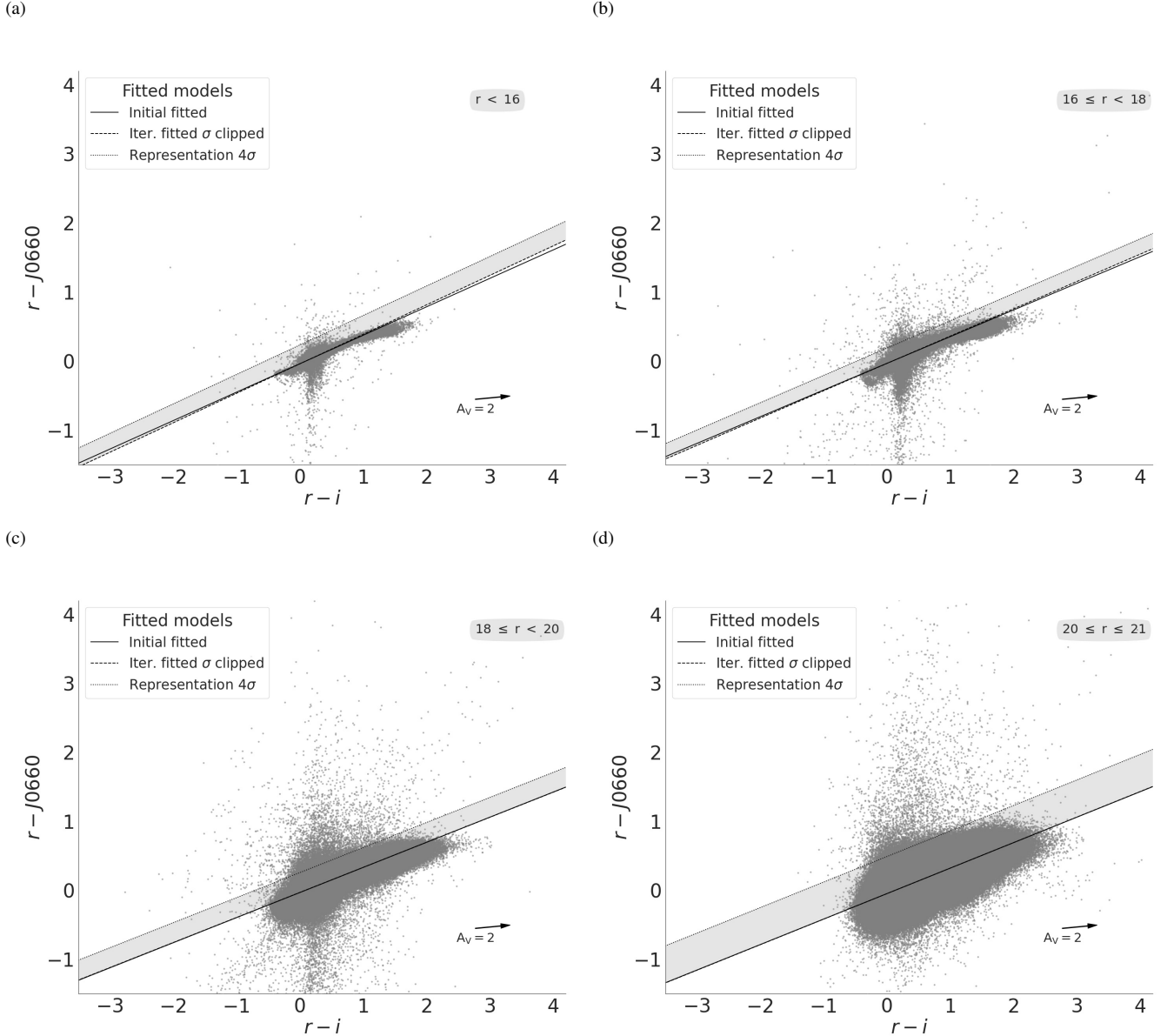


Figure 2. An illustration of the selection criteria used to identify strong emission-line objects via colour-colour plots. The data shown here are all from the S-PLUS DR3. The data are split up into four magnitude bins, as shown in the four panels. Objects with H α excess should be located near the top of the colour-colour diagrams. The thin red lines illustrate the original linear fit to all the data (grey points). The dashed lines represent the final fits to the stellar locus of points which were obtained by applying an iterative σ -clipping technique to the initial fit. The actual cuts used to select H α emitters are shown by the dotted lines. Objects selected as H α emitters must be located above. Note that the cut lines (selection criteria) shown here are only approximate, as the actual selection criterion also considers the errors on each source. This means that an object could be in the bottom right-hand panel is not selected despite clearly lying above the cut line (EXPLICAR ESTA ÚLTIMA FRASE MEJOR).

distributions (see inset plots of the Fig. 7). The two peaks of the ($g - r$) and ($z - g$) distributions clearly correspond to blue and red sources, respectively. This histograms also show that the fraction of blue objects is considerable higher than the red ones.

3.3.2 Hierarchical agglomerative clustering

Hierarchical clustering belong to the family of clustering algorithms on which are constructed clusters by merging and splitting them suc-

cessively. It is an unsupervised algorithm that yields a dendrogram⁶ represents the nested grouping of patterns and the levels of similarity at which the groupings change (Jain et al. 1999). There is two type of hierarchical clustering: one is the *hierarchical agglomerative clustering* (that we have used in this work) which is “bottom-up” approach. Hierarchical agglomerative clustering (HAC) consists of building a binary merge tree, starting from each data element stored at the leaves

⁶ Dendrogram is a diagram representing tree, which shows hierarchical relationship between objects.

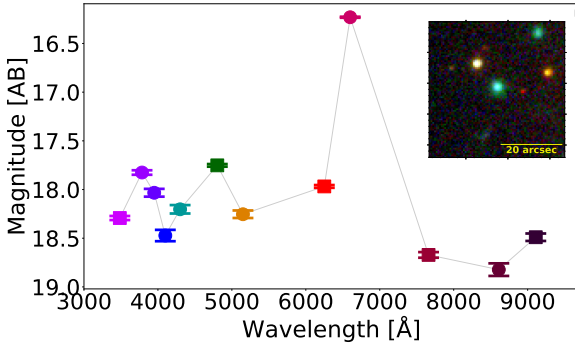


Figure 3. S-spectra of a random object with emission lines select with algorithm explained above. Squares represent the SDSS-like broad-band filters. From left to right they are u , g , r , i and z . Circle symbols are the narrow-band filters, which from left to right represent J0378, J0395, J0410, J0515, J0660 and J0861.

(interpreted as individual clusters) and proceed by merging two by two the “closest” sub-sets (stored at nodes) until it reaches the root -unique cluster- of the tree that contains all the elements of the data set. Agglomerative term is used to define it since the individual data point are successively agglomerated into higher-level. In each iteration, two cluster are selected that are considered as close as possible. These cluster are merged and replaced with a newly created merged cluster. Thus, each merging step reduces the number of cluster by “1”. Therefore, the method needs to be designated for measuring proximity between cluster containing multiple data points, so that they may be merged (Mann & Kaur 2013; Aggarwal 2015). We could describe how to work the algorithm in three simple steps:

- (i) Initially, each data point represents the clusters i.e. leaves.
- (ii) It loops merges the nodes (clusters) that have the maximum similarity between them.
- (iii) At the end of the process all the nodes belong to an unique cluster. This is known as the root of the tree structure.

The other type is the *hierarchical divisive clustering*. This is a “top-down” approach. The data start in one cluster (the root of the tree), and splits step by step are performed recursively as one moves down the hierarchy. It is the inverse procedure of HAC.

In simple words, hierarchical clustering approaches can be interpreted as an algorithm that groups similar objects into groups called clusters or nodes. The endpoint is a set of clusters, where each cluster is distinct from each other cluster, and the objects within each cluster are broadly similar to each other.

Choosing the number of cluster. Firstly, the Hierarchical cluster output dendrogram (tree) can be implemented to obtain the desired clustering. Secondly, the dendrogram schema allows a convenient way to establish the entity relationship between at all levels of granularity. In conclusion, a dendrogram is a visualization in form of a tree showing the order and distances of merges during the hierarchical clustering.

- On the x axis you see labels. If you do not specify anything else they are the indices of your samples in X .
- On the y axis you see the distances (of the “ward” method in our case).

3.3.3 Dendrogram Truncation

As you might have noticed, the above is pretty big for many samples already and you probably have way more in real scenarios, so let me spend a few seconds on highlighting some other features of the `dendrogram()` function:

Starting from each label at the bottom, you can see a vertical line up to a horizontal line. The height of that horizontal line tells you about the distance at which this label was merged into another label or cluster. You can find that other cluster by following the other vertical line down again. If you don’t encounter another horizontal line, it was just merged with the other label you reach, otherwise it was merged into another cluster that was formed earlier.

Hierarchical clustering can be performed with either a distance matrix or raw data. When raw data is provided, the software will automatically compute a distance matrix in the background. The distance matrix below shows the distance between six objects.

Hierarchical clustering starts by treating each observation as a separate cluster. Then, it repeatedly executes the following two steps: (1) identify the two clusters that are closest together, and (2) merge the two most similar clusters. This iterative process continues until all the clusters are merged together. This is illustrated in the diagrams below.

Hierarchical clustering 2

3.3.4 Hierarchical density-based cluster selection

Hierarchical density-based cluster selection (HDBSCAN, Campello et al. 2013) is another unsupervised machine learning algorithm that hinges on clustering. It is based on a slightly modified version of Density-based Spatial Clustering of Applications with Noise (DBSCAN; Ester et al. 1996) which declare points as noise. It is a algorithm that assumes clusters are characterized by “islands” of high density in the sea of the parameter space, such that clusters are regarded as data partitions that have a higher density than their surroundings (Ntwaetsile & Geach 2021). HDBSCAN takes forward the DBSCAN concept by introducing a hierarchy to the clustering, with “persistent” clusters finally extracted from the hierarchical tree. The main advantage of HDBSCAN in comparison with the predecessor consists in the possibility in finding clusters of variables densities and different shape. Following Malzer & Baum (2021) and Ntwaetsile & Geach (2021) works as follows:

- (i) In HDBSCAN is consider the “core” distance for a point x , $\text{core}_k(x)$ which defines the distance of an object to the k th nearest neighbor that is an efficient way of measurement of density. Low values of $\text{core}_k(x)$ represents high density and vice-versa.
- (ii) The “mutual readability distance” between two points a and b is defined as $d_m(a, b) = \min\{\text{core}_k(a), \text{core}_k(b), d(a, b)\}$, where $d(a, b)$ is the distance between a and b according, for instance, Euclidean metric. The mutual readability distance allows points in dense regions stay close together and those that are in less dense regions pushed away.
- (iii) The mutual readability graph is used to construct the minimum spanning tree, and sorting its edges by the mutual readability distance results in a hierarchical tree structure. The hierarchy of connected components is defined by sorting the edges of the tree by distance in reverse order, describing a dendrogram. This is the structure from which cluster will be identified.
- (iv) HDBSCAN allows to extract clusters of variable density, effectively by cutting the dendrogram at different points.
- (v) The cluster tree is condensed into a simpler structure. Considering the single main trunk which contains all of the data points,

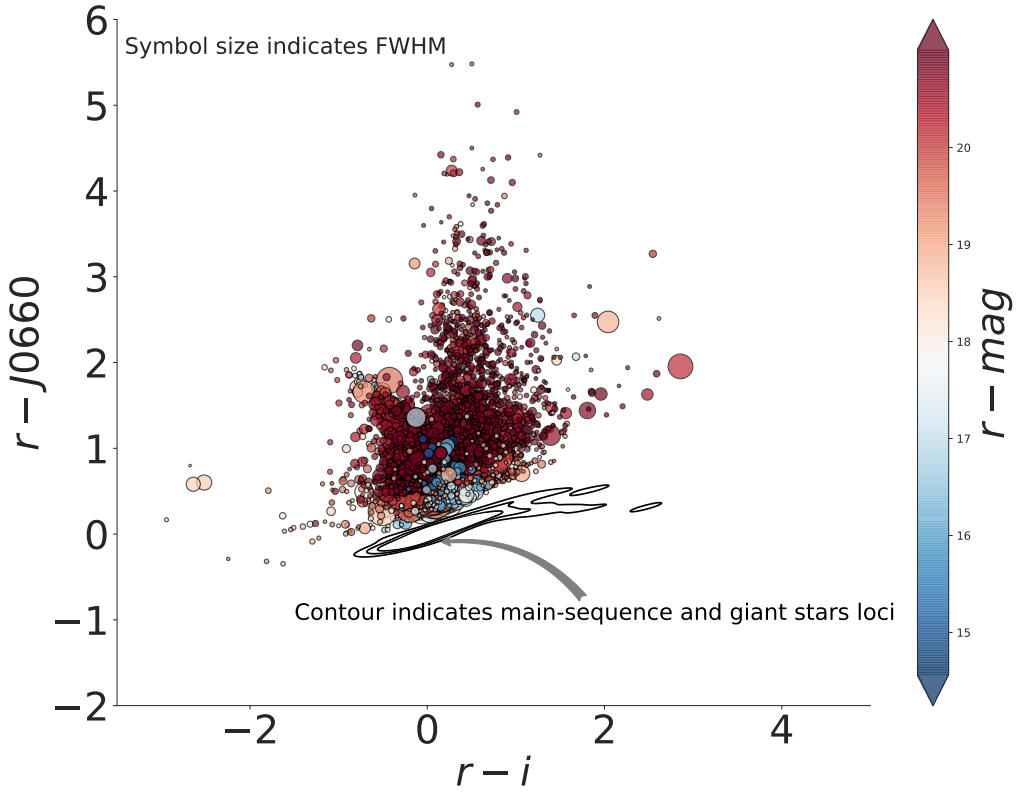


Figure 4. Colour-colour diagram with all the emission line objects selected from S-PLUS DR3. Size of the symbols represent the measured FWHM assuming a Gaussian core (for more detail see Almeida-Fernandes et al. 2021). Coloured bar indicates the magnitude values in the r-band. The contours represent the S-PLUS synthetic photometry of main-sequence and giant stars loci from the library of stellar spectral energy distributions of Pickles (1998).

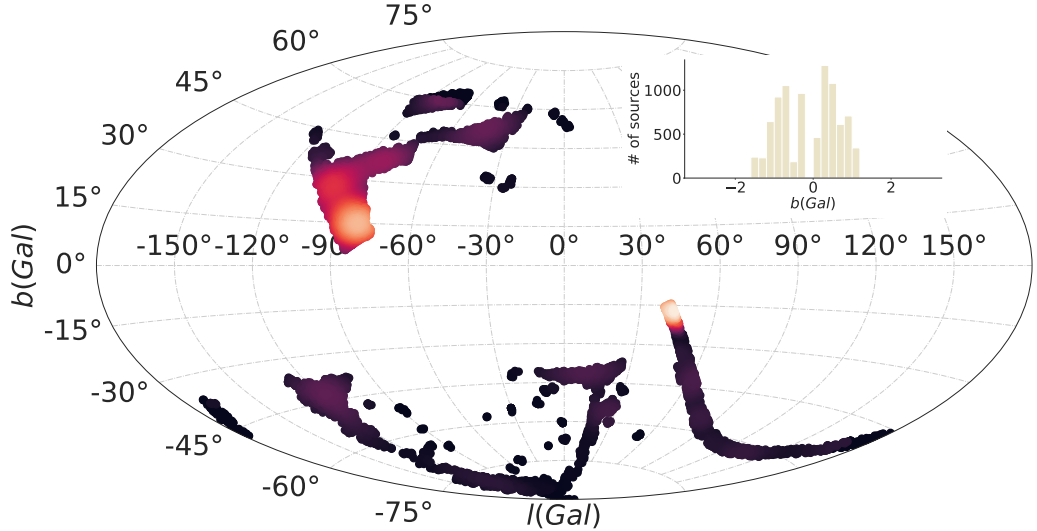


Figure 5. Distribution of H α emitters in Galactic longitude and latitude coordinate. Inset figure represents distribution of the objects in Galactic latitude.

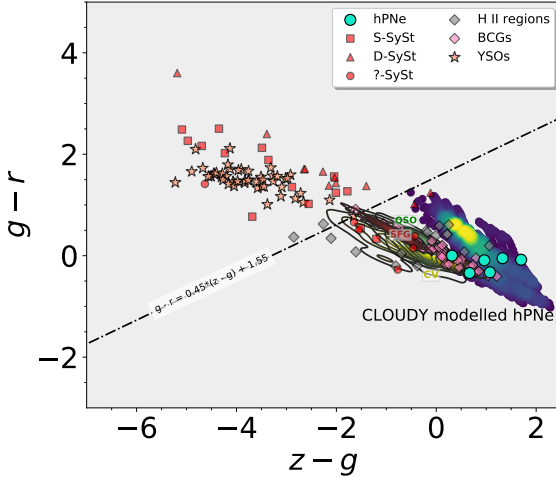


Figure 6. The $(g-r)$ versus $(z-g)$ synthetic color-color diagram of several classes of emission lines objects. Included in the diagrams, there are families of CLOUDY modelled halo PNe spanning a range of properties (density map region). Cyan circles represent S-PLUS photometry from observed spectra Grey diamonds represent H II regions in NGC 55. Red boxes display symbiotic stars, this group also includes Galactic and external SySt from NGC 205 IC 10 and NGC 185,. Yellow circles correspond to cataclysmic variables (CVs) from SDSS. Pink circles indicate blue compact galaxies (BCGs) from SDSS. Orange triangles refer to SDSS star-forming galaxies (SDSS SFGs). SDSS QSOs at different redshift ranges are shown as light blue diamonds, and YSOs from Lupus and Sigma Orionis are represented by salmon stars. The diagonal line represent a subjective criterion to separate the objects into two color types.

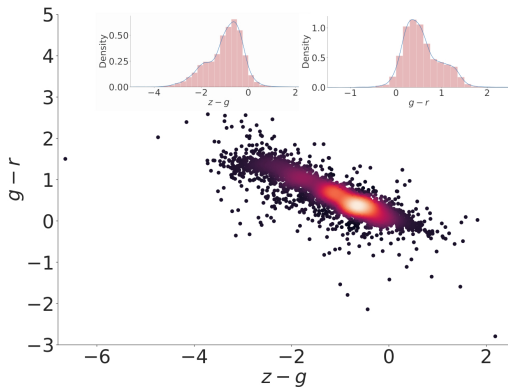


Figure 7. The $(g-r)$ versus $(z-g)$ color-color diagram with all the emission line objects selected in S-PLUS. The inset figures represent the $(g-r)$ and $(z-g)$ distributions.

the tree splits into branches. A condensed cluster hierarchy can be described by considering the number points kept in each branch as it splits. If a given branch splits into two, with a branch containing fewer points than the minimum cluster size means, the large branch “persists” and the smaller split branch “falls out” of the cluster. If a branch splits into two with both branches exceeding the minimum cluster size, both new branches persist.

(vi) The clusters are extracted on the notion of persistence in the hierarchy. The parameter $\lambda = d_m^{-1}$ is defined, and each cluster has a λ_{birth} (the point at which the cluster split off) and λ_{death} (the point when the cluster split into other clusters). In each cluster, we have

λ_p describing when each point fell out of the cluster (or was split off into new cluster), $\lambda_{\text{birth}} \leq \lambda_p \leq \lambda_{\text{death}}$. Cluster stability S is defined as the sum of $\lambda_p - \lambda_{\text{birth}}$ for all points in the cluster. To extract cluster the following procedure is implemented: First, select all leaves as cluster. Then, working through the hierarchy, consider the stability of a parent cluster S_p and its n descendants $S_d^{0,1,2,\dots,n}$. If $S_p > \sum_{i=0}^n S_d^i$ we unselect all the descendants. If $S_p < \sum_{i=0}^n S_d^i$ then the cluster stability is set such that $S_p = \sum_{i=0}^n S_d^i$. At the root node we have our set of selected cluster. Any point in the sample that does not fall into one of the selected clusters is defined as noise.

(vii) The selected cluster are used the label points. Furthermore, the definition of λ_p within a cluster, when normalized between 0 and 1 provides a means of characterization a probability that a given point belongs to the cluster or alternative a measure of the strength of membership.

The algorithm starts off much the same as DBSCAN: we transform the space according to density, exactly as DBSCAN does, and perform single linkage clustering on the transformed space. Instead of taking an epsilon value as a cut level for the dendrogram however, a different approach is taken: the dendrogram is condensed by viewing splits that result in a small number of points splitting off as points “falling out of a cluster”. This results in a smaller tree with fewer clusters that “lose points”. That tree can then be used to select the most stable or persistent clusters. This process allows the tree to be cut at varying height, picking our varying density clusters based on cluster stability. The immediate advantage of this is that we can have varying density clusters; the second benefit is that we have eliminated the epsilon parameter as we no longer need it to choose a cut of the dendrogram. Instead we have a new parameter `min_cluster_size` which is used to determine whether points are “falling out of a cluster” or splitting to form two new clusters. This trades an unintuitive parameter for one that is not so hard to choose for EDA (what is the minimum size cluster I am willing to care about?).

Hierarchical Density-Based Spatial Clustering of Applications with Noise (Campello, Moulavi, and Sander 2013), (Campello et al. 2015). Performs DBSCAN overvarying epsilon values and integrates the result to find a clustering that gives the best stability over epsilon. This allows HDBSCAN to find clusters of varying densities (unlike DBSCAN), and be more robust to parameter selection. The library also includes support for Robust Single Linkage clustering (Chaudhuri et al. 2014), (Chaudhuri and Dasgupta 2010), GLOSH outlier detection (Campello et al. 2015), and tools for visualizing and exploring cluster structures. Finally support for prediction and soft clustering is also available.

In the last years, HDBSCAN have been in astronomy for different tasks. Jayasinghe et al. (2019) presented the second data release Milky Way Project (MWP), a citizen science initiative on the Zooniverse platform, presents internet users with infrared (IR) images from Spitzer on which were aggregate ~ 3 million classifications made by volunteers during the years 2012–2017 to produce the DR2 catalogue, which contains 2600 IR bubbles and 599 candidate bow shock driving stars. The reliability of bubble identifications was made by using HDBSCAN. On the other hand, Webb et al. (2020) used HDBSCAN for transient discovery. Recently, Ntwaetsile & Geach (2021) used it to group radio sources into a sequence of morphological classes, illustrating a simple methodology to classify and label new, unseen galaxies in large samples.

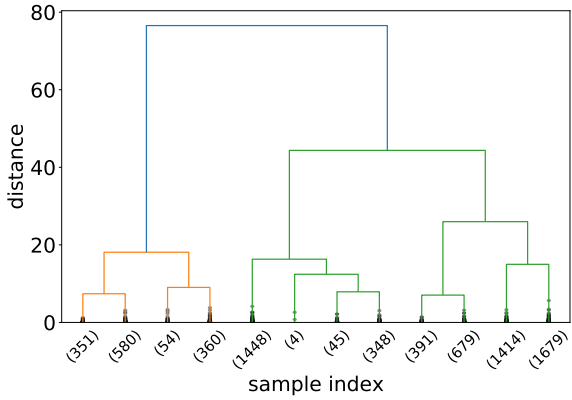


Figure 8. Customer dendrogram...

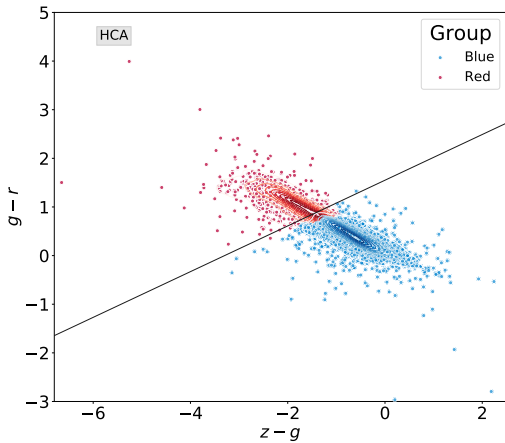


Figure 9. The $(g - r)$ versus $(z - g)$ color-color diagram with the two population found bi implementing HAC algorithm. The blue symbols represent the sources with intense blue continuum and the red symbols are the objects with intense red continuum.

3.4 Grouping the $\text{H}\alpha$ emitters into blue and red sources

3.4.1 HAC

In this work, we implemented HAC by using the python machine learning library `Scikit-learn`⁷ (Pedregosa et al. 2011). There are some parameters to have in count when the algorithm is applied: `n_clusters` which is the number cluster to find. Given that our goal is to divide our sample in two groups we set this value in 2. `Affinity`, Metric used to compute the linkage. We found that a simple “Euclidean” distance metric was effective. `Linkage` which determines which distance to use between sets of observation. The algorithm merge the pairs of cluster that minimize this criterion. Here was implemented “ward” which minimizes the variance of the clusters being merged. As was mentioned, the input variables are the colors; $(g - r)$ and $(z - g)$.

Fig. 8 shows the dendrogram truncated diagram visualization that

shows the branching of the sample from the main root. And Fig. 9 shows the position of the two groups that resulted after to applying HAC in the color-color diagram. The two clusters represent the blue sources (blue symbols) and red sources (blue symbols) as already by analyzing the diagram of the Fig. 6. Now, we have divided our list in two groups in agreement with the nature of their continuum. We found that the number of blue $\text{H}\alpha$ emitter is bigger than the red one.

3.4.2 HDBSCAN

We also used HDBSCAN to separate the blue sources from the red ones. This just for comparing the performance of two algorithms and show that the our resulted are consistent. We used the python implementation of HDBSCAN⁸ (McInnes et al. 2017). Like HAC, in addition to the colors input parameters, there are key parameters that should be considered when the algorithm is applied. “Euclidean” metric is implemented which results to be very efficient. The two most critical parameters to be implemented are the “minimum cluster size” and “minimum number of samples”. The former refers to the smallest size grouping that we wish to consider a cluster. We have adopted the value “80”. The latter provides a measure of how conservative we want our clustering to be and expressed as the fraction of data classified as noise. The value implemented was “40”. With this configuration of our model we found two cluster. If we use values of minimum number of samples smaller than “40” several small cluster are found that do not make sense.

Left panel of Fig. 10 the resulted cluster found with HDBSCAN. Two group are found and these results are consistent with results found with HAC. In fact, by applying the `condensed_tree_` to the data colors two clusters are selected (for mare detail about `condensed_tree_` attribute see appendix A and related Fig. A1). The two primary clusters are located in the same region in the $(g - r)$ versus $(z - g)$ color-color diagram where lie the group found by the other algorithm. The main difference between the two algorithm is that HDBSCAN is much conservative, then many data points are classified as noise. The two final cluster contain, which we are labeled blue and red sources contain xxx and xxx objects, respectively.

3.5 Soft clustering for HDBSCAN

Perhaps, the main disadvantage of HDBSCAN is that many of the sources are labelled as “noise”, on which some sources are not assigned to any cluster. As was mentioned, this comes from the conservative nature of HDBSCAN and that they are located far away of the cluster cores. An alternative to avoid the outlier classification consists in used the concept of “soft clustering”. We have carried out here soft clustering for HDBSCAN to assign every object to its most likely cluster. This means that with this approach, points are not assigned cluster labels, instead are assigned a vector of probabilities. The probability value at the i th entry of the vector is the probability that a data point is a member of the i th cluster. We can then simply assign cluster labels for every point by taking the most likely cluster it belongs to, using probability thresholds. Soft clustering for HDBSCAN is based on the Global-Local Outlier Score from Hierarchies (GLOSH) algorithm (Campello et al. 2015) and combines this with a measure of distance from a given cluster to produce an estimate of the probability that any given data point belongs to any of the fixed clusters extracted from the condensed tree.

The right panel of Fig. 10 shows at what most likely cluster belongs

⁷ <https://scikit-learn.org/stable/>

⁸ <https://hdbSCAN.readthedocs.io/en/latest/>

the data points classified as the noise by HDBSCAN. We have used blue and red colors for the points that have the highest probability of being in the blue and red groups, respectively. This fills out the clusters nicely. We see that there were many noise points that are most likely to belong to the clusters we would expect, e. g. in agreement with the results obtained with HAC. Indeed, We now have improved our classification of our list into sources with blue and red continuum because we have estimated the probability of each source to belong to every group.

4 RESULTS AND DISCUSSION

We found a total of 389 emission line sources in all S-PLUS DR3. To understand the nature of the objects and the fractional contribution of different classes of objects with emission lines to the overall sample cross-matching with some catalogs available were carried out.

4.1 Simbad

We made cross-match between our sample of objects with a excess of emission of the $J0660$ and SIMBAD. We searched for all objects in SIMBAD using a radius of 2 arcsec around the position of the optical source in question. We found 1000 matches that include a great variety of emission line objects. In table 1 is showed the different categories of objects found in SIMBAD.

4.1.1 Nebulae

As was mentioned, objects with nebulosity include several types of objects such as H II region and planetary nebulae. The H II regions are objects with gas that being ionized by amounts of UV light come from massive stars (OB type) on which are formed the emission lines. In these clouds of ionized gas, new stars are formed. Unlike H II regions, planetary nebulae represent the final stages of low- and intermediate-mass stars where the gas previously ejected in the phase of AGB is ionized by the high energetic radiation come from their central stars.

In our list of $H\alpha$ emission line a PN appears cataloged in SIMBAD on which the S-PLUS photometry and spectrum is displayed on panel (a) of Fig 11. Emission lines like $H\alpha$ and [N II] are clearly perceptible in its spectrum, agreeing with PLUS photometry. This object is a very interesting because is one of the twelves PNe that belong to the Galactic halo. These PNe are low metallizite and present large velocities that can give count of the origin and nucleosynthesis of the early universe. 30 objects cataloged as HII regions on the SIMBAD database are in our list of $H\alpha$ emitters. Panel (b) on the figure shows the S-PLUS photometry and SDSS spectrum of the extragalactic HII region GALEX 2417063145906373262.

4.1.2 Binary systems

25 known CVs and 5 candidate CVs (from SIMBAD) were selected with algorithm. CVs are binary systems of very short orbital period, in which a low-mass and early-type star fills its Roche region and transfers mass to a companion stars, a dwarf white (Patterson 1984). Fig. 11 the S-PLUS photometry overlapped to the SDSS spectrum of the CV FASTT 1560. As expected, this object was classified as blue source by the machine learning approaches. Other binary system in our list are the X-binary sources, eclipsing binary, variable stars of RR Lyr type.

4.1.3 Stars

Several stars were selected as shows the matches with SIMBAD. The SIMBAD types include normal stars, white dwarf stars (WD*), white dwarf candidates (Candidate_WD*), blue stars, blue super-giant stars (BlueSG*), high proper-motion stars (PM*) and low-mass star (low-mass*; $M < 1M_\odot$). All these objects appears in the S-PLUS catalog as $H\alpha$ emitters. Some of them can be early/late-type emission-line stars and/or different types of stars with the $H\alpha$ emission lines. Although some of these stars could represent the fraction of contaminant of our sample.

4.1.4 Galaxies

Several type of emission line galaxies were selected. This category include several class of galaxies according to SIMBAD class: emission-line galaxy (EmG), blue compact galaxy (BlueCompG), HII galaxy (HII G), galaxy in cluster of galaxies (GinCl), galaxy in group of galaxies (GinGroup), low surface brightness galaxy (LSB G), interacting galaxies (IG), part of a Galaxy (PartofG), Seyfert 1 and Seyfert 2 galaxies, AGN and galaxy.

All the emission line galaxies of these category form part of the universe local. This mean that their redshift cover the range on which the $H\alpha$ emission line still falls into the $J0660$ filter. Objects with $z > 0.02$ the $H\alpha$ is outside of the $J0660$ filter. Table B1 of the appendices shows the red-shift of the emission line galaxies of our sample that have SIMBAD matches, probing that mostly of these galaxies are real $H\alpha$ emitters. In these kind of galaxies such as the blue compact and/or H II galaxies their starburst regions that consist of ensemble of massive ionizing stars and their respective giant H II regions cover the extension of the optical images and the emission lines of their spectra.

On the other hand, several AGN, Seyfert 1 and Seyfert 2 galaxies have red-shift between 0.31 and 0.37 indicating that the excess on the $J0660$ filter is not due to the $H\alpha$ emission but if due to the $H\beta$ and [O III] 4959, 5007 Å emission lines. These emission lines at the red-shift range $0.306 < z < 0.376$ are detected in the $J0660$ band. It is well known that the AGNs have very strong emission lines such as $H\beta$, [O III] 4959, 5007 Å and $H\alpha$.

One interesting discussion here, is that the type part of a Galaxy (PartofG) on SIMBAD are actually galaxies with Wolf-Rayet (WR) signature in the low red shift universe also named “WR galaxy” (Osterbrock & Cohen 1982). WR stars in galaxies is perceptible in their spectra with strong emission lines such as $H\alpha$ and [NII]. These spectral features can be of them very similar to extragalactic H II regions present typically of the outskirt of spiral galaxies. Panel (e) of Fig. 11 displays the S-PLUS and SDSS spectra of the Wolf-Rayet [BKD2008] WR 14 which belong to the galaxy nnnnn.

Many of the objects have as main type “galaxy” in SIMBAD. This galaxies could be spiral galaxies on which the star formation is present. It is known that in the spiral arms of the galaxies are present H II regions as well as neutral gas (H I) and molecular gas. Actually some of these galaxies have secondary type H I. The reservoir of H I gas in galaxies must ultimately feed their star formation, after cooling and forming molecular clouds (van Driel et al. 2016). Fig. shows the S-PLUS photometry and the SDSS spectra of star-forming galaxy with clearly emission lines. Note that almost all these galaxies are classified as blue color type objects by the HAC and HDBSCAN. However, Mostly of the Seyfert 2 galaxies and a handful of galaxies are classified as red sources, why?

Table 1. A summary of the results obtained of the positional cross-match between the S-PLUS list of emission line objects and the SIMBAD database. We used a search radius of 2 arcsec.

| Main type | Associated SIMBAD types | Number of S-PLUS objects with SIMBAD match |
|---------------------------------------|---|--|
| H II region | HII | 26 |
| Planetary nebula | PN | 1 |
| Supernova | SN, Candidate_SN* | 9 |
| Nova | Nova | 1 |
| Cataclysmic variable star | CataclyV*, Candidate_CV* | 30 |
| Variable star of RR Lyr type | RRLyr, Candidate_RRLyr | 19 |
| X-ray source | HMXB, X | 6 |
| Eclipsing binary | EB* | 8 |
| BL Lac - type object | BLLac | 2 |
| Emission object | EmObj | 4 |
| Star | star, WD*, Candidate_WD*, Blue, BlueSG*, PM*, low-mass* | 57 |
| UV-emission source | UV | 2 |
| Cluster of stars | Cl* | 3 |
| Far-infrared source | FIR | 2 |
| Mid-infrared source | MIR | 1 |
| Radio-source | Radio | 7 |
| Molecular cloud | MolCld | 2 |
| Emission line galaxy | EmG, HII_G, StarburstG, BlueCompG | 102 |
| Part of a galaxy | PartofG | 9 |
| Interacting galaxies | IG | 10 |
| Radio galaxy | RadioG | 2 |
| Galaxy in pair of galaxies | GinPair | 12 |
| Galaxy in group of galaxies | GinGroup | 18 |
| Galaxy in cluster of galaxies | GinCl | 23 |
| Low surface brightness galaxy | LSB_G | 10 |
| Brightest galaxy in a cluster | BCIG | 3 |
| Globular cluster | GICl | 1 |
| QSO | QSO, QSO_Candidate | 225 |
| AGN | AGN, AGN_Candidate | 18 |
| Seyfert 1 | Seyfert_1 | 38 |
| Seyfert 2 | Seyfert_2 | 7 |
| Galaxy | Galaxy | 421 |
| Possible gravitationally lensed image | Possible_lensImage | 1 |
| Total | | 10 |

4.1.5 QSOs

Other extragalactic objects with emission lines that were selected are the QSOs. In the case of the QSOs is not the H α emission line who impact on the J0660 filter. This filter is affected by strong emission lines present in these objects that to specific redshift drop into the J0660 filter. Some of these emission lines are H β , C IV 1550 Å, C III] 1909 Å, Mg II 2798 Å (see, also [Gutiérrez-Soto et al. 2020](#); [Nakazono et al. 2021](#)). All the objects were classified as blue sources which was the expected. Fig. show the S-PLUS photometry and SDSS spectrum of the QSO 2SLAQ J220529.34-003110.6 which has red-shift of ~ 2.45 indicating that the emission line corresponds to the line C III].

4.1.6 Other type of objects

Miscellanies the objects were selected on which are include as it can see in the table 1. They include FIR sources, MIR objects, molecular clouds,

4.2 SDSS and LAMOST

We also made cross-match between the sample of H α emission line objects and SDSS DR16 ([Ahumada et al. 2020](#)). We used use the 2σ error circle as the cross-matching radius. We got 200 spectra from which 195 objects exhibit strong emission lines. 5 objects do not show emission lines, they probably are stars or galaxies.

We also cross-correlate our list with Large Sky Area Multi-Object Fiber Spectroscopic Telescope (LAMOST; [Wu et al. 2011](#)) using a radius of 2 arcsec for the match. These spectra also show strong emission lines. These results shows that this technique actually are very effective for selecting sources with strong emission lines.

4.3 Magnitudes and color distributions

Fig. 13 shows the magnitude and color distribution of the blue and red sources –classification performed with machine learning on Section 3.3–. Upper panel of the figure shows the distribution of the blue and red sources of the r magnitude. The peaks of the r distribution is the same for the blue and red sources, which is around $r \sim 19.9$. However, the density at the peak is higher in red sources than the blue ones indicating that the proportion of objects with value r of 19.9 is higher than the blue sources. The fraction of object is very small

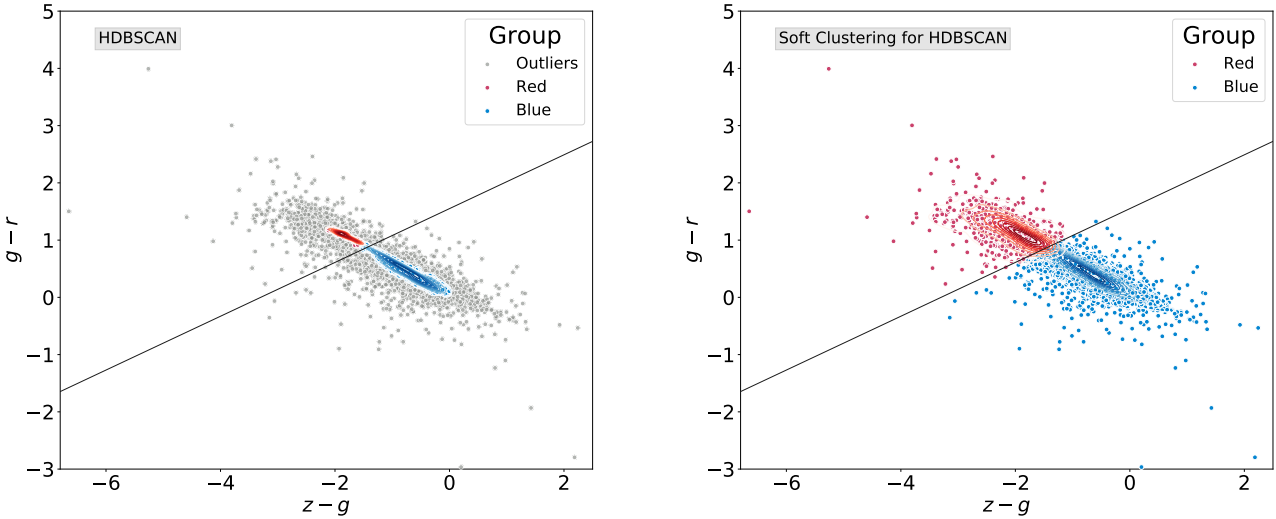


Figure 10. ($r - g$) versus ($g - z$) color-color diagram to separate the blue objects from the red ones.

at $r < 16$ for each group of objects. The distribution of the objects for both group increase in the range $16 \geq r \geq 19.9$. However the density as indicating the Kernel density estimation curves is higher in the blue sources. This implies that the fraction of sources with the magnitude range is considerable higher in comparison with the red group. In conclusion the blue sources tends to be brighter than the red ones.

Middle panel of figure displays the ($r - i$) distribution of the blue and red emission line objects. The peaks of the ($r - i$) distributions are distinct for the blue and red sources. The peaks of the red sources at high red continuum, $(r - i) = 0.5$, compared to the value of the blue sample, $(r - i) = -0.9$. All these results are consistent because the ($r - i$) color is an indicating of reddened sources. This is also consistent with previous works. For instance, Wevers et al. (2017) used different algorithms based on the ($r - i$) color to successfully select blue outliers from the the Galactic Bulge Survey (GBS; Jonker et al. 2011).

Botton panel of Fig. 13 shows the ($r - J0660$) color distribution of the blue and red objects. The fraction of objects selected as emitter rises drastically with $J0660$ excess, until at sufficiently large excesses. The peaks of the ($r - J0660$) color distribution are relatively different for both groups of sources. Having the blue sources the peaks at $(r - J0660) = 0.5$ while for the red one the value peak is $(r - J0660) = 0.7$.

5 CONCLUSIONS

We have created an usefully and important sample of emission line objects. By identifying the locus of main-sequence and giant star and considering as $J0660$ -excess the objects that above of the locus, we have found the emission line sources in S-PLUS DR3. In agreement with the results after to find the coincidences with SIMBAD several type of emission objects are included in our list which including nebulae, binary systems, stars, emission line galaxies, quasars,

globular clusters among other.

We also found that using the colors $g - r$ and $(z - g)$ is very efficient to separate the blue sources from the red ones.

We also found that using this colors as the input to implement unsupervised machine learning in better to group the source in the red or blue sources.

ACKNOWLEDGEMENTS

The S-PLUS project, including the T80-South robotic telescope and the S-PLUS scientific survey, was founded as a partnership between the Fundação de Amparo à Pesquisa do Estado de São Paulo (FAPESP), the Observatório Nacional (ON), the Federal University of Sergipe (UFS), and the Federal University of Santa Catarina (UFSC), with important financial and practical contributions from other collaborating institutes in Brazil, Chile (Universidad de La Serena), and Spain (Centro de Estudios de Física del Cosmos de Aragón, CEFCA). We further acknowledge financial support from the São Paulo Research Foundation (FAPESP), the Brazilian National Research Council (CNPq), the Coordination for the Improvement of Higher Education Personnel (CAPES), the Carlos Chagas Filho Rio de Janeiro State Research Foundation (FAPERJ), and the Brazilian Innovation Agency (FINEP).

Funding for the SDSS and SDSS-II has been provided by the Alfred P. Sloan Foundation, the Participating Institutions, the National Science Foundation, the U.S. Department of Energy, the National Aeronautics and Space Administration, the Japanese Monbukagakusho, the Max Planck Society, and the Higher Education Funding Council for England. The SDSS Web Site is <http://www.sdss.org/>.

The SDSS is managed by the Astrophysical Research Consortium for the Participating Institutions. The Participating Institutions are the American Museum of Natural History, Astrophysical Insti-

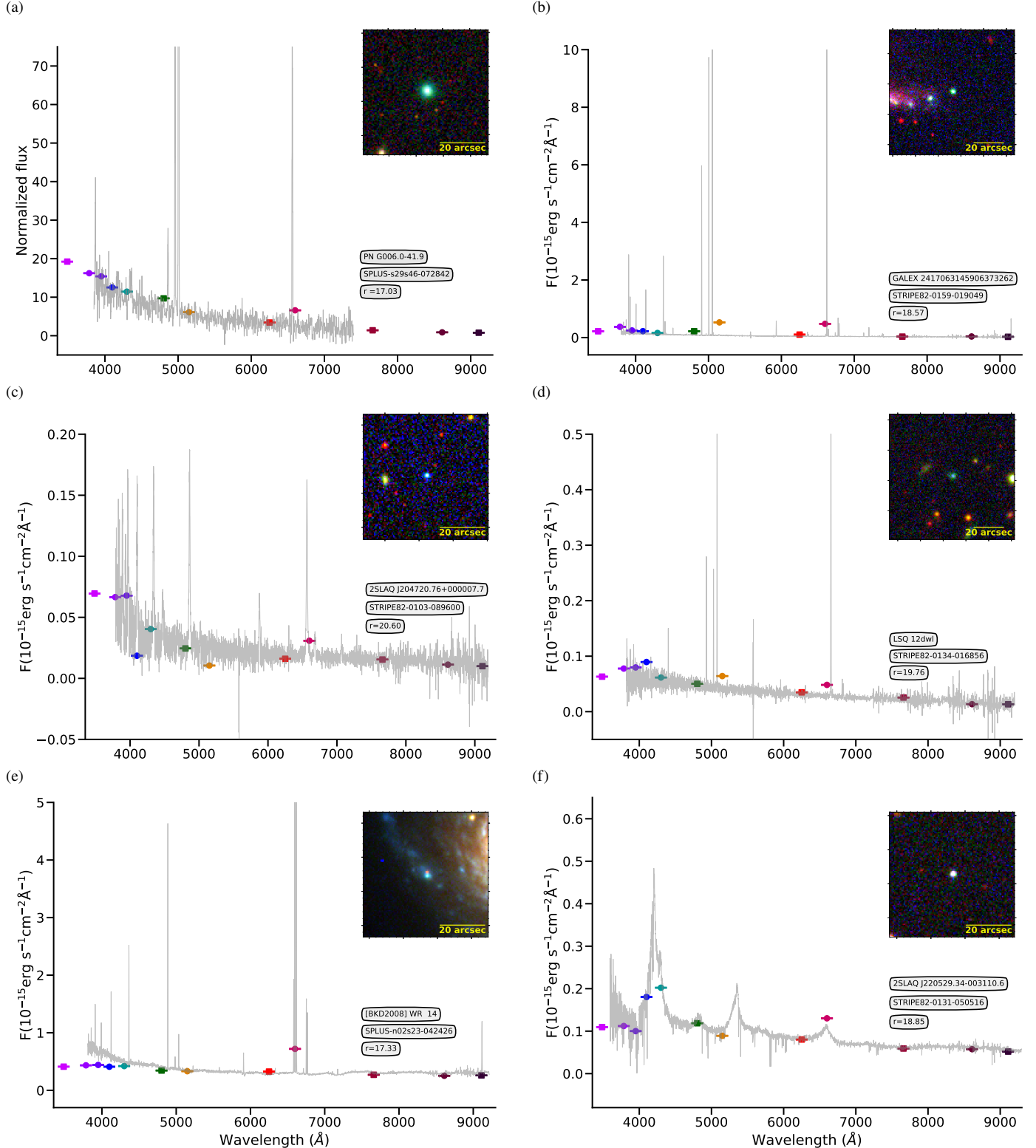


Figure 11. Summary of our selection results showing the spectrum (gray line in each panel) of different classes of emission line sources identified in our target list. A spectrum of a PN (a) from REF. The SDSS spectra of an external H II region (b), a cataclysmic variable star (c), a super nova (d), a WR in a galaxy (e) and a QSO (f) with red-shift of ~ 2.45 . As in Figure 3, colored square and circles symbols represent the S-PLUS photometry. All these objects show a significance excesses on the $J0660$ filter in comparison with the broad-bands.

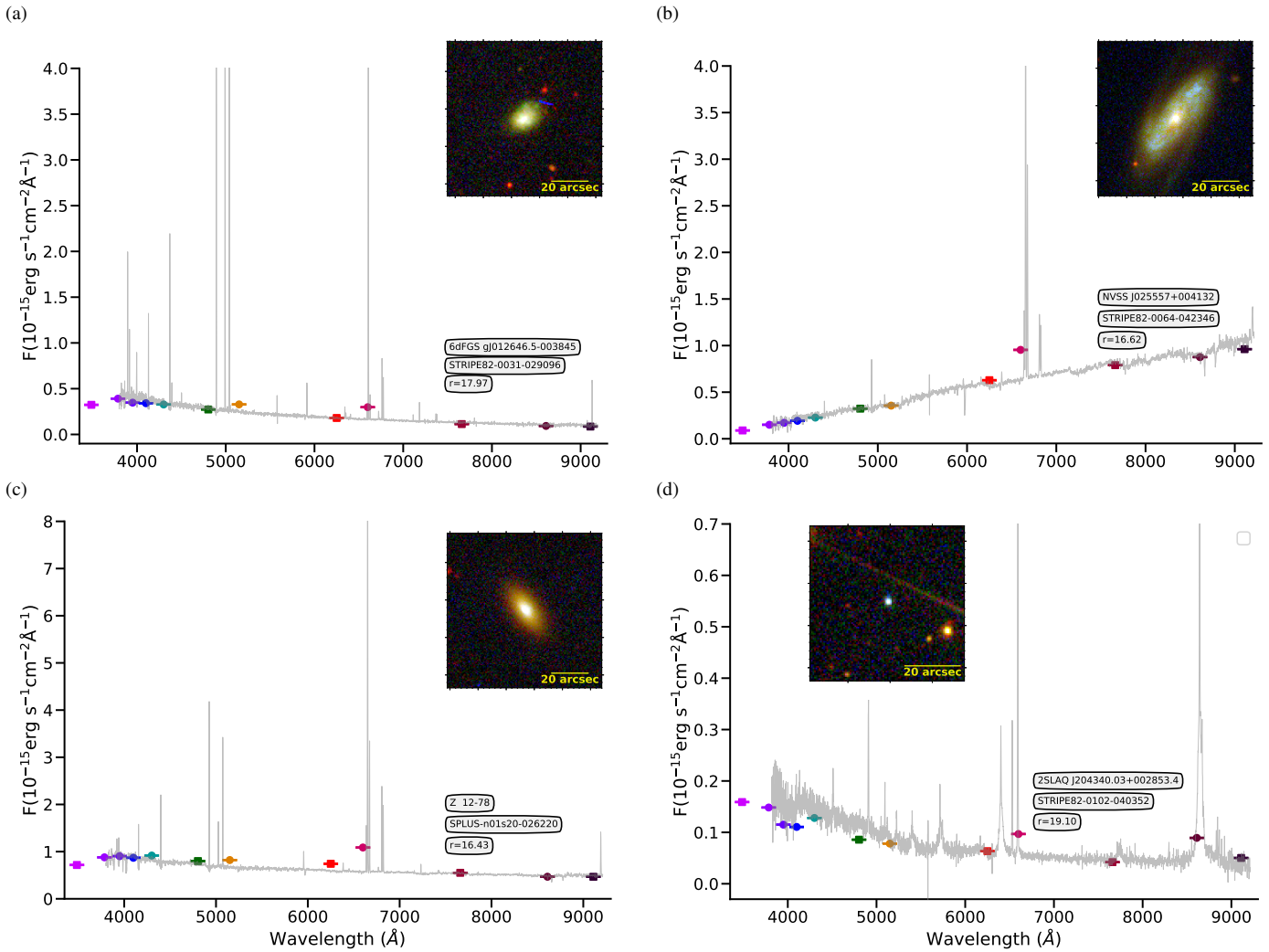


Figure 12. SDSS spectra of a H II galaxy with $z = 0.006$ (a), a radio galaxy with $z = 0.014$ (b), a star-forming galaxy with $z = 0.013$ (c). For this object, the H α line is responsible for the J0660 magnitude. And a Seyfert 1 with $z = 0.317$ (d). For this last object, the excess on the J0660 is due to the [O III] 4959, 5007 \AA emission lines (d). As in Figure 11 coloured symbols indicate the S-PLUS photometry.

tute Potsdam, University of Basel, University of Cambridge, Case Western Reserve University, University of Chicago, Drexel University, Fermilab, the Institute for Advanced Study, the Japan Participation Group, Johns Hopkins University, the Joint Institute for Nuclear Astrophysics, the Kavli Institute for Particle Astrophysics and Cosmology, the Korean Scientist Group, the Chinese Academy of Sciences (LAMOST), Los Alamos National Laboratory, the Max-Planck-Institute for Astronomy (MPIA), the Max-Planck-Institute for Astrophysics (MPA), New Mexico State University, Ohio State University, University of Pittsburgh, University of Portsmouth, Princeton University, the United States Naval Observatory, and the University of Washington.

Guoshoujing Telescope (the Large Sky Area Multi-Object Fiber Spectroscopic Telescope LAMOST) is a National Major Scientific Project built by the Chinese Academy of Sciences. Funding for the project has been provided by the National Development and Reform Commission. LAMOST is operated and managed by the National Astronomical Observatories, Chinese Academy of Sciences.

DATA AVAILABILITY

REFERENCES

- Aggarwal C. C., 2015, Data Mining: The Textbook. Springer, Cham, doi:10.1007/978-3-319-14142-8
- Ahumada R., et al., 2020, *ApJS*, 249, 3
- Akras S., Guzman-Ramirez L., Gonçalves D. R., 2019, *MNRAS*, 488, 3238
- Akras S., Guzman-Ramirez L., Leal-Ferreira M., Ramos-Larios G., 2019a, *ApJS*, 240, 21
- Almeida-Fernandes F., et al., 2021, arXiv e-prints, p. arXiv:2104.00020
- Barentsen G., et al., 2014, *MNRAS*, 444, 3230
- Campello R. J. G. B., Moulavi D., Sander J., 2013, in Pei J., Tseng V. S., Cao L., Motoda H., Xu G., eds, Advances in Knowledge Discovery and Data Mining. Springer Berlin Heidelberg, Berlin, Heidelberg, pp 160–172
- Campello R., Moulavi D., Zimek A., Sander J., 2015, *ACM Transactions on Knowledge Discovery from Data*, 10, 1
- Casares J., 2015, *ApJ*, 808, 80
- Casares J., 2016, *ApJ*, 822, 99
- Cenarro A. J., et al., 2018, preprint, (arXiv:1804.02667)
- Corradi R. L. M., Giannanco C., 2010, *A&A*, 520, A99
- Corradi R. L. M., et al., 2008, *A&A*, 480, 409
- Corradi R. L. M., Sabin L., Munari U., Cetrulo G., Englare A., Angeloni R.,

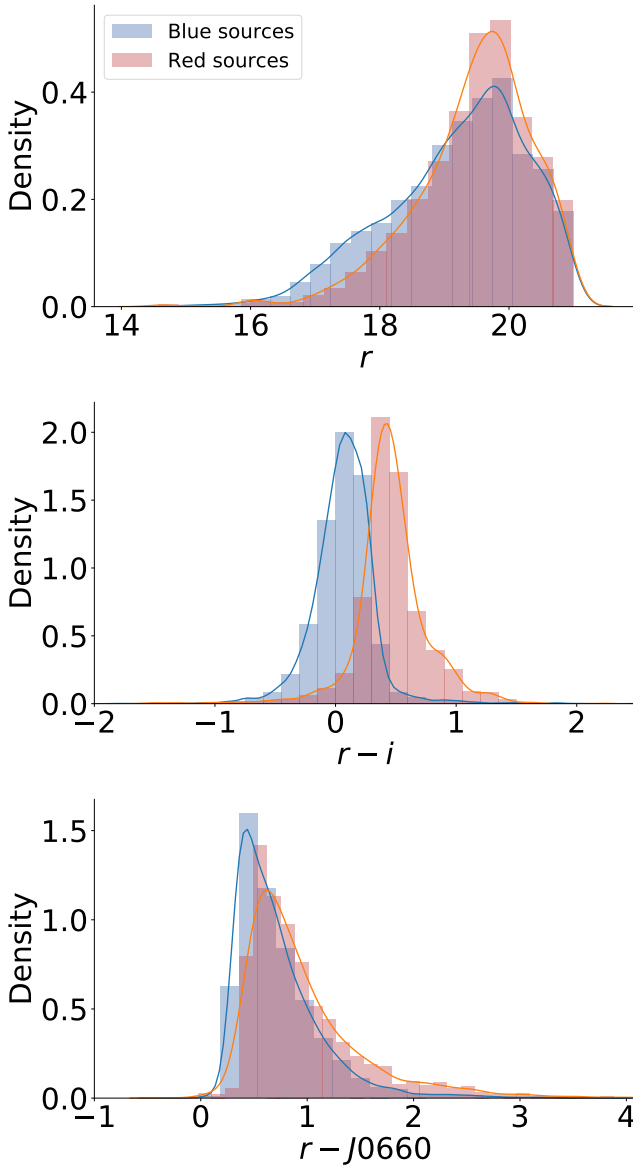


Figure 13. Distribution of r magnitude (left panel), $(r - i)$ color (middle panel), and $(r - J0660)$ color (right panel) for the blue and red sources of the sample of $H\alpha$ emitters. Both sample are normalized to their maximum counts, xx and xx objects for blue and red sources, respectively. The smooth curves represent a Kernel density estimation for both samples.

- Greimel R., Mampaso A., 2011, [A&A, 529, A56](#)
 Drew J. E., et al., 2005, [MNRAS, 362, 753](#)
 Drew J. E., Greimel R., Irwin M. J., Sale S. E., 2008, [MNRAS, 386, 1761](#)
 Drew J. E., et al., 2014, [MNRAS, 440, 2036](#)
 Ester M., Kriegel H.-P., Sander J., Xu X., 1996, in Proc. of 2nd International Conference on Knowledge Discovery and Data Mining (KDD-96). pp 226–231
 Fukugita M., Ichikawa T., Gunn J. E., Doi M., Shimasaku K., Schneider D. P., 1996, [AJ, 111, 1748](#)
 Geach J. E., 2012, [MNRAS, 419, 2633](#)
 Gutiérrez-Soto L. A., et al., 2020, [A&A, 633, A123](#)
 Horne K., Marsh T. R., 1986, [MNRAS, 218, 761](#)
 Jain A. K., Murty M. N., Flynn P. J., 1999, [ACM Comput. Surv., 31, 264](#)
 Jayasinghe T., et al., 2019, [MNRAS, 488, 1141](#)
 Jonker P. G., et al., 2011, [ApJS, 194, 18](#)

- Malzer C., Baum M., 2021, [Sensors, 21](#)
 Mann A., Kaur N., 2013.
 Marín-Franch A., et al., 2012, in Navarro R., Cunningham C. R., Prieto E., eds, Society of Photo-Optical Instrumentation Engineers (SPIE) Conference Series Vol. 8450, Modern Technologies in Space- and Ground-based Telescopes and Instrumentation II. p. 84503S, doi:10.1117/12.925430
 Martin G., Kaviraj S., Hocking A., Read S. C., Geach J. E., 2020, [MNRAS, 491, 1408](#)
 McInnes L., Healy J., Astels S., 2017, [The Journal of Open Source Software, 2](#)
 Mendes de Oliveira C., et al., 2019, [MNRAS, 489, 241](#)
 Nakazono L., et al., 2021, [MNRAS](#)
 Ntwaetsile K., Geach J. E., 2021, [MNRAS, 502, 3417](#)
 Oke J. B., Gunn J. E., 1983, [ApJ, 266, 713](#)
 Osterbrock D. E., Cohen R. D., 1982, [ApJ, 261, 64](#)
 Osterbrock D. E., Ferland G. J., 2006, Astrophysics Of Gas Nebulae and Active Galactic Nuclei. Sausalito: University Science Books, <https://books.google.com.br/books?id=HgfrkDjBD98C>
 Parker Q. A., Bojićić I. S., Frew D. J., 2016, in Journal of Physics Conference Series. p. 032008 ([arXiv:1603.07042](#)), doi:10.1088/1742-6596/728/3/032008
 Patterson J., 1984, [ApJS, 54, 443](#)
 Pedregosa F., et al., 2011, Journal of Machine Learning Research, 12, 2825
 Pickles A. J., 1998, [PASP, 110, 863](#)
 Ratti E. M., Steeghs D. T. H., Jonker P. G., Torres M. A. P., Bassa C. G., Verbunt F., 2012, [MNRAS, 420, 75](#)
 Sabin L., Zijlstra A. A., Wareing C., Corradi R. L. M., Mampaso A., Viironen K., Wright N. J., Parker Q. A., 2010, [Publ. Astron. Soc. Australia, 27, 166](#)
 Scaringi S., Groot P. J., Verbeek K., Greiss S., Knigge C., Körding E., 2013, [MNRAS, 428, 2207](#)
 Schwöpe A. D., Catalán M. S., Beuermann K., Metzner A., Smith R. C., Steeghs D., 2000, [MNRAS, 313, 533](#)
 Steeghs D., Casares J., 2002, [ApJ, 568, 273](#)
 Valenzuela L., Pichara K., 2018, [MNRAS, 474, 3259](#)
 Viironen K., et al., 2009, [A&A, 502, 113](#)
 Vink J. S., Drew J. E., Steeghs D., Wright N. J., Martin E. L., Gänsicke B. T., Greimel R., Drake J., 2008, [MNRAS, 387, 308](#)
 Webb S., et al., 2020, [MNRAS, 498, 3077](#)
 Wevers T., et al., 2017, [MNRAS, 466, 163](#)
 Witham A. R., et al., 2006, [MNRAS, 369, 581](#)
 Witham A. R., et al., 2007, [MNRAS, 382, 1158](#)
 Witham A. R., Knigge C., Drew J. E., Greimel R., Steeghs D., Gänsicke B. T., Groot P. J., Mampaso A., 2008, [MNRAS, 384, 1277](#)
 Wu Y., et al., 2011, [Research in Astronomy and Astrophysics, 11, 924](#)
 van Driel W., et al., 2016, [A&A, 595, A118](#)
 van Spaandonk L., Steeghs D., Marsh T. R., Torres M. A. P., 2010, [MNRAS, 401, 1857](#)

APPENDIX A: CONDENSED TREES

The question now is what does the cluster hierarchy look like - which clusters are near each other, or could perhaps be merged, and which are far apart. We can access the basic hierarchy via the `condensed_tree_` attribute of the `clusterer` object. It is possible to see that HDBSCAN has found two cluster that in agreement with previous results are the blue and red sources.

APPENDIX B: SIMBAD OBJECTS

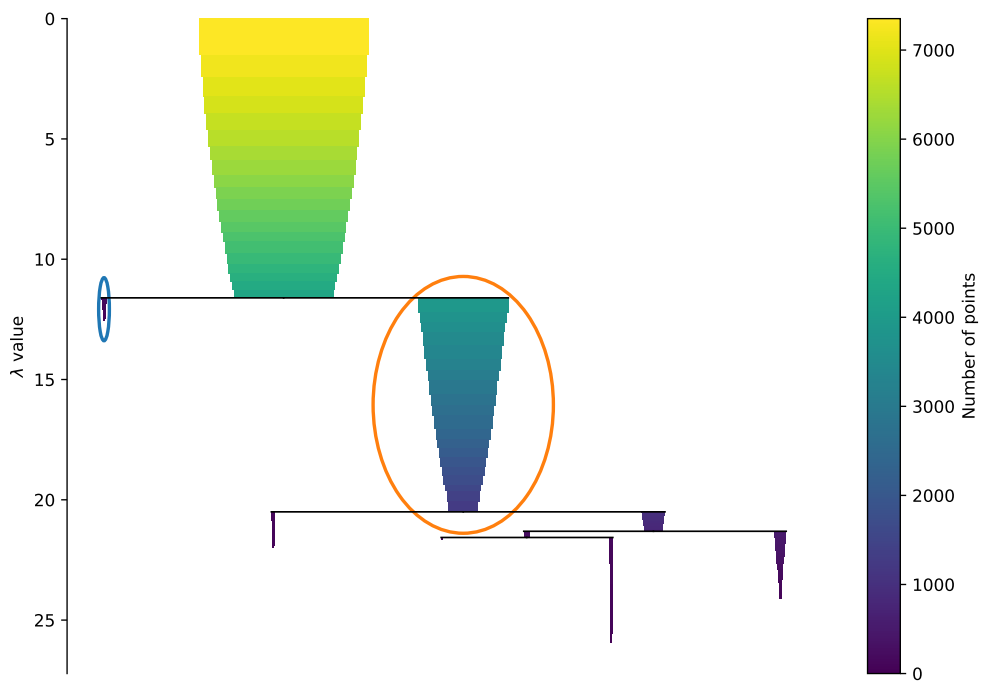


Figure A1. Branches were selected by the HDBSCAN* algorithm.

Table B1: Simbad sources.

| Id Object | RA | Dec | Type | Redshift | Group | P(Blue) | P(Red) |
|---------------------------|-------------|-------------|------------|----------|-------|---------|---------|
| | | | | | | HAC | HDBSCAN |
| CTLGD 9478 | 00:01:59.25 | -29:18:40.4 | Star | — | Blue | 0.98 | 0.02 |
| QSO B2359+005 | 00:02:30.71 | 00:49:59.2 | QSO | 1.354 | Blue | 0.74 | 0.08 |
| [GMB2011] 1808 | 00:02:47.58 | -00:22:23.5 | CIG | 0.351 | — | — | — |
| CTLGD 2037 | 00:05:08.77 | -30:51:04.2 | Star | — | Red | 0.15 | 0.73 |
| SDSS J000637.99-003656.2 | 00:06:37.99 | -00:36:56.2 | QSO | 4.435 | — | — | — |
| LBQS 0004+0036 | 00:07:10.00 | 00:53:29.1 | QSO | 0.316 | Blue | 0.61 | 0.11 |
| SDSS J000809.34+004935.5 | 00:08:09.34 | 00:49:35.3 | QSO | 3.293 | — | — | — |
| 2SLAQ J000918.74-003907.2 | 00:09:18.76 | -00:39:07.0 | Galaxy | — | Blue | 0.71 | 0.07 |
| [VV2006] J001040.1-294428 | 00:10:40.08 | -29:44:27.3 | QSO | 1.361 | Blue | 0.71 | 0.14 |
| CTLGD 7291 | 00:10:48.73 | -29:47:28.8 | Star | — | Red | 0.29 | 0.35 |
| 2QZ J001055.3-304423 | 00:10:55.37 | -30:44:23.5 | Galaxy | 0.307 | Blue | 0.58 | 0.07 |
| [VV2006] J001228.8-310241 | 00:12:28.78 | -31:02:40.0 | QSO | 1.360 | Blue | 0.49 | 0.07 |
| LBQS 0010+0035 | 00:13:27.32 | 00:52:32.2 | Seyfert 1 | 0.363 | Blue | 0.77 | 0.08 |
| [GPM2009] J0014-0044 2 | 00:14:28.79 | -00:44:43.8 | EmG | 0.014 | Blue | 0.15 | 0.06 |
| 2SLAQ J001455.99+001903.5 | 00:14:55.99 | 00:19:03.7 | Star | — | Blue | 0.79 | 0.07 |
| 2SLAQ J001526.52+001813.2 | 00:15:26.52 | 00:18:13.4 | QSO | 1.362 | Blue | 0.51 | 0.09 |
| [VV2006] J001535.5+005355 | 00:15:35.55 | 00:53:56.1 | QSO | 1.358 | Blue | 0.77 | 0.03 |
| SDSS J001628.25+010801.9 | 00:16:28.24 | 01:08:02.0 | Galaxy | 0.010 | Blue | 0.70 | 0.13 |
| [VV2006] J001641.9-312657 | 00:16:41.87 | -31:26:56.6 | QSO | 0.360 | Blue | 0.74 | 0.09 |
| 2SLAQ J001731.27-004859.3 | 00:17:31.26 | -00:48:59.2 | QSO | 1.357 | Blue | 0.76 | 0.11 |
| LEDA 1156 | 00:17:39.97 | 00:30:22.5 | StarburstG | 0.017 | Blue | 0.94 | 0.01 |
| SDSS J001753.82+005057.6 | 00:17:53.82 | 00:50:57.7 | QSO | 1.358 | — | — | — |
| 2SLAQ J001912.39+000319.6 | 00:19:12.39 | 00:03:19.8 | QSO | 1.372 | Blue | 0.75 | 0.07 |
| 2SLAQ J001940.23-005435.9 | 00:19:40.24 | -00:54:35.8 | QSO | 1.374 | Blue | 0.70 | 0.05 |
| [VV2006] J001950.1-004040 | 00:19:50.06 | -00:40:40.7 | QSO | 4.340 | — | — | — |

Table B1: –continued

| Id Object | RA | Dec | Type | Redshift | Group | P(Blue) | P(Red) |
|----------------------------|-------------|-------------|-----------|----------|-------|---------|---------|
| | | | | | | HAC | HDBSCAN |
| 2SLAQ J002237.90+000519.0 | 00:22:37.90 | 00:05:19.2 | QSO | 1.373 | Blue | 0.56 | 0.03 |
| UM 240 | 00:25:07.40 | 00:18:45.2 | EmObj | 0.011 | Blue | 0.74 | 0.12 |
| 2MASX J00251994+0031312 | 00:25:19.92 | 00:31:31.7 | Seyfert 1 | 0.014 | Blue | 0.82 | 0.03 |
| LEDA 3107905 | 00:27:53.84 | -00:58:00.2 | Galaxy | 0.014 | Blue | 0.96 | 0.02 |
| SDSS J002916.79-010021.5 | 00:29:16.81 | -01:00:23.1 | Galaxy | 0.013 | Blue | 1.00 | 0.00 |
| SDSS J002940.01+010528.5 | 00:29:40.02 | 01:05:28.7 | QSO | 1.387 | Blue | 0.55 | 0.05 |
| [VV2010c] J002951.5+004159 | 00:29:51.45 | 00:42:00.0 | AGN | 0.315 | Red | 0.34 | 0.18 |
| SDSS J003117.70+001705.0 | 00:31:17.69 | 00:17:05.1 | QSO | 4.335 | – | – | – |
| 2QZ J003137.5-292815 | 00:31:37.50 | -29:28:15.3 | Unknown | – | Blue | 0.67 | 0.03 |
| 2dFGRS TGS283Z142 | 00:31:50.70 | -28:55:36.7 | Galaxy | 0.013 | Blue | 0.90 | 0.01 |
| 2QZ J003152.5-293534 | 00:31:52.56 | -29:35:33.3 | Galaxy | 0.313 | Blue | 0.86 | 0.07 |
| 2SLAQ J003208.53-005303.7 | 00:32:08.53 | -00:53:03.6 | QSO | 1.344 | Blue | 0.36 | 0.06 |
| SDSS J003234.62-001557.1 | 00:32:34.62 | -00:15:57.1 | QSO | 3.243 | Blue | 0.41 | 0.08 |
| LEDA 559945 | 00:32:34.69 | -42:40:10.4 | Galaxy | – | Blue | 0.70 | 0.04 |
| [VV2006] J003242.7+003111 | 00:32:42.74 | 00:31:11.1 | QSO | 0.360 | Blue | 0.21 | 0.07 |
| 2dFGRS TGS365Z059 | 00:33:54.71 | -29:56:12.7 | Galaxy | 0.006 | Blue | 0.78 | 0.02 |
| SWIRE J003517.14-420518.6 | 00:35:17.11 | -42:05:19.0 | AGN | 0.320 | Red | 0.03 | 0.66 |
| [VV2006] J003545.9+002306 | 00:35:45.86 | 00:23:06.0 | QSO | 3.237 | Blue | 0.82 | 0.02 |
| 2MASS J00362543-0029075 | 00:36:25.39 | -00:29:07.1 | AGN | 0.308 | Red | 0.16 | 0.75 |
| 2dFGRS TGS440Z027 | 00:36:38.44 | -32:34:44.7 | Galaxy | 0.006 | Blue | 0.28 | 0.08 |
| [VV2006] J003714.1-005602 | 00:37:14.11 | -00:56:04.0 | QSO | 4.361 | – | – | – |
| [VV2006] J003722.2-001140 | 00:37:22.17 | -00:11:40.6 | QSO | 1.370 | Blue | 0.70 | 0.04 |
| UM 260 | 00:37:41.13 | 00:33:20.0 | EmObj | 0.014 | Blue | 0.70 | 0.08 |
| SDSS J003859.34-004252.2 | 00:38:59.35 | -00:42:52.0 | QSO | 2.502 | Blue | 0.12 | 0.04 |
| SDSS J003930.30+012021.6 | 00:39:30.28 | 01:20:20.9 | BlueCompG | 0.015 | Blue | 0.31 | 0.06 |
| IRAS 00370+0035 | 00:39:34.78 | 00:51:36.9 | FIR | – | Blue | 0.82 | 0.04 |
| IRAS 00370+0035 | 00:39:34.78 | 00:51:36.9 | FIR | – | Blue | 0.82 | 0.04 |
| 2QZ J004215.6-321257 | 00:42:15.62 | -32:12:57.2 | Galaxy | 0.317 | Blue | 0.91 | 0.03 |
| GALEX 2673249256393934953 | 00:42:43.87 | 01:17:02.2 | QSO | 1.366 | Blue | 0.75 | 0.08 |
| 2dFGRS TGS501Z235 | 00:43:21.88 | -33:19:02.9 | Galaxy | 0.015 | Blue | 0.58 | 0.14 |
| 2SLAQ J004335.13-003729.7 | 00:43:35.16 | -00:37:29.6 | CataclyV* | – | Blue | 0.55 | 0.14 |
| SDSS J004415.83-004303.1 | 00:44:15.81 | -00:43:03.1 | QSO | 3.248 | – | – | – |
| [VV2006] J004544.4-315729 | 00:45:44.35 | -31:57:29.2 | QSO | 1.344 | Blue | 0.78 | 0.09 |
| 2SLAQ J004626.30-011417.0 | 00:46:26.30 | -01:14:16.8 | Galaxy | – | Blue | 0.86 | 0.03 |
| [VV98] J004826.9-341340 | 00:48:26.97 | -34:13:38.7 | QSO | 1.910 | Blue | 0.70 | 0.11 |
| SDSS J004918.52+011308.9 | 00:49:18.52 | 01:13:09.1 | QSO | 1.339 | Blue | 0.59 | 0.09 |
| LEDA 3034 | 00:51:49.42 | 00:33:53.8 | Seyfert 1 | 0.015 | Blue | 0.85 | 0.02 |
| QSO B0049-272 | 00:51:55.64 | -26:57:43.3 | QSO | 2.484 | Blue | 0.21 | 0.05 |
| [BKD2008] WR 353 | 00:51:59.72 | -00:29:20.8 | PartofG | 0.005 | Blue | 0.54 | 0.08 |
| ESO 411-27 | 00:52:51.61 | -27:19:32.8 | Galaxy | 0.006 | Blue | 0.98 | 0.02 |
| SDSS J005343.78+012147.6 | 00:53:43.76 | 01:21:47.5 | QSO | 1.358 | Blue | 0.60 | 0.07 |
| RESOLVE rf554 | 00:54:15.54 | -01:04:56.0 | Galaxy | 0.015 | Blue | 0.97 | 0.03 |
| 2QZ J005440.1-320042 | 00:54:40.12 | -32:00:42.2 | EmG | 0.324 | Blue | 0.56 | 0.04 |
| QSO B0052-307 | 00:54:43.95 | -30:30:54.1 | QSO | 2.450 | Blue | 0.67 | 0.10 |
| [VV2006] J005532.1-311538 | 00:55:32.08 | -31:15:37.8 | QSO | 1.350 | Blue | 0.77 | 0.08 |
| [TYZ2012] II 11 | 00:55:41.32 | -00:56:30.6 | Galaxy | 0.015 | Blue | 0.80 | 0.02 |
| [CT83] 219 | 00:55:51.35 | -30:56:42.8 | UV | – | Blue | 0.58 | 0.07 |
| RGO 8439 | 00:55:53.16 | -28:54:57.3 | Star | – | Blue | 0.99 | 0.01 |
| 2dFGRS TGS502Z028 | 00:55:53.31 | -33:39:01.5 | Galaxy | 0.325 | Blue | 0.70 | 0.14 |
| [VV2006] J005609.9-312209 | 00:56:09.93 | -31:22:08.6 | QSO | 2.460 | Blue | 0.33 | 0.07 |
| [VV2006] J005639.0-315759 | 00:56:39.05 | -31:57:58.6 | QSO | 1.350 | Blue | 1.00 | 0.00 |
| [GPM2009] 0057-0022 | 00:57:12.60 | -00:21:57.7 | Galaxy | 0.010 | Blue | 0.78 | 0.13 |
| [VV2000] J005840.5-300203 | 00:58:40.42 | -30:02:00.1 | QSO | 1.361 | Blue | 0.35 | 0.06 |
| LEDA 3530 | 00:59:04.10 | 01:00:04.2 | GinCl | 0.018 | Blue | 0.97 | 0.03 |
| 2dFGRS TGS503Z245 | 00:59:13.57 | -34:19:15.7 | Galaxy | 0.012 | Blue | 0.97 | 0.03 |
| 2MASX J00593609-3020390 | 00:59:36.09 | -30:20:39.0 | Galaxy | 0.155 | Red | 0.05 | 0.75 |
| LBQS 0057-0135 | 00:59:48.81 | -01:19:05.2 | QSO | 0.325 | Blue | 0.44 | 0.08 |
| QSO B0057-3948 | 00:59:53.21 | -39:31:57.3 | QSO | 3.240 | Blue | 0.85 | 0.05 |

Table B1: –continued

| Id Object | RA | Dec | Type | Redshift | Group | P(Blue) | P(Red) |
|----------------------------|-------------|-------------|-----------|----------|-------|---------|---------|
| | | | | | | HAC | HDBSCAN |
| CAIRNS J005959.59-005157.2 | 00:59:59.58 | -00:51:57.1 | GinCl | 0.166 | Red | 0.00 | 1.00 |
| SCMS 679 | 01:00:04.44 | -33:39:32.5 | Star | — | Blue | 0.53 | 0.05 |
| 2QZ J010009.9-320131 | 01:00:09.94 | -32:01:31.1 | Unknown | — | Blue | 1.00 | 0.00 |
| 2dFGRS TGS561Z059 | 01:00:16.17 | -34:57:40.6 | Galaxy | 0.113 | Blue | 0.52 | 0.06 |
| 2SLAQ J010121.76-000301.7 | 01:01:21.76 | -00:03:01.8 | Galaxy | — | Blue | 0.14 | 0.05 |
| QSO B0059-304B | 01:02:14.65 | -30:07:53.8 | QSO | 3.240 | Blue | 0.88 | 0.01 |
| 2SLAQ J010230.03-003206.8 | 01:02:30.02 | -00:32:06.8 | Seyfert 1 | 0.343 | Blue | 0.50 | 0.08 |
| 2MASX J01023175+0120363 | 01:02:31.78 | 01:20:36.1 | GinCl | 0.016 | Blue | 0.85 | 0.02 |
| [VV2006] J010336.4-005508 | 01:03:36.39 | -00:55:08.8 | QSO | 2.443 | Blue | 0.55 | 0.06 |
| SDSS J010413.86-011552.1 | 01:04:13.86 | -01:15:52.0 | QSO | 1.366 | Blue | 0.96 | 0.04 |
| QSO B0103+00 | 01:06:19.23 | 00:48:23.4 | QSO | 4.435 | Red | 0.03 | 0.04 |
| 6dFGS gJ010653.4-324342 | 01:06:53.44 | -32:43:41.9 | AGN | 0.371 | Blue | 0.64 | 0.03 |
| LIRAS J010658.95+010438.3 | 01:06:58.93 | 01:04:38.2 | AGN | 0.327 | Red | 0.12 | 0.74 |
| [VV2006] J010705.6+000609 | 01:07:05.55 | 00:06:09.0 | QSO | 1.357 | Blue | 0.74 | 0.08 |
| UGC 695 | 01:07:46.47 | 01:03:50.3 | LSB G | 0.002 | Blue | 0.88 | 0.07 |
| SDSS J010748.62+004453.5 | 01:07:48.62 | 00:44:53.7 | BCIG | 0.266 | Red | 0.14 | 0.44 |
| MCG+00-04-011 | 01:09:01.58 | 01:22:41.5 | GinCl | 0.018 | Blue | 0.74 | 0.07 |
| MCG+00-04-011 | 01:09:01.58 | 01:22:41.5 | GinCl | 0.018 | Blue | 0.74 | 0.07 |
| 2SLAQ J010907.59+000649.8 | 01:09:07.59 | 00:06:50.0 | QSO | 1.372 | Blue | 0.55 | 0.07 |
| LEDA 1185205 | 01:09:07.95 | 01:07:15.5 | HII G | 0.004 | Blue | 0.75 | 0.13 |
| SDSS J010918.56+005419.3 | 01:09:18.56 | 00:54:19.4 | QSO | 1.356 | Blue | 0.64 | 0.08 |
| 2SLAQ J010925.95-003739.0 | 01:09:25.96 | -00:37:39.0 | QSO | 1.360 | Blue | 0.69 | 0.04 |
| 2QZ J011014.0-302445 | 01:10:13.97 | -30:24:44.5 | EmG | 0.313 | Blue | 0.60 | 0.05 |
| 2QZ J011119.0-300019 | 01:11:19.02 | -30:00:18.2 | EmG | 0.309 | Blue | 0.83 | 0.05 |
| SDSS J011128.38+000143.7 | 01:11:28.35 | 00:01:43.3 | QSO | 0.765 | Blue | 0.13 | 0.10 |
| 2dFGRS TGS505Z356 | 01:12:12.64 | -33:56:31.1 | Galaxy | 0.333 | Red | 0.43 | 0.13 |
| 2SLAQ J011230.55+001441.5 | 01:12:30.55 | 00:14:41.7 | QSO | 3.259 | Blue | 0.84 | 0.03 |
| PB 6318 | 01:12:58.01 | 00:58:37.0 | Star | — | Blue | 0.65 | 0.04 |
| 2dFGRS TGS447Z027 | 01:13:13.03 | -32:26:09.9 | Galaxy | 0.017 | Blue | 0.86 | 0.05 |
| UGC 772 | 01:13:40.42 | 00:52:39.0 | LSB G | 0.004 | — | — | — |
| 2SLAQ J011402.35-004750.9 | 01:14:02.35 | -00:47:50.8 | Seyfert 1 | 0.350 | Blue | 0.55 | 0.07 |
| [VV2006] J011405.3-310903 | 01:14:05.25 | -31:09:02.8 | QSO | 1.333 | Blue | 0.21 | 0.05 |
| 2dFGRS TGS505Z120 | 01:14:36.11 | -32:38:41.0 | Galaxy | 0.020 | Blue | 0.79 | 0.09 |
| SDSS J011531.90-005144.5 | 01:15:31.89 | -00:51:44.3 | HII G | 0.005 | Blue | 0.89 | 0.06 |
| 2SLAQ J011533.07-005134.9 | 01:15:33.06 | -00:51:34.8 | Galaxy | — | Blue | 0.56 | 0.08 |
| [BKD2008] WR 354 | 01:15:33.79 | -00:51:31.5 | HII G | 0.006 | Blue | 0.22 | 0.07 |
| [BKD2008] WR 354 | 01:15:33.79 | -00:51:31.5 | HII G | 0.006 | Blue | 0.22 | 0.07 |
| 2SLAQ J011542.18+002300.2 | 01:15:42.18 | 00:23:00.4 | QSO | 1.373 | Blue | 0.69 | 0.04 |
| 2dFGRS TGS505Z064 | 01:16:38.40 | -32:55:39.1 | Galaxy | 0.018 | Blue | 0.94 | 0.02 |
| 2dFGRS TGS505Z018 | 01:17:40.21 | -33:04:40.7 | Galaxy | 0.018 | Blue | 0.67 | 0.08 |
| 2dFGRS TGS377Z137 | 01:17:56.44 | -30:26:25.8 | Galaxy | 0.018 | Blue | 0.87 | 0.08 |
| 2dFGRS TGS506Z276 | 01:18:05.71 | -33:03:09.1 | Galaxy | 0.012 | Blue | 0.88 | 0.07 |
| 2SLAQ J011818.13+001455.2 | 01:18:18.12 | 00:14:55.5 | QSO | 1.372 | Blue | 0.62 | 0.03 |
| 2SLAQ J011829.63+004549.4 | 01:18:29.62 | 00:45:49.4 | Seyfert 1 | 0.314 | Blue | 0.67 | 0.14 |
| 2dFGRS TGS506Z243 | 01:18:49.15 | -33:20:13.1 | Galaxy | 0.012 | Blue | 0.83 | 0.07 |
| 2MASX J01195427-3414599 | 01:19:54.23 | -34:15:00.0 | EmG | 0.019 | Blue | 0.99 | 0.01 |
| 2dFGRS TGS506Z158 | 01:20:09.99 | -33:14:10.7 | Galaxy | 0.011 | Blue | 1.00 | 0.00 |
| 2SLAQ J012110.74-005037.2 | 01:21:10.74 | -00:50:37.1 | QSO | 1.352 | Blue | 0.71 | 0.02 |
| [HB93] 0119-341B | 01:21:52.19 | -33:56:15.8 | Star | — | Red | 0.33 | 0.18 |
| SDSS J012213.85+005731.4 | 01:22:13.87 | 00:57:31.6 | HII G | 0.008 | Blue | 1.00 | 0.00 |
| 2dFGRS TGS565Z149 | 01:22:17.09 | -34:02:41.6 | Galaxy | 0.012 | Blue | 0.87 | 0.05 |
| 2SLAQ J012226.76+000327.5 | 01:22:26.75 | 00:03:27.9 | QSO | 2.480 | Blue | 0.86 | 0.04 |
| QSO B0120-002 | 01:23:01.78 | 00:03:23.6 | QSO | 1.356 | Blue | 0.81 | 0.08 |
| 2dFGRS TGS297Z222 | 01:23:50.87 | -29:11:46.4 | Galaxy | 0.000 | Blue | 0.05 | 0.03 |
| MCG+00-04-113 | 01:23:54.75 | 00:16:56.4 | GinCl | 0.018 | Blue | 0.70 | 0.05 |
| SDSS J012356.34+001230.6 | 01:23:56.35 | 00:12:31.0 | Galaxy | — | Blue | 0.99 | 0.01 |
| ESO 352-67 | 01:23:57.47 | -33:48:07.5 | Galaxy | 0.005 | Blue | 0.89 | 0.06 |
| SDSS J012405.73+005905.0 | 01:24:05.73 | 00:59:04.9 | Galaxy | 0.007 | — | — | — |

Table B1: –continued

| Id Object | RA | Dec | Type | Redshift | HAC | P(Blue) | P(Red) |
|----------------------------------|-------------|-------------|-----------|----------|------|---------|---------|
| | | | | | | HDBSCAN | HDBSCAN |
| QSO B0121-324 | 01:24:16.18 | -32:12:21.7 | QSO | 1.358 | Blue | 0.61 | 0.08 |
| 2dFGRS TGS507Z113 | 01:24:30.16 | -33:38:45.5 | Galaxy | 0.305 | Red | 0.45 | 0.39 |
| QSO B0122-3232 | 01:25:04.59 | -32:17:14.6 | QSO | 2.450 | Blue | 0.41 | 0.09 |
| 2QZ J012526.2-304433 | 01:25:26.24 | -30:44:32.8 | EmG | 0.311 | Blue | 0.57 | 0.07 |
| 2QZ J012549.3-280944 | 01:25:49.29 | -28:09:43.6 | Galaxy | 0.324 | – | – | – |
| LEDA 1180903 | 01:26:27.03 | 00:58:51.9 | Galaxy | 0.008 | Blue | 0.98 | 0.02 |
| 2dFGRS TGS566Z338 | 01:26:37.73 | -34:35:13.8 | Galaxy | 0.012 | Blue | 0.89 | 0.02 |
| 6dFGS gJ012646.5-003845 | 01:26:46.51 | -00:38:44.7 | HII G | 0.006 | Blue | 0.54 | 0.08 |
| ESO 413-7 | 01:27:59.31 | -29:05:12.0 | GinCl | 0.005 | Blue | 1.00 | 0.00 |
| 6dFGS gJ012926.6-011159 | 01:29:26.54 | -01:11:59.0 | GinCl | 0.016 | Red | 0.42 | 0.24 |
| SDSS J013034.18-002106.6 | 01:30:34.17 | -00:21:06.5 | QSO | 3.234 | Blue | 0.64 | 0.04 |
| 2dFGRS TGS509Z295 | 01:31:21.84 | -33:06:06.2 | Galaxy | 0.017 | Blue | 0.81 | 0.07 |
| 2dFGRS TGS508Z142 | 01:31:45.65 | -32:56:56.8 | Galaxy | 0.017 | Blue | 0.96 | 0.02 |
| LEDA 679811 | 01:31:47.24 | -33:10:55.1 | Galaxy | – | Blue | 1.00 | 0.00 |
| 2dFGRS TGS509Z242 | 01:32:53.43 | -33:26:42.7 | Galaxy | 0.017 | Blue | 0.62 | 0.12 |
| 2MASS J01330450+0003553 | 01:33:04.52 | 00:03:56.1 | low-mass* | 0.000 | Red | 0.13 | 0.47 |
| 2SLAQ J013400.41-010358.2 | 01:34:00.46 | -01:03:59.2 | Galaxy | – | Blue | 0.99 | 0.01 |
| RESOLVE rf246 | 01:34:52.04 | -00:38:55.2 | Galaxy | 0.017 | Blue | 0.66 | 0.12 |
| [VV2006] J013500.8-004054 | 01:35:00.83 | -00:40:54.2 | QSO | 1.007 | Blue | 0.17 | 0.04 |
| FBQS J0135-0019 | 01:35:17.53 | -00:19:39.0 | Seyfert 1 | 0.312 | Blue | 0.45 | 0.11 |
| 2QZ J013531.1-313651 | 01:35:31.16 | -31:36:51.0 | Galaxy | 0.320 | Blue | 0.46 | 0.07 |
| SDSS J013701.72-012059.3 | 01:37:01.71 | -01:20:59.1 | QSO | 2.496 | Blue | 0.85 | 0.07 |
| [VV2006] J013729.4-320715 | 01:37:29.40 | -32:07:15.7 | QSO | 1.368 | Blue | 0.56 | 0.05 |
| [VV2006] J013837.3+002818 | 01:38:37.28 | 00:28:18.5 | QSO | 1.348 | Blue | 0.82 | 0.08 |
| 2SLAQ J013951.07+002537.9 | 01:39:51.07 | 00:25:38.0 | QSO | 1.342 | Blue | 0.96 | 0.04 |
| 2E 458 | 01:40:17.06 | -00:50:03.0 | Seyfert 1 | 0.334 | Blue | 0.27 | 0.05 |
| SDSS J014125.63+000755.6 | 01:41:25.64 | 00:07:55.8 | QSO | 0.322 | Red | 0.04 | 0.85 |
| [VV2006] J014224.7-320414 | 01:42:24.73 | -32:04:13.7 | QSO | 2.460 | Blue | 0.55 | 0.09 |
| [VV2006] J014303.6-295255 | 01:43:03.49 | -29:52:54.8 | QSO | 2.450 | Blue | 0.45 | 0.07 |
| ESO 353-36 | 01:43:18.29 | -34:12:22.4 | EmG | 0.013 | Red | 0.06 | 0.37 |
| SDSS J014721.12-004505.3 | 01:47:21.12 | -00:45:05.3 | QSO | 1.348 | Red | 0.33 | 0.35 |
| [VV2006] J014739.2-285259 | 01:47:39.21 | -28:52:59.2 | QSO | 0.360 | Blue | 0.75 | 0.05 |
| [VV2006] J014739.2-285259 | 01:47:39.21 | -28:52:59.3 | QSO | 0.360 | Blue | 0.84 | 0.05 |
| SDSS J014806.25-002841.6 | 01:48:06.25 | -00:28:41.6 | Galaxy | 0.215 | Blue | 0.70 | 0.04 |
| [VV2006] J014812.2+000154 | 01:48:12.24 | 00:01:53.5 | QSO | 1.712 | Blue | 0.07 | 0.03 |
| 2QZ J014844.1-275610 | 01:48:44.17 | -27:56:11.0 | Star | – | Blue | 0.73 | 0.07 |
| IC 1734 | 01:49:17.03 | -32:44:33.1 | Galaxy | 0.017 | Blue | 0.59 | 0.06 |
| [VV2006] J014921.5-003220 | 01:49:21.53 | -00:32:20.9 | QSO | 1.379 | Blue | 0.81 | 0.08 |
| [RGD2013] J015239.744+010557.768 | 01:52:39.74 | 01:05:57.9 | Galaxy | 0.331 | Red | 0.15 | 0.63 |
| [RGD2013] J015253.854+011215.480 | 01:52:53.85 | 01:12:15.5 | Galaxy | 0.184 | Red | 0.05 | 0.87 |
| 2QZ J015257.7-284838 | 01:52:57.76 | -28:48:37.8 | Seyfert 1 | 0.326 | Blue | 0.52 | 0.08 |
| 2SLAQ J015331.85+002252.8 | 01:53:31.85 | 00:22:53.0 | QSO | 1.367 | Blue | 0.91 | 0.02 |
| SDSS J015400.48-004509.5 | 01:54:00.50 | -00:45:10.0 | HII G | 0.016 | Blue | 0.66 | 0.04 |
| 2SLAQ J015409.27+002645.2 | 01:54:09.27 | 00:26:45.3 | QSO | 1.355 | Blue | 0.72 | 0.05 |
| [VV2006] J015410.9-285214 | 01:54:10.94 | -28:52:14.6 | QSO | 1.356 | Blue | 0.54 | 0.07 |
| [VV2006] J015415.4-285254 | 01:54:15.48 | -28:52:54.9 | QSO | 1.344 | Blue | 0.61 | 0.07 |
| SDSS J015440.44-000643.9 | 01:54:40.45 | -00:06:43.6 | EmG | 0.019 | Blue | 0.35 | 0.08 |
| 2SLAQ J015526.89+000615.4 | 01:55:26.87 | 00:06:15.8 | Galaxy | 0.016 | Blue | 0.79 | 0.02 |
| 2SLAQ J015529.12-003927.3 | 01:55:29.07 | -00:39:27.1 | Galaxy | – | Blue | 0.70 | 0.07 |
| SDSS J015813.75+010143.5 | 01:58:13.75 | 01:01:43.4 | RRLyr | – | Blue | 0.94 | 0.01 |
| [VV2006] J015832.1-301703 | 01:58:32.15 | -30:17:02.8 | QSO | 1.380 | Blue | 0.76 | 0.09 |
| [VV2006] J015832.1-301703 | 01:58:32.16 | -30:17:02.7 | QSO | 1.380 | Blue | 0.61 | 0.04 |
| [VV2006] J015850.2-300438 | 01:58:50.22 | -30:04:38.1 | QSO | 1.351 | – | – | – |
| [VV2006] J015935.44+000401 | 01:59:35.48 | 00:04:01.5 | QSO | 3.277 | Blue | 0.63 | 0.08 |
| SDSS J020025.40+002916.5 | 02:00:25.40 | 00:29:16.8 | QSO | 0.313 | Red | 0.05 | 0.68 |
| [VV2006] J020055.0-293527 | 02:00:55.02 | -29:35:26.5 | QSO | 1.349 | Blue | 0.64 | 0.05 |
| ESO 414-22 | 02:01:14.49 | -31:43:42.9 | GinGroup | 0.019 | Blue | 0.66 | 0.09 |
| [VV98] J020115.4+003136 | 02:01:15.53 | 00:31:35.1 | QSO | 0.362 | Blue | 0.34 | 0.06 |

Table B1: –continued

| Id Object | RA | Dec | Type | Redshift | Group | P(Blue) | P(Red) |
|-----------------------------|-------------|-------------|-----------|----------|-------|---------|---------|
| | | | | | | HAC | HDBSCAN |
| 2SLAQ J020200.06-000921.2 | 02:02:00.06 | -00:09:21.2 | QSO | 1.359 | Blue | 0.59 | 0.04 |
| [VV96] J020435.5-455923 | 02:04:35.46 | -45:59:24.0 | QSO | 3.240 | Blue | 0.73 | 0.05 |
| LEDA 1193771 | 02:05:00.83 | 01:24:03.7 | Galaxy | – | Blue | 0.59 | 0.06 |
| 2dFGRS TGS514Z164 | 02:07:20.33 | -33:01:54.3 | Galaxy | 0.011 | – | – | – |
| 2SLAQ J020804.48-000023.2 | 02:08:04.49 | -00:00:23.0 | QSO | 1.339 | Blue | 0.53 | 0.04 |
| 2SLAQ J020827.06-005208.1 | 02:08:27.07 | -00:52:07.9 | QSO | 1.341 | Blue | 0.77 | 0.06 |
| SDSS J020921.99-005455.5 | 02:09:22.00 | -00:54:55.4 | QSO | 1.367 | Blue | 0.97 | 0.03 |
| 2dFGRS TGS515Z070 | 02:12:25.05 | -33:04:59.0 | Galaxy | 0.106 | – | – | – |
| 2dFGRS TGS515Z311 | 02:14:24.22 | -33:14:52.0 | Galaxy | 0.012 | Blue | 0.86 | 0.09 |
| 2dFGRS TGS461Z092 | 02:14:47.63 | -32:42:35.2 | Galaxy | 0.012 | Blue | 0.82 | 0.06 |
| 2SLAQ J021529.02-005314.8 | 02:15:29.02 | -00:53:14.9 | QSO | 1.369 | Blue | 0.63 | 0.05 |
| 2dFGRS TGS460Z130 | 02:16:01.62 | -31:36:51.8 | Galaxy | 0.012 | Blue | 0.92 | 0.02 |
| 2dFGRS TGS387Z025 | 02:16:13.75 | -30:50:56.8 | Galaxy | 0.012 | Blue | 1.00 | 0.00 |
| SDSS J021617.19-011046.9 | 02:16:17.19 | -01:10:46.7 | QSO | 3.264 | Blue | 0.96 | 0.01 |
| 2SLAQ J021810.52-010147.4 | 02:18:10.52 | -01:01:47.2 | QSO | 1.353 | Blue | 0.68 | 0.06 |
| V* AX For | 02:19:28.00 | -30:45:46.0 | CataclyV* | – | Blue | 0.45 | 0.07 |
| 2QZ J022112.5-302559 | 02:21:12.54 | -30:25:59.0 | EmG | 0.315 | Blue | 0.80 | 0.08 |
| 2SLAQ J022316.91-010049.7 | 02:23:16.93 | -01:00:49.6 | Galaxy | – | Blue | 0.85 | 0.06 |
| SHOC 120 | 02:24:17.14 | 00:06:26.1 | Seyfert 1 | 0.060 | – | – | – |
| LEDA 667000 | 02:24:52.74 | -34:06:34.3 | Galaxy | – | Blue | 0.78 | 0.06 |
| SDSS J022530.93-005007.0 | 02:25:30.92 | -00:50:07.1 | Galaxy | 0.059 | Blue | 0.61 | 0.07 |
| [BKD2008] WR 346 | 02:26:28.28 | 01:09:37.6 | PartofG | 0.005 | Blue | 1.00 | 0.00 |
| [BKD2008] WR 346 | 02:26:28.28 | 01:09:37.6 | PartofG | 0.005 | Blue | 1.00 | 0.00 |
| LEDA 546974 | 02:26:46.27 | -43:35:29.6 | Galaxy | – | Blue | 0.65 | 0.07 |
| SDSS J022714.48+010536.1 | 02:27:14.47 | 01:05:36.3 | EmG | 0.349 | Blue | 0.66 | 0.07 |
| RESOLVE rf668 | 02:27:19.29 | 01:01:32.2 | Galaxy | 0.015 | Blue | 0.98 | 0.02 |
| [VV2006] J022738.3-313627 | 02:27:38.28 | -31:36:26.4 | QSO | 1.350 | Blue | 0.46 | 0.06 |
| [VV2006] J022758.2+000226 | 02:27:58.20 | 00:02:25.6 | QSO | 1.066 | – | – | – |
| LCRS B022613.7-392927 | 02:28:14.52 | -39:16:04.0 | Galaxy | – | Blue | 0.68 | 0.05 |
| [BKD2008] WR 315 | 02:28:28.73 | -01:08:58.6 | PartofG | 0.005 | Blue | 0.91 | 0.01 |
| 2SLAQ J022945.34+000856.2 | 02:29:45.34 | 00:08:56.4 | Star | – | Blue | 0.54 | 0.09 |
| 2QZ J022954.6-303558 | 02:29:54.69 | -30:35:58.4 | Seyfert 1 | 0.372 | Blue | 0.34 | 0.06 |
| Pul -3 180355 | 02:29:57.00 | -01:00:32.3 | Star | – | Red | 0.04 | 0.06 |
| 2dFGRS TGS463Z130 | 02:30:09.77 | -31:36:18.2 | Galaxy | 0.015 | Blue | 1.00 | 0.00 |
| SDSS J023020.93+001355.5 | 02:30:20.93 | 00:13:55.8 | Seyfert 1 | 0.335 | Blue | 0.20 | 0.06 |
| UGC 2009 | 02:32:09.34 | -01:23:10.3 | Galaxy | 0.015 | Red | 0.03 | 0.88 |
| 2dFGRS TGS518Z089 | 02:32:18.08 | -33:50:43.0 | Galaxy | 0.016 | Blue | 0.59 | 0.14 |
| SDSS J023230.63-011654.5 | 02:32:30.63 | -01:16:54.5 | QSO | 1.364 | Blue | 0.61 | 0.05 |
| 6dFGS gJ023241.8-391744 | 02:32:41.88 | -39:17:42.8 | Galaxy | 0.005 | Blue | 0.51 | 0.08 |
| SDSS J023248.71+005138.8 | 02:32:48.71 | 00:51:38.8 | Galaxy | 0.344 | Blue | 0.57 | 0.06 |
| V* HP Cet | 02:33:22.62 | 00:50:59.4 | Nova | -0.000 | Blue | 0.54 | 0.09 |
| NGC 986 | 02:33:34.29 | -39:02:40.9 | EmG | 0.007 | Blue | 0.93 | 0.07 |
| [VV2006] J023335.4-010744 | 02:33:35.37 | -01:07:44.6 | QSO | 0.367 | Blue | 0.50 | 0.06 |
| SDSS J023628.77-005829.7 | 02:36:28.75 | -00:58:30.0 | Galaxy | 0.008 | Blue | 0.78 | 0.08 |
| [VV2006] J023635.7-003203 | 02:36:35.69 | -00:32:03.4 | QSO | 1.362 | – | – | – |
| SDSS J024059.15+004545.8 | 02:40:59.14 | 00:45:45.9 | QSO | 3.233 | Blue | 0.99 | 0.01 |
| [VV2006] J024235.0-010351 | 02:42:34.91 | -01:03:51.9 | QSO | 1.373 | Blue | 0.56 | 0.03 |
| [EKS96] NGC 1068 91 | 02:42:46.94 | 00:01:26.2 | HII | – | Blue | 0.14 | 0.06 |
| [ZBF2015] NGC1073 1 | 02:43:35.61 | 01:22:37.9 | HII | – | Blue | 0.27 | 0.06 |
| [ZBF2015] NGC1073 16 | 02:43:37.69 | 01:22:22.5 | HII | – | Blue | 0.94 | 0.06 |
| [ZBF2015] NGC1073 21 | 02:43:42.74 | 01:21:34.4 | HII | – | Blue | 0.50 | 0.07 |
| [ZBF2015] NGC1073 10 | 02:43:44.03 | 01:22:40.5 | HII | – | Blue | 0.80 | 0.05 |
| 6dFGS gJ024605.3-330500 | 02:46:05.28 | -33:04:59.4 | Galaxy | 0.017 | Blue | 0.83 | 0.01 |
| 2MASS J02462415-0029539 | 02:46:24.14 | -00:29:52.9 | Star | – | Blue | 0.76 | 0.03 |
| Gaia DR2 249776434864940160 | 02:46:24.75 | -00:30:16.3 | QSO | – | Blue | 0.53 | 0.07 |
| [BKD2008] WR 316 | 02:46:25.42 | -00:30:09.8 | PartofG | 0.005 | Blue | 0.57 | 0.04 |
| 2SLAQ J024626.59-003000.2 | 02:46:26.57 | -00:30:00.4 | Star | – | Blue | 1.00 | 0.00 |
| 2SLAQ J025100.64+001707.2 | 02:51:00.64 | 00:17:07.3 | QSO | 2.466 | Blue | 0.70 | 0.07 |

Table B1: –continued

| Id Object | RA | Dec | Type | Redshift | Group HAC | P(Blue) | P(Red) |
|----------------------------------|-------------|-------------|---------------|----------|--------------|---------|---------|
| | | | | | | HDBSCAN | HDBSCAN |
| 2SLAQ J025216.75+001741.2 | 02:52:16.73 | 00:17:41.2 | Galaxy | 0.005 | Blue | 0.89 | 0.06 |
| 2SLAQ J025252.02-002211.7 | 02:52:52.00 | -00:22:11.6 | QSO | 1.370 | Blue | 0.85 | 0.05 |
| SHOC 143 | 02:54:26.13 | -00:41:22.7 | Seyfert 1 | 0.015 | Blue | 0.88 | 0.08 |
| NVSS J025557+004132 | 02:55:57.24 | 00:41:33.5 | RadioG | 0.014 | Red | 0.12 | 0.32 |
| QSO B0253+0058 | 02:56:07.25 | 01:10:38.8 | QSO | 1.349 | Blue | 0.66 | 0.08 |
| HBQS 0253+0022 | 02:56:25.32 | 00:34:29.4 | HII | 0.013 | Blue | 0.99 | 0.01 |
| LEDA 1170514 | 02:56:28.43 | 00:36:28.2 | Galaxy | 0.009 | Blue | 0.64 | 0.05 |
| 2dFGRS TGS522Z138 | 02:57:45.54 | -33:28:55.5 | Galaxy | 0.335 | Red | 0.43 | 0.28 |
| 2MASSI J0259103-002239 | 02:59:10.38 | -00:22:39.8 | Seyfert 1 | 0.360 | Blue | 0.54 | 0.09 |
| 2SLAQ J030309.82+001337.5 | 03:03:09.83 | 00:13:37.8 | Galaxy | – | – | – | – |
| UGC 2517 | 03:04:12.47 | -01:11:33.8 | Galaxy | 0.013 | Red | 0.53 | 0.20 |
| 2SLAQ J030417.77-004931.7 | 03:04:17.77 | -00:49:31.5 | Galaxy | – | Blue | 0.62 | 0.11 |
| LEDA 1142424 | 03:04:34.76 | -00:28:30.7 | Seyfert 1 | 0.006 | Blue | 0.98 | 0.02 |
| LBQS 0302-0019 | 03:04:49.85 | -00:08:13.4 | QSO | 3.295 | Blue | 0.95 | 0.02 |
| 2MASS J03045799+0057131 | 03:04:57.98 | 00:57:14.0 | Blue | 0.012 | Blue | 0.99 | 0.01 |
| MCG+00-08-089 | 03:05:18.24 | -00:09:34.1 | Galaxy | 0.009 | Blue | 0.72 | 0.04 |
| LBQS 0303+0110 | 03:06:12.72 | 01:21:57.3 | QSO | 1.335 | Blue | 0.70 | 0.07 |
| WISE J030629.21-335332.3 | 03:06:29.22 | -33:53:32.3 | AGN | 0.780 | Blue | 0.67 | 0.11 |
| SDSS J030630.33-000622.9 | 03:06:30.33 | -00:06:22.9 | Galaxy | 0.106 | Red | 0.12 | 0.72 |
| SDSS J030715.63+004352.1 | 03:07:15.60 | 00:43:52.6 | Galaxy | 0.010 | Blue | 1.00 | 0.00 |
| 2SLAQ J030757.55+000712.0 | 03:07:57.55 | 00:07:12.1 | QSO | 1.343 | Blue | 0.74 | 0.04 |
| 2SLAQ J031129.69-001701.4 | 03:11:29.70 | -00:17:01.5 | QSO | 1.357 | Blue | 0.72 | 0.05 |
| 2QZ J031130.9-315250 | 03:11:30.92 | -31:52:51.1 | WD* | – | Blue | 0.58 | 0.13 |
| ESO 417-20 | 03:12:48.61 | -31:29:10.7 | GinGroup | 0.013 | Blue | 0.96 | 0.03 |
| SDSS J031258.36-000453.6 | 03:12:58.36 | -00:04:53.6 | | 0.117 | Blue | 0.76 | 0.02 |
| 2dFGRS TGS398Z109 | 03:13:56.08 | -31:28:12.6 | Galaxy | 0.014 | Blue | 0.32 | 0.09 |
| 2SLAQ J031428.25+004506.6 | 03:14:28.25 | 00:45:07.0 | Galaxy | – | Blue | 1.00 | 0.00 |
| 2dFGRS TGS471Z114 | 03:16:15.31 | -31:12:33.3 | Galaxy | 0.004 | Blue | 0.81 | 0.04 |
| 2SLAQ J031618.00-003025.2 | 03:16:18.01 | -00:30:24.9 | Galaxy | – | Blue | 1.00 | 0.00 |
| 2dFGRS TGS524Z054 | 03:16:50.65 | -33:18:03.8 | Galaxy | 0.006 | Blue | 0.94 | 0.02 |
| 2dFGRS TGS524Z054 | 03:16:50.66 | -33:18:04.0 | Galaxy | 0.006 | Blue | 0.96 | 0.04 |
| 2SLAQ J031829.06-000040.3 | 03:18:29.06 | -00:00:40.5 | Galaxy | – | Blue | 0.65 | 0.04 |
| [VV2006] J031845.2-001844 | 03:18:45.17 | -00:18:45.3 | QSO | 3.224 | Blue | 0.97 | 0.03 |
| 2SLAQ J031937.30-002641.1 | 03:19:37.29 | -00:26:41.0 | QSO | 1.371 | Blue | 0.37 | 0.08 |
| SDSS J032244.90+004442.4 | 03:22:44.90 | 00:44:42.3 | QSO Candidate | 0.304 | Blue | 0.94 | 0.03 |
| 6dFGS gJ032504.2-365540 | 03:25:04.15 | -36:55:39.9 | | 0.006 | Blue | 0.64 | 0.08 |
| 6dFGS gJ032512.9-362210 | 03:25:13.07 | -36:22:09.7 | Galaxy | 0.004 | Blue | 0.75 | 0.12 |
| [JPB2015] 051.4803133-32.8829964 | 03:25:55.27 | -32:52:58.9 | GICl | – | Blue | 0.83 | 0.08 |
| SDSS J033226.29-011126.2 | 03:32:26.29 | -01:11:26.0 | QSO | 1.361 | Blue | 0.52 | 0.07 |
| SDSS J033226.29-011126.2 | 03:32:26.30 | -01:11:26.3 | QSO | 1.361 | Blue | 0.53 | 0.05 |
| SDSS J033310.10+000849.1 | 03:33:10.08 | 00:08:49.2 | Seyfert 2 | 0.327 | Red | 0.13 | 0.37 |
| [VV2006] J033458.5-000744 | 03:34:58.48 | -00:07:43.9 | | 1.357 | Blue | 0.77 | 0.02 |
| [VV2006] J033821.6+003106 | 03:38:21.51 | 00:31:06.6 | QSO | 1.349 | Blue | 0.64 | 0.04 |
| 2XMM J033841.3-353134 | 03:38:41.36 | -35:31:34.4 | BLLac | 0.360 | Blue | 0.26 | 0.06 |
| 2XMM J033841.3-353134 | 03:38:41.37 | -35:31:34.2 | BLLac | 0.360 | Blue | 0.25 | 0.05 |
| [VV2006] J033927.5-344707 | 03:39:27.45 | -34:37:07.0 | QSO | 1.364 | Blue | 0.55 | 0.04 |
| CXO J034012.4-353740 | 03:40:12.39 | -35:37:40.1 | HMXB | – | Blue | 0.18 | 0.05 |
| SDSS J034019.89+010330.7 | 03:40:19.89 | 01:03:30.7 | EmG | 0.322 | Blue | 0.72 | 0.11 |
| [VV2006] J034023.0-351606 | 03:40:22.99 | -35:16:07.0 | QSO | 1.372 | Blue | 0.55 | 0.08 |
| 2XMM J034050.4-352620 | 03:40:50.48 | -35:26:21.7 | AGN | 1.366 | Blue | 0.59 | 0.08 |
| ESO 358-51 | 03:41:32.55 | -34:53:19.0 | GinGroup | 0.006 | Blue | 0.88 | 0.07 |
| 2MASS J03424773+0109331 | 03:42:47.72 | 01:09:33.0 | | 0.360 | Blue | 0.16 | 0.07 |
| 2SLAQ J034304.64+002512.1 | 03:43:04.65 | 00:25:12.3 | Star | – | Blue | 0.43 | 0.09 |
| LCRS B034214.4-381736 | 03:44:04.68 | -38:08:11.9 | Galaxy | – | Red | 0.00 | 1.00 |
| [VV2006] J034408.3-003106 | 03:44:08.25 | -00:31:05.8 | QSO | 1.646 | Blue | 0.93 | 0.03 |
| SDSS J034427.73-002740.4 | 03:44:27.73 | -00:27:40.2 | Galaxy | 0.041 | Red | 0.53 | 0.25 |
| SDSS J034517.02-001549.8 | 03:45:17.01 | -00:15:49.7 | QSO | 1.335 | Blue | 1.00 | 0.00 |
| 6dFGS gJ034545.4-362046 | 03:45:45.38 | -36:20:46.1 | GinCl | 0.004 | Blue | 0.84 | 0.02 |

Table B1: –continued

| Id Object | RA | Dec | Type | Redshift | Group | P(Blue) | P(Red) |
|------------------------------|-------------|-------------|------------------|----------|-------|---------|---------|
| | | | | | | HAC | HDBSCAN |
| SDSS J034602.53-000058.7 | 03:46:02.53 | -00:00:58.6 | Seyfert 2 | 0.308 | Red | 0.18 | 0.50 |
| 2MASX J03472195-3251054 | 03:47:21.94 | -32:51:05.2 | GinCl | 0.116 | Red | 0.29 | 0.56 |
| SDSS J034907.92+010943.3 | 03:49:07.93 | 01:09:43.2 | LSB G | 0.014 | Blue | 0.96 | 0.04 |
| MCG+00-10-021 | 03:49:08.87 | 01:09:46.3 | LSB G | 0.014 | Blue | 0.85 | 0.05 |
| FASTT 83 | 03:51:19.36 | 00:32:16.6 | EB* | – | Red | 0.12 | 0.54 |
| LEDA 607287 | 03:55:02.55 | -38:35:40.2 | Galaxy | – | Red | 0.17 | 0.75 |
| Gaia DR2 4857261601188886016 | 03:55:16.01 | -37:29:44.7 | Candidate WD* | – | – | – | – |
| [ZJM2003] SA 95-2230 | 03:55:38.45 | 00:28:34.9 | Star | – | Blue | 0.98 | 0.02 |
| 2dFGRS TGS817Z154 | 03:56:05.58 | -49:28:40.7 | Galaxy | 0.003 | Blue | 0.98 | 0.01 |
| SDSSCGB 74387.1 | 03:56:50.79 | -00:14:34.9 | Galaxy | – | Red | 0.37 | 0.27 |
| 2dFGRS TGS848Z501 | 03:57:22.10 | -37:01:54.1 | Galaxy | 0.016 | Blue | 0.97 | 0.03 |
| 6dFGS gJ035732.5-000047 | 03:57:32.27 | -00:00:47.6 | Galaxy | 0.017 | Blue | 0.69 | 0.06 |
| UGC 2913 | 03:59:03.91 | 01:21:33.6 | Galaxy | 0.013 | Blue | 0.55 | 0.09 |
| UGC 2913 | 03:59:03.91 | 01:21:33.6 | Galaxy | 0.013 | Blue | 0.55 | 0.09 |
| ESO 201-14 | 04:00:29.38 | -49:01:48.4 | EmG | 0.004 | Blue | 0.78 | 0.05 |
| 2MASS J04004608-3424277 | 04:00:46.07 | -34:24:27.7 | AGN Candidate | – | Blue | 0.53 | 0.11 |
| 6dFGS gJ040053.2-351416 | 04:00:53.13 | -35:14:16.2 | Galaxy | 0.015 | Blue | 0.80 | 0.04 |
| QSO B0401-3505 | 04:03:10.56 | -34:56:56.8 | QSO | 3.251 | Blue | 0.67 | 0.04 |
| LCRS B040209.0-382209 | 04:03:56.75 | -38:13:58.5 | Galaxy | – | Blue | 0.54 | 0.14 |
| 6dFGS gJ040441.2-345756 | 04:04:41.14 | -34:57:55.8 | Galaxy | 0.008 | Blue | 0.80 | 0.07 |
| 6dFGS gJ040520.4-364859 | 04:05:20.40 | -36:48:59.0 | Galaxy | 0.003 | Blue | 0.39 | 0.11 |
| 6dFGS gJ040520.4-364859 | 04:05:20.40 | -36:48:58.8 | Galaxy | 0.003 | Blue | 0.40 | 0.12 |
| Gaia DR2 4845009910624639232 | 04:05:27.97 | -38:11:22.1 | Star | – | Blue | 0.99 | 0.01 |
| [VV96] J041130.5-335331 | 04:11:30.51 | -33:53:31.1 | QSO | 1.350 | Blue | 0.76 | 0.04 |
| 2dFGRS TGS894Z351 | 04:11:58.37 | -37:58:44.0 | Galaxy | 0.013 | Blue | 0.96 | 0.04 |
| ESO 420-11 | 04:12:53.30 | -31:18:30.2 | GinGroup | 0.005 | Blue | 0.97 | 0.03 |
| 2dFGRS TGS894Z291 | 04:13:00.00 | -38:19:42.5 | Galaxy | 0.012 | Blue | 0.98 | 0.02 |
| Gaia DR2 4872129059981617536 | 04:20:06.78 | -32:51:20.0 | Candidate WD* | – | – | – | – |
| LEDA 685147 | 04:20:56.84 | -32:50:42.8 | Galaxy | – | – | – | – |
| 2MASX J04255940-4316225 | 04:25:59.40 | -43:16:22.6 | Galaxy | 0.078 | Blue | 0.98 | 0.02 |
| LEDA 579779 | 04:26:32.58 | -41:01:56.6 | Galaxy | – | Blue | 1.00 | 0.00 |
| LEDA 125483 | 04:26:44.34 | -42:15:41.2 | Galaxy | 0.015 | Blue | 1.00 | 0.00 |
| LEDA 568379 | 04:26:44.87 | -42:05:40.5 | Galaxy | – | Blue | 0.98 | 0.01 |
| LEDA 554934 | 04:26:44.91 | -42:58:38.4 | Galaxy | – | Blue | 0.90 | 0.03 |
| MCG-07-10-009 | 04:27:42.24 | -42:38:20.4 | Galaxy | 0.016 | Blue | 0.83 | 0.06 |
| 2MASX J04282877-4314283 | 04:28:28.71 | -43:14:29.1 | Galaxy | 0.015 | Blue | 0.70 | 0.04 |
| 6dFGS gJ043139.6-301514 | 04:31:39.57 | -30:15:14.1 | CataclyV* | -0.000 | Blue | 0.27 | 0.08 |
| LEDA 697927 | 04:32:44.32 | -32:01:20.1 | Galaxy | – | Red | 0.10 | 0.85 |
| ESO 251-12 | 04:33:09.79 | -43:46:13.6 | Galaxy | 0.010 | Blue | 0.82 | 0.05 |
| ESO 304-2 | 04:35:19.80 | -42:12:11.8 | Galaxy | 0.007 | Blue | 1.00 | 0.00 |
| LEDA 494343 | 04:35:41.79 | -47:52:43.9 | Galaxy | – | Blue | 0.89 | 0.05 |
| [HM2015b] 236 3 | 04:37:11.17 | -46:41:06.8 | Galaxy | – | Blue | 0.38 | 0.06 |
| LEDA 692923 | 04:37:18.21 | -32:22:10.3 | Galaxy | – | Blue | 1.00 | 0.00 |
| Gaia DR2 4790561549357871744 | 04:37:35.04 | -44:20:28.8 | Candidate RR Lyr | – | Blue | 0.99 | 0.01 |
| LEDA 681270 | 04:38:23.53 | -33:05:08.6 | Galaxy | – | Blue | 0.83 | 0.02 |
| 6dFGS gJ043927.4-425912 | 04:39:27.45 | -42:59:11.8 | Galaxy | 0.362 | Blue | 0.41 | 0.06 |
| LEDA 606705 | 04:45:44.98 | -38:38:48.7 | Galaxy | – | Blue | 1.00 | 0.00 |
| LEDA 88363 | 04:48:23.05 | -44:52:57.7 | Galaxy | – | Blue | 0.97 | 0.03 |
| 2dFGRS TGS880Z325 | 04:50:02.35 | -47:28:39.0 | Galaxy | 0.010 | Blue | 0.68 | 0.10 |
| LEDA 512705 | 04:51:48.86 | -46:37:36.8 | Galaxy | – | Blue | 1.00 | 0.00 |
| Gaia DR2 4811451372635865984 | 04:52:31.12 | -44:11:04.3 | Star | – | Blue | 0.48 | 0.11 |
| LEDA 686311 | 04:53:19.46 | -32:46:32.8 | Galaxy | – | Blue | 0.85 | 0.04 |
| [VV98] J045444.5-481300 | 04:54:43.04 | -48:13:20.2 | Seyfert 1 | 0.363 | Blue | 0.68 | 0.06 |
| SN 2012at | 04:54:52.74 | -37:19:15.5 | SN | – | Blue | 0.56 | 0.13 |
| 2MASX J04550020-3715351 | 04:55:00.19 | -37:15:35.4 | GinPair | 0.008 | Blue | 0.88 | 0.05 |
| LEDA 715392 | 04:55:26.51 | -30:35:28.6 | Galaxy | – | Blue | 0.20 | 0.07 |
| ESO 499-24 | 09:57:01.69 | -26:29:28.5 | Galaxy | 0.015 | Blue | 0.89 | 0.03 |
| LEDA 859547 | 09:57:06.62 | -19:07:06.1 | Galaxy | – | Blue | 0.84 | 0.08 |

Table B1: –continued

| Id Object | RA | Dec | Type | Redshift | Group | P(Blue) | P(Red) |
|------------------------------|-------------|-------------|---------------|----------|-------|---------|---------|
| | | | | | HAC | HDBSCAN | HDBSCAN |
| LEDA 1022680 | 09:57:23.46 | -07:12:51.4 | Galaxy | – | Blue | 0.18 | 0.06 |
| 2MASX J09583711-4704597 | 09:58:37.10 | -47:05:00.4 | Galaxy | 0.012 | Blue | 0.63 | 0.07 |
| [CMI2006b] H42-f02-1939 | 09:59:46.82 | -19:28:00.0 | Galaxy | 0.265 | Blue | 0.99 | 0.01 |
| CRTS J095950.7-383024 | 09:59:50.88 | -38:30:22.9 | RRLyr | – | Blue | 0.97 | 0.03 |
| LEDA 605183 | 10:00:05.44 | -38:47:28.7 | Galaxy | – | Blue | 0.57 | 0.08 |
| NGC 3095 | 10:00:05.83 | -31:33:10.8 | GinGroup | 0.009 | Red | 0.08 | 0.49 |
| LEDA 154528 | 10:00:49.12 | -30:32:41.9 | Galaxy | – | Blue | 0.75 | 0.07 |
| SDSS J100059.08+032751.4 | 10:00:59.07 | 03:27:51.5 | Galaxy | 0.007 | Blue | 0.74 | 0.08 |
| ESO 567-3 | 10:01:09.07 | -19:26:29.7 | LSB G | 0.012 | Blue | 0.99 | 0.01 |
| LEDA 1011555 | 10:01:34.08 | -07:52:55.7 | Galaxy | – | Blue | 0.90 | 0.08 |
| Gaia DR2 5670829935783719936 | 10:02:11.73 | -19:25:37.1 | Star | – | Blue | 0.32 | 0.06 |
| 2QZ J100215.7-001056 | 10:02:15.83 | -00:10:55.8 | QSO | 0.353 | Blue | 0.63 | 0.09 |
| VVDS 100108471 | 10:02:25.38 | 01:19:36.8 | Galaxy | 0.123 | Blue | 1.00 | 0.00 |
| ESO 262-15 | 10:02:38.71 | -45:29:53.9 | GinGroup | 0.012 | Red | 0.17 | 0.48 |
| [BCP93] F2 H6 | 10:02:51.82 | -26:09:23.9 | HII | – | Blue | 1.00 | 0.00 |
| [EBU2007] 7 | 10:02:54.69 | -26:08:59.6 | BlueSG* | 0.001 | Blue | 0.24 | 0.09 |
| [H69] NGC 3109 12 | 10:02:56.31 | -26:08:58.5 | HII | – | Blue | 0.26 | 0.09 |
| [PRS2007] HII 44 | 10:02:59.47 | -26:08:46.4 | HII | – | Blue | 0.43 | 0.11 |
| [PRS2007] HII 44 | 10:02:59.48 | -26:08:46.4 | HII | – | Blue | 0.48 | 0.10 |
| PSO J150.7588-26.1494 | 10:03:02.10 | -26:08:58.7 | AGN Candidate | – | Blue | 0.67 | 0.08 |
| 2MASX J10030450-1949377 | 10:03:04.51 | -19:49:38.1 | Galaxy | 0.012 | Blue | 0.84 | 0.04 |
| 2dFGRS TGN094Z280 | 10:03:15.05 | -05:54:32.8 | Galaxy | 0.013 | Blue | 0.96 | 0.04 |
| [EBU2007] 3 | 10:03:17.64 | -26:10:01.7 | BlueSG* | 0.001 | Blue | 0.26 | 0.08 |
| [VV96] J100342.1-150808 | 10:03:41.93 | -15:08:08.9 | QSO | 0.342 | Blue | 0.43 | 0.07 |
| 2MASX J10035230-3124480 | 10:03:52.32 | -31:24:48.5 | Galaxy | 0.009 | Blue | 0.99 | 0.01 |
| 2MASX J10041992-4425311 | 10:04:19.86 | -44:25:32.6 | Galaxy | 0.012 | Blue | 0.90 | 0.07 |
| 2MASX J10050765-1951299 | 10:05:07.68 | -19:51:30.2 | Galaxy | – | Blue | 0.64 | 0.06 |
| 2dFGRS TGN421Z115 | 10:05:17.31 | 01:38:21.7 | Galaxy | 0.004 | Blue | 0.88 | 0.05 |
| 2MFGC 7816 | 10:05:28.51 | -38:07:30.1 | Galaxy | – | Blue | 1.00 | 0.00 |
| [VV2006] J100539.9+040914 | 10:05:39.88 | 04:09:14.7 | QSO | 1.355 | Blue | 0.59 | 0.07 |
| CRTS J100548.9-254146 | 10:05:48.99 | -25:41:47.1 | RRLyr | – | Blue | 0.99 | 0.01 |
| 2MASX J10061715-0634276 | 10:06:17.20 | -06:34:27.7 | Galaxy | 0.011 | Blue | 0.95 | 0.05 |
| 6dFGS gJ100622.2-264958 | 10:06:22.20 | -26:49:57.2 | Galaxy | 0.015 | Blue | 0.99 | 0.01 |
| 6dFGS gJ100631.4-320236 | 10:06:31.39 | -32:02:35.9 | GinGroup | 0.008 | Red | 0.42 | 0.24 |
| NGC 3125 | 10:06:33.37 | -29:56:07.8 | HII G | 0.004 | Blue | 0.53 | 0.10 |
| 1RXH J100633.9-295612 | 10:06:33.90 | -29:56:11.6 | X | – | Blue | 0.73 | 0.07 |
| 2MASX J10071106-1904039 | 10:07:11.07 | -19:04:04.6 | Galaxy | 0.012 | Blue | 0.87 | 0.05 |
| LEDA 699275 | 10:07:27.24 | -31:55:26.9 | Galaxy | – | Blue | 0.94 | 0.06 |
| CRTS J100733.7-301921 | 10:07:33.84 | -30:19:19.4 | EB* | – | Blue | 0.80 | 0.03 |
| RX J1007.5-2017 | 10:07:34.65 | -20:17:32.4 | CataclyV* | – | Blue | 0.48 | 0.11 |
| RX J1007.5-2017 | 10:07:34.66 | -20:17:32.5 | CataclyV* | – | Blue | 0.18 | 0.08 |
| 2MASX J10081071-3331017 | 10:08:10.76 | -33:31:02.2 | Galaxy | 0.010 | Red | 0.54 | 0.20 |
| 2MASX J10082199-1448362 | 10:08:22.01 | -14:48:36.1 | Galaxy | 0.008 | Blue | 0.75 | 0.06 |
| LEDA 768685 | 10:08:30.09 | -26:21:33.0 | Galaxy | – | Blue | 0.97 | 0.03 |
| 2MASX J10091380-4300089 | 10:09:13.81 | -43:00:09.0 | GinGroup | 0.015 | Red | 0.21 | 0.33 |
| LEDA 648630 | 10:09:50.26 | -35:27:43.3 | Galaxy | – | Blue | 0.97 | 0.03 |
| LEDA 3094360 | 10:09:58.73 | -20:30:59.5 | Galaxy | – | Blue | 0.84 | 0.06 |
| ESO 435-50 | 10:10:50.41 | -30:25:24.4 | Galaxy | 0.009 | Blue | 0.73 | 0.06 |
| LEDA 654529 | 10:10:51.81 | -35:00:28.1 | Galaxy | – | Blue | 1.00 | 0.00 |
| NGC 3146 | 10:11:09.90 | -20:52:14.0 | EmG | 0.013 | Blue | 0.75 | 0.06 |
| LEDA 729120 | 10:11:13.49 | -29:27:27.9 | Galaxy | – | Blue | 0.65 | 0.13 |
| CRTS J101200.8-365725 | 10:12:00.81 | -36:57:25.2 | EB* | – | Red | 0.32 | 0.28 |
| LEDA 691325 | 10:12:03.36 | -32:28:06.8 | Galaxy | – | Blue | 1.00 | 0.00 |
| Gaia DR2 5407412036686860672 | 10:12:47.58 | -47:33:51.1 | Star | – | Blue | 0.63 | 0.10 |
| LEDA 655538 | 10:12:59.65 | -34:56:06.6 | Galaxy | – | Blue | 0.99 | 0.01 |
| 2MASX J10134201-3451194 | 10:13:41.91 | -34:51:18.3 | EmG | 0.015 | Blue | 0.72 | 0.08 |
| LEDA 658182 | 10:13:54.08 | -34:44:23.0 | Galaxy | – | Blue | 0.85 | 0.04 |
| LEDA 713928 | 10:14:25.56 | -30:42:30.1 | Galaxy | – | Blue | 0.67 | 0.03 |

Table B1: –continued

| Id Object | RA | Dec | Type | Redshift | Group | P(Blue) | P(Red) |
|-------------------------------|-------------|-------------|---------------|----------|-------|---------|---------|
| | | | | | | HAC | HDBSCAN |
| 2MASX J10142679-2329036 | 10:14:26.81 | -23:29:04.9 | Galaxy | 0.012 | Blue | 0.99 | 0.01 |
| ESO 263-21 | 10:14:41.74 | -44:51:14.1 | EmG | 0.004 | Blue | 0.80 | 0.03 |
| IC 2559 | 10:14:45.36 | -34:03:33.0 | EmG | 0.010 | Red | 0.29 | 0.36 |
| ESO 263-22 | 10:14:48.13 | -43:31:49.5 | Galaxy | 0.010 | Blue | 0.69 | 0.06 |
| ESO 263-23 | 10:14:57.32 | -43:37:09.2 | Galaxy | 0.010 | Red | 0.35 | 0.23 |
| ESO 567-32 | 10:15:44.54 | -20:17:44.0 | EmG | 0.012 | Red | 0.06 | 0.34 |
| Gaia DR2 5407327747940309248 | 10:15:58.31 | -47:58:09.1 | Star | – | Blue | 0.32 | 0.08 |
| IC 2560 | 10:16:18.68 | -33:33:49.8 | Seyfert 2 | 0.010 | Red | 0.33 | 0.28 |
| ESO 567-39 | 10:17:13.15 | -21:04:00.3 | EmG | 0.012 | Blue | 0.72 | 0.04 |
| LEDA 702814 | 10:18:05.73 | -31:38:49.0 | Galaxy | – | Blue | 0.64 | 0.07 |
| [VV96] J101821.7-214008 | 10:18:21.76 | -21:40:07.7 | QSO | 2.470 | Blue | 0.48 | 0.08 |
| CRTS SSS120320 J101854-400644 | 10:18:53.51 | -40:06:43.7 | Candidate CV* | – | Blue | 0.29 | 0.10 |
| ESO 375-7 | 10:19:01.23 | -37:40:19.2 | | 0.016 | Blue | 1.00 | 0.00 |
| CTS 1011 | 10:19:21.17 | -22:08:33.4 | HII G | 0.012 | Blue | 0.43 | 0.12 |
| CTS 1011 | 10:19:21.28 | -22:08:35.9 | HII G | 0.012 | Blue | 0.58 | 0.14 |
| NGC 3208 | 10:19:41.31 | -25:48:52.9 | EmG | 0.010 | Blue | 0.62 | 0.06 |
| 6dFGS gJ102028.5-232845 | 10:20:28.52 | -23:28:45.3 | Galaxy | 0.012 | Blue | 1.00 | 0.00 |
| LEDA 800754 | 10:20:32.72 | -23:26:54.0 | Galaxy | – | Blue | 0.48 | 0.09 |
| CRTS SSS120215 J102042-335002 | 10:20:42.16 | -33:50:02.4 | Candidate CV* | – | Blue | 0.61 | 0.08 |
| Gaia DR2 5668001579559758720 | 10:20:43.31 | -20:47:54.6 | Star | – | Blue | 0.54 | 0.07 |
| ESO 500-30 | 10:20:48.90 | -23:27:57.1 | EmG | 0.012 | Red | 0.63 | 0.18 |
| 6dFGS gJ102109.3-325140 | 10:21:09.27 | -32:51:39.9 | Galaxy | 0.010 | Blue | 0.96 | 0.04 |
| 6dFGS gJ102121.0-213628 | 10:21:21.03 | -21:36:27.7 | Galaxy | 0.011 | Blue | 0.99 | 0.01 |
| LEDA 592969 | 10:22:02.22 | -39:52:45.9 | Galaxy | – | Blue | 0.89 | 0.06 |
| 6dFGS gJ102239.9-302931 | 10:22:39.94 | -30:29:30.6 | AGN Candidate | 0.317 | Blue | 0.45 | 0.08 |
| ESO 263-30 | 10:22:59.54 | -42:49:38.9 | Galaxy | 0.009 | Blue | 0.83 | 0.03 |
| ESO 317-19 | 10:23:02.34 | -39:09:59.8 | GinGroup | 0.010 | Blue | 0.84 | 0.06 |
| ESO 375-18 | 10:23:40.27 | -35:49:33.5 | EmG | 0.015 | Red | 0.40 | 0.39 |
| ESO 375-18 | 10:23:40.27 | -35:49:33.5 | EmG | 0.015 | Red | 0.29 | 0.45 |
| ESO 263-32 | 10:24:21.47 | -43:55:01.6 | Galaxy | – | Blue | 0.85 | 0.02 |
| ESO 500-34 | 10:24:31.43 | -23:33:09.6 | Seyfert 2 | 0.012 | Red | 0.05 | 0.52 |
| CRTS J102513.4-354014 | 10:25:13.46 | -35:40:16.7 | | EB* | – | Blue | 0.99 |
| 6dFGS gJ102607.5-243321 | 10:26:07.41 | -24:33:20.2 | Galaxy | 0.013 | Blue | 0.75 | 0.08 |
| ESO 436-21 | 10:26:21.70 | -29:11:57.8 | GinCl | – | Blue | 0.96 | 0.01 |
| NAME OT J102706-434341 | 10:27:05.83 | -43:43:41.3 | CataclyV* | – | Blue | 0.75 | 0.05 |
| ESO 500-42 | 10:27:20.27 | -23:48:19.6 | Galaxy | 0.012 | Blue | 0.97 | 0.01 |
| SN 2001db | 10:27:50.35 | -43:54:20.8 | SN | – | Red | 0.57 | 0.34 |
| SN 2001db | 10:27:50.37 | -43:54:20.8 | SN | – | Red | 0.40 | 0.30 |
| [LWZ2002] 5 | 10:27:51.28 | -43:53:58.5 | X | – | Blue | 0.70 | 0.11 |
| NGC 3256 | 10:27:51.29 | -43:54:14.0 | IG | 0.009 | Red | 0.35 | 0.40 |
| NGC 3256 | 10:27:51.30 | -43:54:13.7 | IG | 0.009 | Red | 0.37 | 0.38 |
| [LDT2000] R02 | 10:27:51.73 | -43:54:13.6 | X | – | Blue | 0.94 | 0.06 |
| [LDT2000] R02 | 10:27:51.73 | -43:54:13.3 | X | – | Blue | 0.94 | 0.06 |
| [EF2003] B3 | 10:27:52.88 | -43:54:11.5 | HII | 0.010 | Blue | 0.45 | 0.07 |
| [EF2003] B3 | 10:27:52.89 | -43:54:11.2 | HII | 0.010 | Blue | 0.46 | 0.07 |
| [EF2003] B3 | 10:27:52.89 | -43:54:11.2 | HII | 0.010 | Blue | 0.46 | 0.07 |
| ESO 436-26 | 10:28:42.96 | -31:02:17.7 | AGN | 0.014 | Red | 0.33 | 0.27 |
| CRTS CSS140309 J102844-161303 | 10:28:43.86 | -16:13:03.3 | CataclyV* | – | Blue | 0.13 | 0.07 |
| [SHM2017] J157.24190-30.14112 | 10:28:58.05 | -30:08:27.7 | RRLyr | – | Blue | 0.19 | 0.04 |
| ESO 317-34 | 10:29:00.71 | -40:04:57.9 | GinGroup | 0.009 | Blue | 0.97 | 0.03 |
| IC 2582 | 10:29:11.07 | -30:20:32.7 | EmG | 0.014 | Blue | 0.79 | 0.05 |
| LEDA 636268 | 10:30:30.59 | -36:28:47.1 | Galaxy | – | Blue | 0.76 | 0.08 |
| LEDA 636268 | 10:30:30.59 | -36:28:47.1 | Galaxy | – | Blue | 0.65 | 0.05 |
| LEDA 83158 | 10:30:57.69 | -34:42:28.5 | GinGroup | – | Blue | 0.74 | 0.05 |
| ESO 317-39 | 10:31:00.18 | -40:10:42.5 | Galaxy | 0.015 | Red | 0.13 | 0.29 |
| ESO 436-32 | 10:31:29.90 | -32:42:47.1 | EmG | 0.013 | Blue | 0.51 | 0.11 |
| NGC 3281 | 10:31:52.11 | -34:51:13.0 | Seyfert 2 | 0.011 | Red | 0.05 | 0.36 |
| LEDA 571751 | 10:31:57.37 | -41:48:41.1 | | – | Blue | 0.62 | 0.02 |

Table B1: –continued

| Id Object | RA | Dec | Type | Redshift | Group | P(Blue) | P(Red) |
|--------------------------|-------------|-------------|-----------|----------|-------|---------|---------|
| | | | | | HAC | HDBSCAN | HDBSCAN |
| [BM98] 2 | 10:32:59.22 | -27:32:36.9 | GinCl | 0.016 | Blue | 0.95 | 0.02 |
| 6dFGS gJ103317.5-430444 | 10:33:17.40 | -43:04:43.1 | Galaxy | 0.010 | Blue | 0.64 | 0.07 |
| ESO 375-64 | 10:34:00.75 | -35:16:57.6 | GinGroup | 0.009 | Blue | 0.62 | 0.07 |
| ESO 375-64 | 10:34:00.75 | -35:16:57.3 | GinGroup | 0.009 | Blue | 0.64 | 0.07 |
| LEDA 754029 | 10:34:26.74 | -27:30:04.0 | GinCl | 0.012 | Blue | 0.98 | 0.02 |
| ESO 436-42 | 10:34:38.75 | -28:35:00.1 | EmG | 0.012 | Blue | 0.76 | 0.04 |
| ESO 568-18 | 10:34:54.59 | -20:32:55.6 | EmG | 0.012 | Blue | 0.98 | 0.01 |
| 2MASX J10345852-4054438 | 10:34:58.52 | -40:54:43.3 | Galaxy | 0.016 | Blue | 0.73 | 0.06 |
| 6dFGS gJ103502.9-293024 | 10:35:02.88 | -29:30:23.8 | GinCl | 0.012 | Blue | 0.97 | 0.03 |
| ESO 437-3 | 10:35:07.72 | -27:59:28.7 | EmG | 0.008 | Blue | 0.70 | 0.04 |
| ESO 375-69 | 10:35:18.72 | -36:52:42.5 | EmG | 0.011 | Blue | 0.95 | 0.05 |
| ESO 501-22 | 10:35:21.68 | -27:41:44.5 | GinCl | 0.010 | Blue | 0.96 | 0.04 |
| LEDA 712419 | 10:35:31.70 | -30:50:00.0 | Galaxy | – | Blue | 0.62 | 0.03 |
| LEDA 535830 | 10:35:34.16 | -44:34:41.1 | Galaxy | – | Blue | 0.77 | 0.08 |
| LEDA 784823 | 10:36:02.66 | -24:54:24.1 | Galaxy | – | Blue | 0.81 | 0.03 |
| LEDA 743415 | 10:36:06.94 | -28:17:45.0 | Galaxy | – | Blue | 0.87 | 0.06 |
| ESO 501-32 | 10:36:22.11 | -25:22:35.4 | EmG | 0.013 | Blue | 0.81 | 0.05 |
| [CZ2003] 1060C-393 25 | 10:36:30.34 | -27:54:04.0 | GinCl | 0.008 | Blue | 0.82 | 0.06 |
| 6dFGS gJ103645.4-281005 | 10:36:45.48 | -28:10:02.7 | GinCl | 0.012 | Blue | 0.90 | 0.03 |
| LEDA 769967 | 10:36:54.86 | -26:14:26.0 | HII G | 0.012 | Blue | 0.14 | 0.05 |
| 6dFGS gJ103656.1-265414 | 10:36:56.08 | -26:54:13.6 | Galaxy | 0.096 | Blue | 0.99 | 0.01 |
| LEDA 742546 | 10:37:01.84 | -28:22:01.7 | GinCl | – | Blue | 0.87 | 0.05 |
| 6dFGS gJ103704.4-312157 | 10:37:04.45 | -31:21:57.3 | Galaxy | 0.010 | Blue | 0.81 | 0.03 |
| NGC 3314 | 10:37:12.87 | -27:41:02.2 | EmG | 0.009 | Blue | 0.64 | 0.11 |
| 6dFGS gJ103719.9-281420 | 10:37:19.89 | -28:14:19.9 | GinCl | 0.012 | Blue | 1.00 | 0.00 |
| LEDA 753354 | 10:37:22.21 | -27:32:41.9 | Galaxy | – | Blue | 0.70 | 0.08 |
| WISE J103754.92-242544.5 | 10:37:54.92 | -24:25:44.6 | MIR | – | Red | 0.14 | 0.47 |
| ESO 501-61 | 10:38:05.84 | -25:05:40.1 | IG | 0.012 | Blue | 0.94 | 0.02 |
| [WLH83] 1036-378A | 10:38:14.37 | -38:05:25.5 | HII | – | Blue | 0.93 | 0.03 |
| LEDA 740766 | 10:38:28.68 | -28:30:55.0 | GinCl | – | Blue | 0.97 | 0.03 |
| 2MASX J10383034-2332546 | 10:38:30.34 | -23:32:54.7 | Galaxy | – | Blue | 0.91 | 0.05 |
| ESO 501-65 | 10:38:33.42 | -27:44:13.8 | EmG | 0.015 | Blue | 0.86 | 0.06 |
| WPVS 78 | 10:38:41.50 | -25:35:32.2 | EmG | 0.010 | Blue | 0.49 | 0.12 |
| 6dFGS gJ103857.2-200242 | 10:38:57.24 | -20:02:41.8 | Galaxy | 0.007 | Blue | 0.91 | 0.02 |
| LEDA 838980 | 10:39:13.02 | -20:38:12.5 | Galaxy | – | Blue | 0.64 | 0.04 |
| MCG-04-25-054 | 10:39:26.01 | -23:45:16.8 | EmG | 0.013 | Blue | 0.60 | 0.06 |
| 2MASS J10395999-4701261 | 10:39:59.97 | -47:01:26.3 | CataclyV* | – | Blue | 0.55 | 0.12 |
| 2MASS J10395999-4701261 | 10:39:59.97 | -47:01:26.3 | CataclyV* | – | Blue | 0.55 | 0.12 |
| ESO 437-37 | 10:40:31.01 | -29:16:10.5 | IG | 0.012 | Blue | 0.90 | 0.03 |
| ESO 568-20 | 10:40:58.70 | -21:47:04.3 | EmG | 0.012 | Red | 0.22 | 0.50 |
| 6dFGS gJ104102.1-304740 | 10:41:02.12 | -30:47:40.1 | Galaxy | 0.011 | Blue | 0.82 | 0.05 |
| CRTS J104104.0-341120 | 10:41:03.86 | -34:11:23.4 | RRLyr | – | Blue | 1.00 | 0.00 |
| ESO 568-21 | 10:41:15.17 | -21:01:22.9 | Seyfert 1 | 0.012 | Blue | 0.95 | 0.03 |
| ESO 437-42 | 10:41:27.71 | -31:46:49.1 | Galaxy | 0.009 | Blue | 0.82 | 0.05 |
| ESO 437-42 | 10:41:27.71 | -31:46:49.1 | Galaxy | 0.009 | Blue | 0.82 | 0.05 |
| LEDA 3081775 | 10:41:35.15 | -37:28:09.5 | Galaxy | – | Blue | 0.81 | 0.05 |
| 6dFGS gJ104139.4-274638 | 10:41:39.43 | -27:46:38.2 | Galaxy | 0.014 | Blue | 0.66 | 0.07 |
| ESO 568-22 | 10:42:06.62 | -22:06:20.1 | IG | 0.007 | Blue | 0.74 | 0.05 |
| LEDA 31904 | 10:42:19.50 | -36:19:13.7 | Galaxy | – | Blue | 0.97 | 0.03 |
| 6dFGS gJ104238.0-235609 | 10:42:37.99 | -23:56:08.4 | Galaxy | 0.003 | Blue | 0.90 | 0.02 |
| ESO 437-50 | 10:43:31.00 | -30:46:20.0 | EmG | 0.013 | Blue | 0.76 | 0.03 |
| ESO 437-50 | 10:43:31.00 | -30:46:20.0 | EmG | 0.013 | Blue | 0.76 | 0.03 |
| 6dFGS gJ104409.7-204909 | 10:44:09.71 | -20:49:09.5 | Galaxy | 0.013 | Blue | 0.82 | 0.04 |
| ESO 569-2 | 10:45:00.21 | -22:09:08.2 | IG | 0.010 | Blue | 1.00 | 0.00 |
| 6dFGS gJ104534.8-241702 | 10:45:34.75 | -24:17:01.3 | Galaxy | 0.012 | Blue | 0.80 | 0.07 |
| 6dFGS gJ104617.1-282524 | 10:46:17.11 | -28:25:23.6 | EmG | 0.012 | Blue | 0.73 | 0.04 |
| LEDA 718607 | 10:46:30.26 | -30:19:17.8 | Galaxy | – | Blue | 0.83 | 0.04 |
| ESO 376-20 | 10:46:38.45 | -36:21:11.9 | EmG | 0.014 | Blue | 0.69 | 0.07 |

Table B1: –continued

| Id Object | RA | Dec | Type | Redshift | Group HAC | P(Blue) | P(Red) |
|-------------------------------|-------------|-------------|-----------------|----------|--------------|---------|---------|
| | | | | | | HDBSCAN | HDBSCAN |
| ESO 501-96 | 10:46:47.54 | -23:19:39.8 | Galaxy | 0.011 | Blue | 0.94 | 0.06 |
| Gaia DR2 5391507429181636352 | 10:47:23.91 | -41:59:49.3 | Star | – | Blue | 0.56 | 0.07 |
| EC 10453-2041 | 10:47:44.36 | -20:57:48.8 | EmG | 0.012 | Blue | 0.53 | 0.09 |
| 2MASX J10475221-2004542 | 10:47:52.11 | -20:04:53.3 | HII G | 0.013 | Blue | 0.87 | 0.02 |
| 2MASX J10475221-2004542 | 10:47:52.13 | -20:04:53.5 | HII G | 0.013 | Blue | 1.00 | 0.00 |
| [KRB2015] A | 10:48:23.47 | -25:09:43.6 | Radio | – | Red | 0.62 | 0.19 |
| 2MASX J10482527-2151000 | 10:48:25.30 | -21:51:00.5 | Galaxy | 0.015 | Blue | 0.73 | 0.04 |
| SN 2018aqi | 10:48:25.45 | -25:09:36.1 | SN | 0.012 | Red | 0.20 | 0.07 |
| LEDA 688498 | 10:48:42.32 | -32:38:37.4 | Galaxy | – | Blue | 1.00 | 0.00 |
| LEDA 738826 | 10:49:46.88 | -28:40:37.1 | Galaxy | – | Blue | 0.50 | 0.08 |
| 2MASX J10503963-1832342 | 10:50:39.64 | -18:32:34.4 | Galaxy | 0.014 | Red | 0.43 | 0.22 |
| LEDA 844461 | 10:51:00.37 | -20:14:21.3 | Galaxy | – | Blue | 1.00 | 0.00 |
| 6dFGS gJ105101.9-282017 | 10:51:01.81 | -28:20:16.5 | Galaxy | 0.011 | Blue | 0.85 | 0.03 |
| LEDA 851789 | 10:51:27.40 | -19:41:37.0 | Galaxy | – | Blue | 0.99 | 0.01 |
| 6dFGS gJ105149.2-215323 | 10:51:49.07 | -21:53:17.5 | Galaxy | 0.010 | Blue | 0.67 | 0.05 |
| 6dFGS gJ105233.0-230900 | 10:52:33.04 | -23:08:59.6 | Galaxy | 0.318 | Blue | 0.29 | 0.08 |
| MASTER OT J105440.86-391319.0 | 10:54:40.84 | -39:13:19.0 | Candidate SN* | – | Blue | 0.76 | 0.08 |
| 6dFGS gJ105521.6-232527 | 10:55:21.62 | -23:25:27.3 | Galaxy | 0.012 | Blue | 0.87 | 0.06 |
| 6dFGS gJ105521.6-232527 | 10:55:21.63 | -23:25:27.3 | Galaxy | 0.012 | Blue | 0.90 | 0.04 |
| 2MASX J10563839-2047119 | 10:56:38.39 | -20:47:12.2 | Galaxy | 0.012 | Blue | 0.87 | 0.03 |
| LEDA 849870 | 10:56:48.51 | -19:50:00.4 | Galaxy | – | Blue | 0.85 | 0.08 |
| ESO 376-28 | 10:57:04.32 | -33:09:20.3 | Galaxy | 0.013 | Red | 0.45 | 0.30 |
| ESO 264-52 | 10:57:13.91 | -47:40:11.3 | Galaxy | 0.016 | Red | 0.63 | 0.14 |
| LEDA 648093 | 10:57:36.52 | -35:30:15.8 | Galaxy | – | Blue | 1.00 | 0.00 |
| 2MASX J10584423-1909304 | 10:58:44.25 | -19:09:31.1 | Galaxy | 0.012 | Blue | 1.00 | 0.00 |
| EC 10566-3120 | 10:58:59.03 | -31:36:34.1 | CataclyV* | – | Blue | 0.52 | 0.08 |
| 2MASX J10590982-2759589 | 10:59:09.86 | -27:59:59.3 | Galaxy | 0.005 | Blue | 0.91 | 0.04 |
| Gaia DR2 5386613537284200960 | 11:01:51.26 | -46:53:04.5 | Candidate RRLyr | – | Blue | 1.00 | 0.00 |
| Gaia DR2 3537117430403448320 | 11:01:57.97 | -23:47:27.3 | PM* | – | Blue | 0.53 | 0.10 |
| V* TU Crt | 11:03:36.57 | -21:37:45.9 | CataclyV* | – | Blue | 0.58 | 0.09 |
| NGC 3513 | 11:03:46.16 | -23:14:42.1 | GinPair | 0.004 | Blue | 0.76 | 0.04 |
| FAUST 2807 | 11:03:59.06 | -18:46:36.1 | UV | – | Blue | 1.00 | 0.00 |
| ESO 570-5 | 11:07:13.10 | -19:49:07.2 | IG | 0.012 | Blue | 0.89 | 0.05 |
| NGC 3529 | 11:07:19.13 | -19:33:20.0 | EmG | 0.013 | Blue | 0.96 | 0.03 |
| NGC 3529 | 11:07:19.14 | -19:33:19.5 | EmG | 0.013 | Blue | 0.96 | 0.02 |
| NGC 3565 | 11:07:47.84 | -20:01:20.2 | IG | 0.013 | Blue | 0.89 | 0.04 |
| ESO 570-10 | 11:10:50.57 | -21:58:28.3 | Galaxy | 0.012 | Blue | 0.86 | 0.08 |
| LEDA 821419 | 11:10:57.23 | -21:56:53.3 | Galaxy | – | Blue | 0.89 | 0.03 |
| 6dFGS gJ111351.0-212655 | 11:13:50.97 | -21:26:54.8 | Galaxy | 0.012 | Blue | 0.88 | 0.07 |
| NGC 3597 | 11:14:42.00 | -23:43:39.9 | EmG | 0.012 | Blue | 0.67 | 0.08 |
| [VV96] J111644.8-171127 | 11:16:43.58 | -17:11:41.5 | QSO | 0.375 | Blue | 0.41 | 0.07 |
| LEDA 861413 | 11:17:15.01 | -18:58:24.4 | Galaxy | – | – | – | – |
| LEDA 809402 | 11:17:35.06 | -22:45:06.2 | Galaxy | – | Red | 0.29 | 0.49 |
| CRTS J112256.0-242841 | 11:22:56.09 | -24:28:40.0 | EB* | – | Blue | 1.00 | 0.00 |
| LEDA 786212 | 11:29:34.18 | -24:46:39.1 | Galaxy | – | Blue | 0.50 | 0.08 |
| [VV2010c] J113128.4-195903 | 11:31:28.46 | -19:59:02.8 | AGN | 0.363 | Blue | 0.58 | 0.07 |
| CRTS SSS110509 J113219-213943 | 11:32:19.01 | -21:39:42.9 | Candidate CV* | – | – | – | – |
| 2dFGRS TGN44Z198 | 11:34:24.52 | 01:09:15.7 | Galaxy | 0.017 | Blue | 0.88 | 0.04 |
| MGC 22410 | 11:36:12.70 | 00:04:54.9 | Star | – | Blue | 1.00 | 0.00 |
| UGC 6578 | 11:36:36.73 | 00:49:02.1 | EmG | 0.004 | Blue | 0.58 | 0.13 |
| GAMA 6821 | 11:36:36.79 | 00:48:55.8 | Galaxy | 0.004 | Blue | 0.08 | 0.04 |
| V* RZ Leo | 11:37:22.18 | 01:48:58.9 | CataclyV* | -0.000 | Blue | 0.17 | 0.05 |
| Gaia DR2 3541998025080414336 | 11:37:49.97 | -20:07:37.1 | Candidate WD* | – | Blue | 0.37 | 0.10 |
| 2dFGRS TGN238Z266 | 11:38:54.33 | -01:38:34.1 | Galaxy | 0.006 | Blue | 0.49 | 0.08 |
| CRTS J113855.5-211148 | 11:38:55.60 | -21:11:47.7 | RRLyr | – | Blue | 0.97 | 0.03 |
| SDSS J113901.39+012017.8 | 11:39:01.39 | 01:20:17.7 | Galaxy | 0.005 | Blue | 0.37 | 0.11 |
| LBQS 1136-0109 | 11:39:04.35 | -01:26:25.0 | QSO | 1.375 | Blue | 0.81 | 0.03 |
| 6dFGS gJ114135.0-181141 | 11:41:35.04 | -18:11:40.5 | Galaxy | 0.012 | Blue | 0.95 | 0.02 |

Table B1: –continued

| Id Object | RA | Dec | Type | Redshift | HAC | P(Blue) | P(Red) |
|------------------------------|-------------|-------------|---------------|----------|------|---------|---------|
| | | | | | | HDBSCAN | HDBSCAN |
| 2dFGRS TGN238Z191 | 11:41:45.67 | -01:54:04.8 | HII G | 0.006 | Blue | 0.86 | 0.06 |
| ESO 571-16 | 11:42:09.14 | -18:10:08.7 | Galaxy | 0.012 | Red | 0.05 | 0.40 |
| SDSS J114212.38+002002.5 | 11:42:12.33 | 00:20:03.4 | PartofG | 0.019 | Blue | 0.98 | 0.02 |
| 2QZ J114214.5-023154 | 11:42:14.64 | -02:31:53.3 | Galaxy | 0.319 | Blue | 0.90 | 0.02 |
| CRTS J114238.0-202722 | 11:42:37.96 | -20:27:21.8 | RRLyr | – | Blue | 0.99 | 0.01 |
| 2QZ J114250.9+013057 | 11:42:50.95 | 01:30:58.2 | Seyfert 1 | 0.361 | Blue | 0.80 | 0.08 |
| SDSS J114329.34-020319.7 | 11:43:29.34 | -02:03:19.5 | QSO | 3.304 | – | – | – |
| SDSS J114329.34-020319.7 | 11:43:29.35 | -02:03:19.9 | QSO | 3.304 | – | – | – |
| SDSSCGB 59619.2 | 11:43:46.11 | -01:16:34.0 | Galaxy | – | – | – | – |
| GAMA 396970 | 11:43:47.41 | 01:30:53.9 | Galaxy | 0.102 | Blue | 0.59 | 0.06 |
| LINEAR 2118419 | 11:44:08.82 | 01:24:20.7 | RRLyr | 0.001 | Blue | 0.98 | 0.02 |
| 2QZ J114450.8+014324 | 11:44:50.95 | 01:43:24.8 | EmG | 0.333 | Blue | 0.58 | 0.07 |
| Gaia DR2 3544179185567992320 | 11:44:55.76 | -17:56:39.4 | Candidate WD* | – | Blue | 0.46 | 0.11 |
| 2dFGRS TGN310Z256 | 11:45:08.04 | -00:59:18.2 | Galaxy | 0.004 | Blue | 0.48 | 0.09 |
| SDSS J114511.70-005402.6 | 11:45:11.72 | -00:54:02.5 | Galaxy | 0.204 | Red | 0.15 | 0.75 |
| 2MASX J11451524-2044471 | 11:45:15.26 | -20:44:47.5 | Galaxy | 0.012 | Blue | 0.70 | 0.08 |
| Z 12-78 | 11:45:26.30 | 00:00:14.8 | Galaxy | 0.013 | Blue | 0.95 | 0.05 |
| SDSS J114600.44+001037.4 | 11:46:00.45 | 00:10:37.0 | Galaxy | 0.311 | Red | 0.29 | 0.55 |
| 2dFGRS TGN310Z211 | 11:46:07.72 | -00:27:28.7 | Galaxy | 0.013 | Blue | 0.97 | 0.03 |
| SDSS J114643.10+011118.6 | 11:46:43.12 | 01:11:18.8 | QSO | 3.220 | Blue | 0.80 | 0.05 |
| 2QZ J114711.4-002706 | 11:47:11.47 | -00:27:05.8 | EmG | 0.312 | Blue | 0.98 | 0.02 |
| 2MASX J11481815-0138230 | 11:48:18.21 | -01:38:23.8 | Seyfert 1 | 0.013 | Blue | 0.81 | 0.06 |
| SDSS J114818.33-013830.8 | 11:48:18.35 | -01:38:30.5 | Galaxy | 0.013 | Blue | 0.52 | 0.08 |
| [VV2006] J114939.6+014624 | 11:49:39.60 | 01:46:25.5 | QSO | 1.362 | Blue | 0.56 | 0.06 |
| 2dFGRS TGN378Z115 | 11:50:23.78 | -00:31:41.9 | HII G | 0.013 | Blue | 0.54 | 0.11 |
| [P78] ACO 1392 C | 11:50:36.30 | -00:34:06.6 | GinCl | 0.006 | Blue | 0.58 | 0.13 |
| SDSS J115036.42-003402.0 | 11:50:36.39 | -00:34:02.6 | Galaxy | 0.006 | Blue | 0.57 | 0.13 |
| [VV2006] J115049.2-005149 | 11:50:49.29 | -00:51:49.1 | QSO | 1.354 | Blue | 0.34 | 0.08 |
| LEDA 807513 | 11:51:13.02 | -22:53:25.2 | Galaxy | – | Red | 0.34 | 0.44 |
| SDSS J115129.42-000333.8 | 11:51:29.45 | -00:03:33.6 | Galaxy | 0.326 | Red | 0.20 | 0.34 |
| 2dFGRS TGN242Z154 | 11:51:32.96 | -02:22:21.9 | Galaxy | 0.004 | Blue | 0.26 | 0.09 |
| LEDA 37102 | 11:51:33.35 | -02:22:21.7 | Seyfert 1 | 0.003 | Blue | 0.06 | 0.03 |
| SDSS J115216.86+012327.2 | 11:52:16.88 | 01:23:27.5 | Galaxy | 0.304 | Red | 0.11 | 0.59 |
| 2QZ J115217.3-025303 | 11:52:17.34 | -02:53:02.7 | EmG | 0.320 | Blue | 0.97 | 0.02 |
| ESO 572-7 | 11:52:27.62 | -20:06:14.1 | GinGroup | 0.005 | Blue | 0.80 | 0.03 |
| Mrk 1307 | 11:52:37.30 | -02:28:09.4 | Seyfert 1 | 0.004 | Blue | 0.24 | 0.08 |
| SDSS J115237.67-022806.3 | 11:52:37.67 | -02:28:06.8 | HII G | 0.004 | Blue | 0.27 | 0.09 |
| 2dFGRS TGN311Z206 | 11:52:47.52 | -00:40:07.7 | Seyfert 1 | 0.005 | Blue | 0.25 | 0.09 |
| 2dFGRS TGN311Z206 | 11:52:47.53 | -00:40:07.8 | Seyfert 1 | 0.005 | Blue | 0.26 | 0.09 |
| 2dFGRS TGN176Z274 | 11:53:14.07 | -03:24:32.6 | Galaxy | 0.004 | Blue | 0.66 | 0.07 |
| 2dFGRS TGN243Z103 | 11:53:28.66 | -03:13:48.9 | Galaxy | 0.005 | Blue | 1.00 | 0.00 |
| [VV2006] J115345.5-024320 | 11:53:45.44 | -02:43:20.4 | QSO | 1.347 | Blue | 0.84 | 0.04 |
| UM 465B | 11:54:12.31 | 00:08:12.4 | GinPair | – | Blue | 0.88 | 0.07 |
| SDSS J115456.54+001106.0 | 11:54:56.59 | 00:11:05.5 | Galaxy | 0.004 | – | – | – |
| SDSS J115511.13+002905.1 | 11:55:11.19 | 00:29:05.5 | Galaxy | 0.011 | Blue | 0.30 | 0.09 |
| SDSS J115511.67+002925.0 | 11:55:11.70 | 00:29:25.0 | Galaxy | 0.011 | Blue | 0.39 | 0.09 |
| 2dFGRS TGN243Z202 | 11:57:11.86 | -02:41:12.9 | Galaxy | 0.005 | Blue | 0.57 | 0.13 |
| SDSS J115712.38-024111.2 | 11:57:12.29 | -02:41:11.3 | Galaxy | 0.005 | Blue | 0.58 | 0.14 |
| ESO 572-25 | 11:57:28.04 | -19:37:26.5 | Galaxy | 0.006 | Blue | 0.52 | 0.08 |
| 2QZ J115737.0-020138 | 11:57:37.08 | -02:01:37.3 | Galaxy | 0.328 | Blue | 0.80 | 0.07 |
| 2QZ J115737.0-020138 | 11:57:37.09 | -02:01:37.2 | Galaxy | 0.328 | Blue | 0.84 | 0.04 |
| [VV2006] J115748.0+014320 | 11:57:48.02 | 01:43:20.9 | QSO | 1.364 | Blue | 0.56 | 0.05 |
| [VV2006] J115754.2-013815 | 11:57:54.26 | -01:38:16.0 | QSO | 4.380 | – | – | – |
| LEDA 839904 | 11:57:56.69 | -20:33:56.4 | Galaxy | – | Blue | 0.39 | 0.11 |
| 2MASX J11580803-1753363 | 11:58:08.00 | -17:53:36.2 | Galaxy | 0.008 | Blue | 0.83 | 0.04 |
| 6dFGS gJ115823.8-193103 | 11:58:23.80 | -19:31:03.2 | Galaxy | 0.005 | Blue | 0.54 | 0.07 |
| ESO 572-34 | 11:58:58.18 | -19:01:47.7 | EmG | 0.004 | Blue | 0.55 | 0.13 |
| GAMA 137854 | 11:59:23.49 | -01:43:22.3 | Galaxy | 0.304 | Blue | 0.59 | 0.16 |

Table B1: –continued

| Id Object | RA | Dec | Type | Redshift | Group | P(Blue) | P(Red) |
|------------------------------|-------------|-------------|-----------|----------|-------|---------|---------|
| | | | | | | HAC | HDBSCAN |
| SN 1996W | 11:59:28.93 | -19:15:22.8 | SN | — | Blue | 0.85 | 0.04 |
| LEDA 836770 | 12:00:19.81 | -20:48:07.5 | Galaxy | — | Blue | 0.78 | 0.05 |
| 2MASX J12002013-0106229 | 12:00:20.20 | -01:06:23.8 | Galaxy | 0.005 | Blue | 0.89 | 0.04 |
| SDSS J120021.76-024331.0 | 12:00:21.77 | -02:43:30.9 | QSO | 3.248 | Blue | 0.81 | 0.03 |
| [BKD2008] WR 14 | 12:00:26.30 | -01:06:07.0 | PartofG | 0.005 | Blue | 0.51 | 0.08 |
| [VV2006] J120038.3+011246 | 12:00:38.29 | 01:12:46.5 | QSO | 1.358 | Blue | 0.68 | 0.08 |
| QSO B1158-1842 | 12:00:44.95 | -18:59:44.5 | QSO | 2.453 | Blue | 0.53 | 0.07 |
| 2dFGRS TGN244Z048 | 12:00:47.47 | -03:25:12.1 | Galaxy | 0.005 | Blue | 0.99 | 0.01 |
| [RDS2004] MGS sure 22 | 12:00:47.72 | -00:01:24.3 | HI | 0.006 | Blue | 0.97 | 0.03 |
| UGC 7000 | 12:01:10.85 | -01:17:50.2 | GinPair | 0.005 | Blue | 1.00 | 0.00 |
| QSO B1158+007 | 12:01:23.26 | 00:28:28.5 | QSO | 1.369 | Blue | 0.78 | 0.08 |
| LEDA 802182 | 12:01:30.48 | -23:19:06.8 | Galaxy | — | Blue | 0.71 | 0.02 |
| [CEB2007] Cluster 2 | 12:01:50.41 | -18:52:12.4 | Cl* | — | Blue | 0.54 | 0.08 |
| CXOU J120150.4-185221 | 12:01:50.41 | -18:52:19.8 | HMXB | — | Blue | 0.56 | 0.07 |
| [ZBF2015] Arp244 82 | 12:01:50.49 | -18:52:02.5 | HII | — | Blue | 0.94 | 0.06 |
| [NU2000] 9 3 | 12:01:51.13 | -18:52:28.8 | Radio | — | Blue | 0.85 | 0.03 |
| [NU2000] 13 5 | 12:01:51.24 | -18:51:45.3 | Radio | — | Blue | 0.60 | 0.04 |
| [MLT2008] S2-2 | 12:01:51.90 | -18:52:28.2 | Cl* | — | Blue | 0.78 | 0.03 |
| [ZBF2015] Arp244 123 | 12:01:52.28 | -18:52:19.4 | HII | — | Blue | 0.99 | 0.01 |
| [ZBF2015] Arp244 80 | 12:01:52.96 | -18:52:03.5 | HII | — | Red | 0.31 | 0.60 |
| [ZBF2015] Arp244 5 | 12:01:52.98 | -18:52:08.7 | HII | — | Blue | 0.98 | 0.02 |
| [ZBF2015] Arp244 14 | 12:01:53.52 | -18:51:44.2 | HII | — | Blue | 0.92 | 0.03 |
| [WZ2002] 1 | 12:01:53.57 | -18:53:09.0 | Radio | — | Red | 0.29 | 0.29 |
| [BEK2006] Complex 6 | 12:01:54.54 | -18:52:07.5 | Cl* | — | Blue | 0.56 | 0.03 |
| [WS95] 89 | 12:01:54.54 | -18:53:03.8 | PartofG | — | Blue | 0.57 | 0.07 |
| [WBC2014] 180.48062-18.88025 | 12:01:55.35 | -18:52:48.7 | MolCld | 0.005 | Blue | 0.34 | 0.06 |
| [ZBF2015] Arp244 6 | 12:01:55.54 | -18:52:22.9 | HII | — | Blue | 0.85 | 0.02 |
| [ZFB2014] GMC 98 | 12:01:55.68 | -18:52:14.0 | MolCld | — | Blue | 0.67 | 0.02 |
| [WZ2002] 9 | 12:01:55.70 | -18:52:42.8 | Radio | — | Blue | 0.35 | 0.06 |
| [ZBF2015] Arp244 10 | 12:01:56.29 | -18:52:38.8 | HII | — | Blue | 1.00 | 0.00 |
| CRTS J120206.7-230305 | 12:02:06.75 | -23:03:06.0 | EB* | — | Blue | 0.95 | 0.02 |
| SDSS J120250.38+001931.6 | 12:02:50.39 | 00:19:31.5 | Galaxy | 0.333 | Red | 0.05 | 0.39 |
| SDSS J120515.80-024222.6 | 12:05:15.80 | -02:42:22.6 | WD* | 0.000 | Blue | 0.38 | 0.08 |
| LEDA 913203 | 12:06:37.73 | -15:17:17.2 | Galaxy | — | Blue | 0.97 | 0.03 |
| 6dFGS gJ120650.7-141256 | 12:06:50.66 | -14:12:55.9 | Galaxy | 0.013 | Blue | 0.79 | 0.04 |
| [VV2006] J120700.4+011155 | 12:07:00.41 | 01:11:56.4 | QSO | 1.520 | Blue | 0.75 | 0.07 |
| SDSS J120920.53-002855.3 | 12:09:20.55 | -00:28:55.3 | QSO | 3.237 | Blue | 0.83 | 0.05 |
| [VV2006] J121010.8-003909 | 12:10:10.82 | -00:39:09.7 | QSO | 1.008 | Blue | 0.07 | 0.06 |
| SDSS J121026.38-000513.2 | 12:10:26.41 | -00:05:13.2 | Galaxy | 0.310 | Blue | 0.70 | 0.04 |
| SDSS J121043.55-003907.2 | 12:10:43.59 | -00:39:08.5 | Seyfert 1 | 0.331 | Red | 0.03 | 0.06 |
| 2QZ J121101.0+012024 | 12:11:01.05 | 01:20:25.0 | EmG | 0.333 | Blue | 0.96 | 0.04 |
| Mrk 1313 | 12:12:14.73 | 00:04:20.6 | Seyfert 1 | 0.008 | Blue | 0.77 | 0.08 |
| 2dFGRS TGN246Z007 | 12:12:15.90 | -00:33:53.2 | Galaxy | 0.008 | Blue | 0.54 | 0.07 |
| 2MASS J12125978+0149231 | 12:12:59.78 | 01:49:23.2 | EB* | — | Red | 0.63 | 0.21 |
| SDSS J121304.91-003901.2 | 12:13:04.93 | -00:39:01.2 | Galaxy | 0.189 | Red | 0.06 | 0.64 |
| 2dFGRS TGN247Z167 | 12:13:38.79 | -01:17:36.3 | Galaxy | 0.008 | Blue | 0.86 | 0.03 |
| 6dFGS gJ121348.2-143140 | 12:13:48.16 | -14:31:39.8 | Galaxy | 0.330 | Blue | 0.62 | 0.06 |
| SDSS J121435.24-015924.4 | 12:14:35.26 | -01:59:24.4 | QSO | 3.233 | Blue | 0.86 | 0.09 |
| [VV2006] J121515.2-013542 | 12:15:15.23 | -01:35:40.8 | QSO | 1.350 | Blue | 0.57 | 0.04 |
| 2QZ J121539.4-022149 | 12:15:39.47 | -02:21:47.2 | Galaxy | 0.319 | Blue | 0.78 | 0.05 |
| 2QZ J121607.5-022559 | 12:16:07.54 | -02:25:57.6 | Galaxy | 0.324 | Blue | 1.00 | 0.00 |
| SDSS J121759.99+002558.1 | 12:18:00.05 | 00:25:57.7 | Galaxy | 0.003 | — | — | — |
| 2dFGRS TGN181Z079 | 12:18:07.07 | -03:06:28.8 | Galaxy | 0.001 | Red | 0.12 | 0.71 |
| LEDA 927634 | 12:18:19.06 | -14:12:19.9 | Galaxy | — | Blue | 0.97 | 0.03 |
| LEDA 927634 | 12:18:19.06 | -14:12:20.0 | Galaxy | — | Blue | 0.96 | 0.04 |
| QSO B1216+0216 | 12:18:55.80 | 02:00:02.1 | QSO | 0.327 | Blue | 0.31 | 0.09 |
| [VV2006] J121942.5-001821 | 12:19:42.47 | -00:18:21.4 | QSO | 1.337 | Blue | 0.79 | 0.07 |
| 2dFGRS TGN385Z034 | 12:19:53.13 | 01:46:24.0 | HII G | 0.007 | Blue | 0.88 | 0.05 |

Table B1: –continued

| Id Object | RA | Dec | Type | Redshift | Group | P(Blue) | P(Red) |
|--------------------------------|-------------|-------------|---------------|----------|-------|---------|---------|
| | | | | | | HAC | HDBSCAN |
| SDSS J122003.72+010632.0 | 12:20:03.73 | 01:06:32.4 | Galaxy | 0.315 | Red | 0.07 | 0.21 |
| 2dFGRS TGN385Z025 | 12:20:11.53 | 01:57:31.1 | LSB G | 0.007 | Blue | 0.54 | 0.13 |
| 2dFGRS TGN181Z173 | 12:20:28.80 | -01:50:21.0 | Galaxy | 0.008 | Blue | 0.82 | 0.06 |
| LEDA 1143004 | 12:20:30.39 | -00:27:03.0 | Galaxy | 0.007 | — | — | — |
| [VV2006] J122130.9+010727 | 12:21:30.97 | 01:07:28.1 | QSO | 1.370 | Blue | 0.66 | 0.04 |
| Gaia DR2 3521773745637847552 | 12:21:34.41 | -14:57:50.5 | Star | — | Blue | 0.09 | 0.04 |
| LEDA 3294456 | 12:21:55.83 | -01:35:36.0 | Galaxy | 0.006 | Blue | 0.54 | 0.08 |
| Gaia DR2 3521681421020417408 | 12:22:39.34 | -15:29:12.1 | Star | — | Blue | 0.43 | 0.09 |
| SDSS J122322.39-000801.6 | 12:23:22.39 | -00:08:01.7 | Galaxy | 0.318 | Blue | 0.69 | 0.03 |
| MCG+00-32-004 | 12:24:12.47 | 00:34:01.0 | Galaxy | 0.007 | Blue | 0.96 | 0.04 |
| 2SLAQ J122421.12+002354.1 | 12:24:21.13 | 00:23:54.4 | QSO | 0.334 | Blue | 0.55 | 0.11 |
| NGC 4385 | 12:25:42.74 | 00:34:21.9 | AGN | 0.007 | Blue | 0.60 | 0.04 |
| 2QZ J122547.3-012007 | 12:25:47.38 | -01:20:05.7 | Galaxy | 0.317 | Blue | 0.72 | 0.03 |
| SHOC 373a | 12:26:22.64 | -01:15:17.3 | HII G | 0.007 | Blue | 0.34 | 0.09 |
| SHOC 373b | 12:26:22.73 | -01:15:12.3 | HII G | 0.007 | Blue | 0.21 | 0.07 |
| [VV2006] J122625.7+011604 | 12:26:25.67 | 01:16:04.6 | QSO | 2.478 | Blue | 0.57 | 0.09 |
| 2SLAQ J122641.43-002005.1 | 12:26:41.45 | -00:20:05.1 | Seyfert 1 | 0.353 | Blue | 0.60 | 0.06 |
| MCG+00-32-013 | 12:27:04.54 | -00:54:21.5 | GinPair | 0.007 | Blue | 0.84 | 0.07 |
| MCG+00-32-013 | 12:27:04.56 | -00:54:22.0 | GinPair | 0.007 | Blue | 0.87 | 0.03 |
| [VV2006] J122707.1+010811 | 12:27:07.13 | 01:08:11.3 | QSO | 2.189 | Blue | 0.16 | 0.04 |
| [MIO2012] R1 | 12:27:46.07 | 01:36:01.5 | Cl* | — | Blue | 0.57 | 0.12 |
| 2dFGRS TGN387Z059 | 12:28:15.92 | 01:49:43.7 | Galaxy | 0.003 | Blue | 1.00 | 0.00 |
| 2QZ J122851.2-022630 | 12:28:51.34 | -02:26:29.2 | EmG | 0.331 | Blue | 0.93 | 0.07 |
| 2dFGRS TGN250Z094 | 12:29:14.65 | -01:21:55.2 | Galaxy | 0.007 | Blue | 0.51 | 0.08 |
| 2dFGRS TGN250Z087 | 12:29:46.33 | -01:17:42.0 | LSB G | 0.008 | Blue | 0.76 | 0.15 |
| 2dFGRS TGN321Z099 | 12:29:58.88 | 00:01:37.9 | RadioG | 0.008 | Red | 0.08 | 0.68 |
| 2dFGRS TGN388Z078 | 12:30:54.31 | 00:57:50.5 | Galaxy | 0.008 | Blue | 0.66 | 0.08 |
| [BKD2008] WR 29 | 12:31:48.01 | -02:58:13.0 | PartofG | 0.008 | Blue | 0.80 | 0.03 |
| 2QZ J123202.6+003124 | 12:32:02.70 | 00:31:24.7 | EmG | 0.329 | Blue | 0.79 | 0.07 |
| 2dFGRS TGN251Z016 | 12:32:23.64 | -01:44:24.3 | HII G | 0.007 | Blue | 0.77 | 0.03 |
| GALEX 2414740977348515009 | 12:32:36.17 | -03:18:39.4 | Blue | — | Blue | 0.57 | 0.05 |
| MGC 34804 | 12:32:41.58 | 00:03:26.4 | Star | — | Blue | 0.74 | 0.11 |
| [DCD2013] CSS J123702.3-151643 | 12:37:02.41 | -15:16:43.5 | RRLyr | — | Blue | 0.90 | 0.01 |
| Gaia DR2 3527007524064861312 | 12:39:19.45 | -14:47:31.1 | Star | — | — | — | — |
| 2MASX J12442692-1252359 | 12:44:26.92 | -12:52:35.9 | Galaxy | 0.018 | Blue | 1.00 | 0.00 |
| LEDA 924051 | 12:50:47.04 | -14:29:01.5 | Galaxy | — | Blue | 1.00 | 0.00 |
| LEDA 932206 | 12:58:59.15 | -13:51:42.3 | Galaxy | — | Blue | 0.52 | 0.08 |
| CRTS SSS120721 J125901-133442 | 12:59:00.82 | -13:34:42.0 | Candidate CV* | — | Blue | 0.48 | 0.09 |
| 6dFGS gJ125904.7-144623 | 12:59:04.67 | -14:46:23.5 | | 0.016 | Blue | 0.73 | 0.04 |
| 2MASX J12593269-1514196 | 12:59:32.75 | -15:14:19.3 | Galaxy | — | Blue | 0.31 | 0.10 |
| LEDA 914340 | 13:00:03.04 | -15:12:17.2 | Galaxy | — | Blue | 0.98 | 0.02 |
| NGC 4887 | 13:00:39.30 | -14:39:59.3 | GinPair | 0.009 | Blue | 0.98 | 0.02 |
| LEDA 936912 | 13:01:07.09 | -13:31:02.4 | Galaxy | 0.004 | Blue | 0.33 | 0.09 |
| [VV96] J130243.5-135553 | 13:02:43.59 | -13:55:52.8 | QSO | 1.391 | Blue | 0.54 | 0.07 |
| LEDA 45114 | 13:03:33.44 | -14:19:23.1 | EmObj | 0.008 | Blue | 0.76 | 0.08 |
| 2MASX J13044961-1311288 | 13:04:49.65 | -13:11:28.2 | Galaxy | 0.010 | Blue | 0.72 | 0.06 |
| LCRS B130214.7-120615 | 13:04:52.39 | -12:22:18.7 | Galaxy | — | Blue | 1.00 | 0.00 |
| LEDA 949391 | 13:05:58.52 | -12:40:08.5 | Galaxy | — | Blue | 0.62 | 0.07 |
| LEDA 105081 | 13:10:08.77 | -12:12:20.4 | Galaxy | 0.013 | Blue | 0.90 | 0.02 |
| UGCA 332 | 13:11:58.29 | -12:03:51.4 | EmG | 0.007 | Blue | 0.90 | 0.04 |
| LEDA 976320 | 13:12:28.41 | -10:35:24.4 | Galaxy | — | Blue | 0.86 | 0.07 |
| LCRS B131057.8-121222 | 13:13:36.14 | -12:28:15.2 | EmObj | 0.013 | Blue | 0.49 | 0.12 |
| LEDA 126038 | 13:15:07.97 | -12:31:05.1 | Galaxy | 0.013 | Blue | 1.00 | 0.00 |
| LEDA 981336 | 13:17:40.89 | -10:10:59.5 | Galaxy | — | Blue | 1.00 | 0.00 |
| SDSS J131742.35-002015.8 | 13:17:42.37 | -00:20:15.7 | Galaxy | 0.356 | — | — | — |
| 6dFGS gJ131743.9-010002 | 13:17:43.96 | -01:00:01.1 | AGN | 0.004 | Blue | 0.08 | 0.04 |
| 2MASX J13192221-1509232 | 13:19:22.29 | -15:09:23.6 | Galaxy | 0.009 | Blue | 0.96 | 0.04 |
| MCG-02-34-029 | 13:19:42.72 | -11:28:28.5 | GinGroup | 0.009 | Blue | 0.98 | 0.02 |

Table B1: –continued

| Id Object | RA | Dec | Type | Redshift | HAC | P(Blue) | P(Red) |
|--------------------------------|-------------|-------------|--------------------|----------|------|---------|---------|
| | | | | | | HDBSCAN | HDBSCAN |
| 2SLAQ J131957.59-003446.7 | 13:19:57.60 | -00:34:46.6 | Star | – | Blue | 0.97 | 0.03 |
| QSO B1317-122 | 13:19:59.20 | -12:29:16.8 | QSO | 0.329 | Blue | 0.46 | 0.09 |
| NGC 5088 | 13:20:20.33 | -12:34:18.1 | Galaxy | 0.005 | Blue | 0.89 | 0.03 |
| SDSS J132023.46-004730.9 | 13:20:23.47 | -00:47:30.8 | QSO | 3.255 | – | – | – |
| 6dFGS gJ132134.7-151056 | 13:21:34.68 | -15:10:55.5 | Galaxy | 0.009 | Blue | 1.00 | 0.00 |
| 6dFGS gJ132137.8-145120 | 13:21:37.83 | -14:51:19.7 | Galaxy | 0.009 | Blue | 0.97 | 0.01 |
| 2dFGRS TGN263Z056 | 13:22:17.11 | -00:32:54.4 | EmG | 0.018 | – | – | – |
| [SHM2017] J200.93368-12.05326 | 13:23:44.09 | -12:03:11.8 | RRLyr | – | Blue | 0.96 | 0.03 |
| LEDA 46982 | 13:25:48.67 | -11:36:37.8 | BlueCompG | 0.004 | Blue | 0.06 | 0.03 |
| LEDA 46982 | 13:25:48.68 | -11:36:38.0 | BlueCompG | 0.004 | Blue | 0.06 | 0.03 |
| LEDA 991902 | 13:26:05.10 | -09:22:12.6 | Galaxy | – | Blue | 0.54 | 0.09 |
| BPS CS 22889-0007 | 13:31:59.47 | -09:53:02.6 | RRLyr | 0.001 | Blue | 0.99 | 0.01 |
| NVSS J133618-072251 | 13:36:18.64 | -07:22:51.8 | Radio | – | Blue | 0.73 | 0.08 |
| LCRS B133356.3-061328 | 13:36:33.05 | -06:28:45.2 | Galaxy | – | Red | 0.07 | 0.85 |
| GALEX 2697385722761974216 | 13:39:09.19 | -08:19:40.8 | Blue | – | Blue | 0.65 | 0.03 |
| LEDA 1025584 | 13:41:04.99 | -07:01:05.8 | Galaxy | – | Blue | 0.65 | 0.02 |
| [DCD2013] CSS J134330.9-151858 | 13:43:31.01 | -15:18:58.9 | RRLyr | – | Blue | 1.00 | 0.00 |
| V* HS Vir | 13:43:38.44 | -08:14:03.7 | CataclyV* | – | Blue | 0.86 | 0.06 |
| SN 2018evt | 13:46:39.20 | -09:38:36.0 | SN | 0.029 | Blue | 0.83 | 0.04 |
| GALEX 2697315366902694354 | 13:47:49.82 | -04:10:10.6 | Blue | – | Blue | 0.61 | 0.05 |
| 2dFGRS TGN202Z201 | 13:49:42.20 | -02:11:59.1 | Galaxy | 0.011 | Blue | 0.74 | 0.03 |
| GALEX 2699039396840082228 | 13:50:33.33 | -12:16:42.9 | Blue | – | Blue | 0.55 | 0.07 |
| 6dFGS gJ135123.7-060412 | 13:51:23.70 | -06:04:11.7 | Galaxy | 0.010 | Blue | 0.98 | 0.02 |
| 2dFGRS TGN202Z136 | 13:51:35.65 | -02:33:15.0 | Galaxy | 0.015 | Blue | 0.99 | 0.01 |
| SDSSCGB 287.4 | 13:52:03.90 | -02:07:22.3 | Galaxy | – | Blue | 0.79 | 0.09 |
| SDSSCGB 287.2 | 13:52:04.24 | -02:07:48.9 | Galaxy | 0.015 | Blue | 0.65 | 0.07 |
| LEDA 126156 | 13:54:11.29 | -03:26:27.2 | Galaxy | 0.014 | Blue | 0.80 | 0.08 |
| LEDA 126156 | 13:54:11.40 | -03:26:27.0 | Galaxy | 0.014 | Blue | 0.90 | 0.04 |
| QSO B1352-104 | 13:54:46.53 | -10:41:02.6 | QSO | 0.330 | Blue | 0.41 | 0.06 |
| VV 99b | 13:55:33.98 | -05:58:17.0 | GinPair | – | Blue | 0.87 | 0.07 |
| 2dFGRS TGN141Z158 | 13:55:37.68 | -04:11:43.8 | Galaxy | 0.012 | Blue | 0.33 | 0.10 |
| VV 100a | 13:55:45.46 | -06:00:15.9 | Galaxy | – | Blue | 0.74 | 0.07 |
| VV 100d | 13:55:46.68 | -06:00:40.8 | Galaxy | – | Blue | 0.56 | 0.14 |
| [VV2006] J135602.8-022624 | 13:56:02.79 | -02:26:23.3 | QSO | 1.373 | – | – | – |
| 2dFGRS TGN203Z232 | 13:56:53.48 | -02:38:52.2 | Galaxy | 0.013 | Blue | 0.62 | 0.05 |
| 2dFGRS TGN142Z266 | 13:58:08.62 | -04:08:43.6 | Galaxy | 0.015 | Blue | 0.75 | 0.02 |
| SDSSCGB 16922.1 | 13:58:41.49 | -01:31:15.7 | Galaxy | – | Red | 0.28 | 0.36 |
| LEDA 1020082 | 14:02:45.08 | -07:22:25.8 | Galaxy | – | Blue | 0.52 | 0.08 |
| 2MASS J14265388+0525172 | 14:26:53.89 | 05:25:17.4 | QSO | 0.323 | Blue | 0.45 | 0.10 |
| UGC 9252 | 14:27:10.82 | 05:07:59.3 | Galaxy | 0.005 | Blue | 1.00 | 0.00 |
| [LAM2019] J1428+0500 B | 14:28:55.39 | 05:00:21.9 | Possible lensImage | – | Blue | 0.62 | 0.10 |
| GALEX 2429518413625830432 | 14:28:55.46 | 05:00:19.9 | Blue | – | Blue | 0.81 | 0.07 |
| DES J142943.42+052122.7 | 14:29:43.44 | 05:21:22.9 | GinCl | – | Red | 0.37 | 0.42 |
| SDSS J142958.66+044611.0 | 14:29:58.65 | 04:46:11.3 | BCIG | 0.456 | Red | 0.08 | 0.18 |
| LEDA 1290447 | 14:41:28.04 | 05:51:52.3 | Galaxy | 0.027 | Blue | 1.00 | 0.00 |
| SDSS J145344.51+045645.8 | 14:53:44.52 | 04:56:46.0 | QSO | 3.328 | Blue | 0.71 | 0.03 |
| SDSSCGB 43444.3 | 14:55:33.70 | 04:46:43.2 | AGN | 0.334 | Red | 0.38 | 0.38 |
| SDSS J200143.74+004918.4 | 20:01:43.73 | 00:49:18.4 | QSO | – | Blue | 0.36 | 0.07 |
| SDSS J200432.38+001041.3 | 20:04:32.39 | 00:10:41.4 | low-mass* | – | – | – | – |
| [SHM2017] J302.70083-00.21773 | 20:10:48.20 | -00:13:03.9 | RRLyr | – | Blue | 1.00 | 0.00 |
| [SHM2017] J302.70083-00.21773 | 20:10:48.20 | -00:13:03.9 | RRLyr | – | Blue | 1.00 | 0.00 |
| [SSV2012] 4869177 | 20:22:35.51 | -00:40:09.9 | RRLyr | – | Blue | 0.92 | 0.02 |
| [SSV2012] 4472518 | 20:22:37.80 | -00:02:50.5 | RRLyr | – | Blue | 0.99 | 0.01 |
| UGC 11566 | 20:28:12.02 | 00:17:18.2 | Galaxy | 0.006 | Blue | 0.88 | 0.05 |
| SDSS J202906.80+005453.5 | 20:29:06.81 | 00:54:53.6 | QSO | – | Blue | 0.97 | 0.03 |
| 2SLAQ J204340.03+002853.4 | 20:43:40.04 | 00:28:53.6 | Seyfert 1 | 0.317 | Blue | 0.53 | 0.08 |
| SDSS J204626.10+002337.7 | 20:46:26.11 | 00:23:37.8 | QSO | 0.332 | Red | 0.24 | 0.39 |
| 2SLAQ J204720.76+000007.7 | 20:47:20.76 | 00:00:07.8 | CataclyV* | 0.001 | Blue | 1.00 | 0.00 |

Table B1: –continued

| Id Object | RA | Dec | Type | Redshift | Group HAC | P(Blue) | P(Red) |
|-------------------------------|-------------|-------------|---------------|----------|--------------|---------|---------|
| | | | | | | HDBSCAN | HDBSCAN |
| 2SLAQ J204720.76+000007.7 | 20:47:20.76 | 00:00:07.7 | CataclyV* | 0.001 | Blue | 0.70 | 0.07 |
| 2SLAQ J204910.96+001557.2 | 20:49:10.95 | 00:15:57.5 | Seyfert 1 | 0.363 | Blue | 0.41 | 0.07 |
| [VV2006] J204956.6-001201 | 20:49:56.62 | -00:12:01.7 | QSO | 0.369 | Blue | 0.46 | 0.09 |
| [VV2006] J204956.6-001201 | 20:49:56.62 | -00:12:01.7 | QSO | 0.369 | Blue | 0.53 | 0.08 |
| [VV2006] J205316.7+005920 | 20:53:16.77 | 00:59:21.1 | QSO | 4.299 | – | – | – |
| 2SLAQ J205352.03-001601.5 | 20:53:52.04 | -00:16:01.5 | QSO | 0.363 | Blue | 0.68 | 0.11 |
| 2SLAQ J205614.55-004050.9 | 20:56:14.55 | -00:40:50.6 | Star | – | – | – | – |
| 2SLAQ J205712.69+001211.3 | 20:57:12.69 | 00:12:11.4 | QSO | 0.335 | Blue | 0.50 | 0.11 |
| SDSS J205740.76+005418.5 | 20:57:40.75 | 00:54:19.0 | QSO | 0.332 | Red | 0.13 | 0.68 |
| Gaia DR2 6794425304909258752 | 20:58:06.45 | -30:08:18.1 | Candidate WD* | – | Blue | 0.40 | 0.07 |
| LEDA 687146 | 20:58:24.54 | -32:43:22.5 | Galaxy | – | Blue | 1.00 | 0.00 |
| 2MASX J20584976-4420243 | 20:58:49.69 | -44:20:24.7 | Galaxy | 0.018 | Blue | 0.98 | 0.02 |
| 6dFGS gJ205957.5-213935 | 20:59:57.53 | -21:39:34.9 | Galaxy | -0.001 | Blue | 0.72 | 0.06 |
| SDSS J210014.12+004446.0 | 21:00:14.11 | 00:44:45.9 | CataclyV* | 0.000 | Blue | 0.57 | 0.10 |
| SDSSCGB 52599.6 | 21:01:55.95 | -00:31:24.9 | Galaxy | – | Red | 0.15 | 0.64 |
| LEDA 598660 | 21:01:56.43 | -39:23:40.3 | Galaxy | – | Blue | 0.70 | 0.03 |
| QSO B2059-330 | 21:02:41.71 | -32:52:44.1 | QSO | 3.280 | Blue | 0.76 | 0.07 |
| QSO B2059-330 | 21:02:41.72 | -32:52:44.4 | QSO | 3.280 | Blue | 0.98 | 0.02 |
| LEDA 528866 | 21:03:02.23 | -45:14:41.1 | Galaxy | – | Blue | 0.88 | 0.04 |
| Gaia DR2 6808104805812408064 | 21:03:56.66 | -21:47:27.1 | Star | – | Blue | 0.89 | 0.03 |
| ESO 286-33 | 21:04:08.52 | -43:32:03.2 | IG | 0.017 | Blue | 0.68 | 0.05 |
| ESO 286-35 | 21:04:11.17 | -43:35:33.8 | GinGroup | 0.017 | Blue | 0.58 | 0.15 |
| LEDA 720203 | 21:04:21.46 | -30:11:50.0 | Galaxy | – | Red | 0.06 | 0.19 |
| [GPM2009] J2104-0035 1 | 21:04:55.31 | -00:35:21.8 | EmG | 0.005 | Blue | 0.75 | 0.15 |
| LEDA 520361 | 21:05:20.69 | -45:59:19.3 | Galaxy | – | Blue | 0.63 | 0.06 |
| ESO 286-44 | 21:05:38.68 | -42:46:52.4 | Galaxy | 0.008 | Blue | 0.71 | 0.13 |
| PN G006.0-41.9 | 21:05:53.57 | -37:08:40.4 | PN | – | Blue | 0.04 | 0.02 |
| EC 21035-4032 | 21:06:48.02 | -40:20:03.7 | Star | – | Blue | 0.38 | 0.11 |
| 2MASX J21071198-4733258 | 21:07:11.98 | -47:33:25.2 | GinPair | – | Blue | 0.94 | 0.01 |
| 2MASX J21071385-4733258 | 21:07:13.86 | -47:33:25.3 | GinPair | 0.015 | Blue | 1.00 | 0.00 |
| [GPM2009] J2112-0016 2 | 21:12:00.92 | -00:16:49.2 | EmG | 0.012 | Blue | 0.97 | 0.03 |
| 6dFGS gJ211224.6-412854 | 21:12:24.59 | -41:28:53.3 | AGN | 0.349 | Blue | 0.66 | 0.05 |
| CRTS J211328.1+000332 | 21:13:28.17 | 00:03:32.6 | EB* | – | Blue | 1.00 | 0.00 |
| ESO 402-20 | 21:15:19.13 | -33:13:34.6 | Galaxy | 0.018 | Blue | 0.93 | 0.07 |
| CTCV J2118-3412 | 21:18:04.28 | -34:13:43.5 | CataclyV* | – | Blue | 0.53 | 0.06 |
| AT20G J212302-291504 | 21:23:02.82 | -29:15:04.0 | Radio(cm) | – | Blue | 0.52 | 0.08 |
| CRTS CSS120613 J212655-012054 | 21:26:54.54 | -01:20:54.1 | Candidate CV* | – | Blue | 0.32 | 0.06 |
| LEDA 710984 | 21:27:08.26 | -30:57:08.4 | Galaxy | – | Blue | 1.00 | 0.00 |
| 2SLAQ J212954.20-010323.3 | 21:29:54.22 | -01:03:23.3 | EmG | 0.335 | Blue | 0.70 | 0.03 |
| LBQS 2128-4555 | 21:31:29.53 | -45:41:50.5 | QSO | 0.623 | Blue | 0.63 | 0.07 |
| 2SLAQ J213242.28-010309.0 | 21:32:42.29 | -01:03:09.2 | Galaxy | – | Blue | 0.87 | 0.05 |
| 2SLAQ J213245.24+000146.4 | 21:32:45.26 | 00:01:46.8 | Seyfert 1 | 0.234 | Blue | 0.28 | 0.07 |
| 2MASS J21333817+0126291 | 21:33:38.14 | 01:26:29.0 | QSO | 1.004 | Blue | 0.97 | 0.03 |
| SDSS J213455.08+001056.9 | 21:34:55.09 | 00:10:56.8 | QSO | 3.289 | Blue | 0.76 | 0.03 |
| WISEA J213649.75-012852.2 | 21:36:49.75 | -01:28:52.2 | QSO | 3.280 | Blue | 1.00 | 0.00 |
| QSO B2134-453 | 21:38:07.49 | -45:08:18.0 | QSO | 4.360 | – | – | – |
| 2MASS J21381896+0112224 | 21:38:18.96 | 01:12:22.5 | Seyfert 1 | 0.344 | Blue | 0.44 | 0.10 |
| CRTS J213937.6-023913 | 21:39:37.58 | -02:39:13.0 | Candidate CV* | – | Blue | 0.36 | 0.08 |
| 2SLAQ J214106.46+004733.3 | 21:41:06.44 | 00:47:33.5 | QSO | 2.452 | Blue | 0.45 | 0.08 |
| SDSSCGB 15831.2 | 21:41:42.73 | 00:45:34.9 | Galaxy | – | Blue | 0.91 | 0.02 |
| SDSS J214155.04-011734.3 | 21:41:55.04 | -01:17:34.2 | QSO | 3.286 | Blue | 1.00 | 0.00 |
| SDSS J214155.04-011734.3 | 21:41:55.04 | -01:17:34.3 | QSO | 3.286 | Blue | 0.47 | 0.06 |
| SN 2017hxv | 21:44:22.94 | -29:54:59.0 | SN | 0.019 | Red | 0.12 | 0.19 |
| 2SLAQ J214455.94+002305.8 | 21:44:55.92 | 00:23:06.1 | EmG | 0.330 | Blue | 0.86 | 0.05 |
| 6dFGS gJ214540.0-291937 | 21:45:40.01 | -29:19:36.9 | Galaxy | 0.341 | Red | 0.17 | 0.22 |
| 2SLAQ J214830.60-004752.6 | 21:48:30.61 | -00:47:52.6 | EmG | 0.332 | Blue | 0.90 | 0.03 |
| 2SLAQ J214830.60-004752.6 | 21:48:30.61 | -00:47:52.5 | EmG | 0.332 | – | – | – |
| SDSS J215002.69+011343.8 | 21:50:02.70 | 01:13:43.8 | QSO | 3.267 | Blue | 0.98 | 0.02 |

Table B1: –continued

| Id Object | RA | Dec | Type | Redshift | Group | P(Blue) | P(Red) |
|---------------------------|-------------|-------------|-----------|----------|-------|---------|---------|
| | | | | | | HAC | HDBSCAN |
| 2SLAQ J215010.52-001000.6 | 21:50:10.53 | -00:10:00.6 | QSO | 0.335 | Blue | 0.48 | 0.10 |
| 2dFGRS TGS406Z223 | 21:53:05.55 | -31:28:17.9 | Galaxy | 0.019 | Blue | 0.54 | 0.09 |
| 2dFGRS TGS406Z223 | 21:53:05.55 | -31:28:17.9 | Galaxy | 0.019 | Blue | 0.54 | 0.09 |
| 2dFGRS TGS406Z223 | 21:53:05.55 | -31:28:17.9 | Galaxy | 0.019 | Blue | 0.54 | 0.09 |
| 2dFGRS TGS406Z223 | 21:53:05.55 | -31:28:17.9 | Galaxy | 0.019 | Blue | 0.54 | 0.09 |
| 2MASX J21541799+0056318 | 21:54:18.00 | 00:56:31.9 | Galaxy | 0.010 | Blue | 1.00 | 0.00 |
| LEDA 214792 | 21:56:13.83 | -01:09:42.8 | Galaxy | – | Blue | 0.85 | 0.03 |
| LEDA 214792 | 21:56:13.85 | -01:09:43.2 | Galaxy | – | Blue | 0.97 | 0.03 |
| SDSSCGB 16345.1 | 21:56:19.79 | -01:10:03.6 | Galaxy | 0.016 | Blue | 0.78 | 0.12 |
| SDSSCGB 16345.1 | 21:56:19.81 | -01:10:03.7 | Galaxy | 0.016 | Blue | 0.79 | 0.12 |
| 2dFGRS TGS059Z257 | 21:57:20.89 | -25:08:02.4 | Galaxy | 0.009 | Blue | 0.96 | 0.04 |
| SDSS J215824.23-004413.7 | 21:58:24.28 | -00:44:13.7 | HII G | 0.016 | Blue | 0.94 | 0.03 |
| SDSS J215902.90-003318.4 | 21:59:02.89 | -00:33:18.0 | Galaxy | – | Blue | 0.73 | 0.08 |
| LEDA 214793 | 21:59:03.11 | -01:57:18.3 | Galaxy | – | Blue | 0.66 | 0.05 |
| LEDA 1136721 | 22:01:50.08 | -00:42:26.7 | Galaxy | 0.018 | Blue | 0.96 | 0.04 |
| 2dFGRS TGS114Z230 | 22:02:07.08 | -26:26:38.0 | Galaxy | 0.309 | Blue | 0.59 | 0.11 |
| PB 5049 | 22:03:15.14 | 01:17:21.0 | Star | – | Blue | 0.06 | 0.03 |
| 2dFGRS TGS115Z105 | 22:04:53.68 | -25:03:05.2 | Galaxy | 0.009 | Blue | 0.97 | 0.03 |
| 2SLAQ J220529.34-003110.6 | 22:05:29.34 | -00:31:10.7 | QSO | 2.454 | Blue | 0.66 | 0.05 |
| NGC 7204 | 22:06:55.31 | -31:03:10.6 | IG | 0.009 | Red | 0.25 | 0.29 |
| 2dFGRS TGS251Z159 | 22:07:34.55 | -28:39:29.3 | Galaxy | 0.018 | Blue | 0.58 | 0.14 |
| NGC 7208 | 22:08:24.43 | -29:03:03.6 | GinGroup | 0.009 | Blue | 0.96 | 0.04 |
| 2dFGRS TGS333Z140 | 22:08:51.96 | -30:38:58.8 | | 0.008 | – | – | – |
| [VV2006] J220852.0-010603 | 22:08:51.97 | -01:06:03.7 | QSO | 0.351 | Blue | 0.46 | 0.09 |
| [VV2006] J220852.0-010603 | 22:08:51.97 | -01:06:03.7 | QSO | 0.351 | Blue | 0.48 | 0.08 |
| MCG-05-52-033a | 22:08:55.90 | -27:13:22.0 | GinPair | 0.009 | Blue | 0.78 | 0.06 |
| 2dFGRS TGS061Z180 | 22:09:19.05 | -24:07:12.4 | QSO | 0.320 | Red | 0.16 | 0.17 |
| 2dFGRS TGS116Z088 | 22:09:22.91 | -25:25:04.6 | Galaxy | 0.008 | Blue | 0.58 | 0.08 |
| 2QZ J220948.6-301357 | 22:09:48.63 | -30:13:55.8 | WD* | – | Blue | 0.21 | 0.08 |
| SDSSCGB 41857.2 | 22:09:51.35 | 01:09:00.0 | Galaxy | 0.149 | Red | 0.38 | 0.38 |
| SDSS J220954.57-012717.6 | 22:09:54.57 | -01:27:17.6 | QSO | 3.296 | Blue | 0.57 | 0.03 |
| 2QZ J221000.7-311400 | 22:10:00.75 | -31:14:00.0 | EmG | 0.328 | Blue | 0.63 | 0.05 |
| 2dFGRS TGS116Z082 | 22:10:03.74 | -25:20:07.3 | Galaxy | 0.009 | Blue | 0.99 | 0.01 |
| 2QZ J221005.7-275439 | 22:10:05.76 | -27:54:38.7 | Galaxy | 0.330 | Blue | 0.95 | 0.03 |
| 6dFGS gJ221058.1-250431 | 22:10:58.01 | -25:04:31.1 | Galaxy | 0.017 | Blue | 0.78 | 0.03 |
| 2QZ J221058.3-273930 | 22:10:58.33 | -27:39:29.4 | Galaxy | 0.313 | Blue | 0.81 | 0.07 |
| LSQ 12dw1 | 22:12:41.57 | 00:30:43.1 | SN | 0.014 | Blue | 0.51 | 0.10 |
| [VV2006] J221335.7-282542 | 22:13:35.65 | -28:25:41.7 | QSO | 2.469 | Blue | 0.41 | 0.08 |
| 2dFGRS TGS175Z009 | 22:14:02.86 | -27:32:21.4 | Galaxy | 0.014 | Blue | 1.00 | 0.00 |
| 2dFGRS TGS175Z009 | 22:14:02.88 | -27:32:21.5 | Galaxy | 0.014 | Blue | 0.96 | 0.04 |
| NGC 7229 | 22:14:03.23 | -29:22:57.8 | EmG | 0.014 | Blue | 0.77 | 0.05 |
| 2dFGRS TGS254Z244 | 22:14:05.10 | -29:22:52.9 | Galaxy | 0.015 | Blue | 0.97 | 0.03 |
| ESO 467-25 | 22:14:24.23 | -29:58:51.5 | EmG | 0.015 | Blue | 0.74 | 0.03 |
| 2dFGRS TGS254Z138 | 22:14:41.93 | -28:26:39.6 | Galaxy | 0.012 | Blue | 1.00 | 0.00 |
| 2dFGRS TGS334Z074 | 22:14:47.16 | -29:41:12.4 | Galaxy | 0.006 | Blue | 0.76 | 0.02 |
| 2QZ J221517.1-285358 | 22:15:17.10 | -28:53:57.5 | EmG | 0.312 | Blue | 0.74 | 0.07 |
| [VV2006] J221532.6-281805 | 22:15:32.58 | -28:18:03.9 | QSO | 1.330 | Blue | 0.67 | 0.04 |
| 2QZ J221630.0-290054 | 22:16:30.07 | -29:00:53.3 | EmG | 0.330 | Red | 0.18 | 0.09 |
| 6dFGS gJ221706.5-303447 | 22:17:06.52 | -30:34:46.1 | Galaxy | 0.337 | Red | 0.34 | 0.24 |
| [VV2006] J221722.5+010436 | 22:17:22.44 | 01:04:36.3 | QSO | 1.403 | Blue | 0.10 | 0.05 |
| 2dFGRS TGS176Z011 | 22:17:41.15 | -27:21:54.6 | Galaxy | 0.009 | Blue | 0.76 | 0.03 |
| SDSS J221813.90+001625.1 | 22:18:13.91 | 00:16:25.3 | Galaxy | 0.333 | – | – | – |
| 2MASX J22181503+0115169 | 22:18:15.03 | 01:15:16.9 | Galaxy | 0.049 | Blue | 0.80 | 0.04 |
| SDSS J221817.26+003623.6 | 22:18:17.26 | 00:36:23.7 | AGN | 0.331 | Red | 0.08 | 0.20 |
| 2QZ J221819.4-271544 | 22:18:19.39 | -27:15:44.2 | Seyfert 1 | 0.355 | Blue | 0.44 | 0.09 |
| 2SLAQ J221846.76-011119.0 | 22:18:46.74 | -01:11:18.8 | Galaxy | – | Blue | 0.77 | 0.03 |
| 2SLAQ J221846.76-011119.0 | 22:18:46.74 | -01:11:18.8 | Galaxy | – | Blue | 0.84 | 0.03 |
| SDSS J221852.63-010310.1 | 22:18:52.65 | -01:03:10.5 | Galaxy | 0.016 | Blue | 0.69 | 0.11 |

Table B1: –continued

| Id Object | RA | Dec | Type | Redshift | Group HAC | P(Blue) | P(Red) |
|---------------------------|-------------|-------------|---------------|----------|--------------|---------|---------|
| | | | | | | HDBSCAN | HDBSCAN |
| 2QZ J221925.9-305108 | 22:19:25.92 | -30:51:07.7 | EmG | 0.307 | Blue | 0.66 | 0.04 |
| SDSSCGB 28259.2 | 22:19:44.75 | -00:14:40.0 | Galaxy | – | Red | 0.21 | 0.38 |
| 2QZ J221945.1-293414 | 22:19:45.08 | -29:34:13.4 | EmG | 0.343 | Blue | 0.97 | 0.03 |
| [DD2013] W4+2-1 115196 | 22:19:53.86 | 00:29:04.8 | Galaxy | 0.087 | Blue | 0.61 | 0.11 |
| 2SLAQ J222021.37+004040.2 | 22:20:21.36 | 00:40:40.5 | Star | – | Blue | 0.57 | 0.06 |
| 2QZ J222113.6-280421 | 22:21:13.62 | -28:04:20.9 | Seyfert 1 | 0.332 | Red | 0.27 | 0.18 |
| 2dFGRS TGS337Z130 | 22:22:54.92 | -30:42:28.4 | Galaxy | 0.014 | Blue | 0.94 | 0.02 |
| 6dFGS gJ222313.7-285844 | 22:23:13.70 | -28:58:44.6 | Galaxy | 0.006 | Blue | 0.45 | 0.11 |
| 2SLAQ J222332.83-010614.8 | 22:23:32.84 | -01:06:14.8 | QSO | 2.460 | Blue | 0.52 | 0.06 |
| 2QZ J222336.0-283140 | 22:23:36.03 | -28:31:39.6 | EmG | 0.333 | Blue | 0.82 | 0.07 |
| 2SLAQ J222403.36-005724.2 | 22:24:03.35 | -00:57:24.2 | QSO | 0.313 | Blue | 0.56 | 0.11 |
| 2SLAQ J222403.36-005724.2 | 22:24:03.36 | -00:57:24.1 | QSO | 0.313 | Blue | 0.48 | 0.11 |
| 2QZ J222416.2-292421 | 22:24:16.26 | -29:24:21.7 | Candidate CV* | – | Blue | 0.59 | 0.11 |
| 2dFGRS TGS338Z083 | 22:27:38.90 | -31:08:10.3 | Galaxy | 0.015 | Blue | 0.80 | 0.06 |
| 2SLAQ J222825.11-002217.4 | 22:28:25.12 | -00:22:17.2 | Galaxy | – | Red | 0.51 | 0.18 |
| LEDA 711478 | 22:28:47.80 | -30:54:43.2 | Galaxy | – | Blue | 0.41 | 0.12 |
| LEDA 711478 | 22:28:47.82 | -30:54:43.2 | Galaxy | – | Blue | 0.43 | 0.11 |
| 2dFGRS TGS337Z266 | 22:28:53.67 | -30:58:51.4 | Galaxy | 0.013 | Blue | 0.85 | 0.05 |
| 2dFGRS TGS337Z266 | 22:28:53.67 | -30:58:51.4 | Galaxy | 0.013 | Blue | 0.80 | 0.03 |
| SDSS J222923.00-020042.7 | 22:29:23.00 | -02:00:42.4 | QSO | 3.294 | – | – | – |
| 2SLAQ J222956.53+003126.5 | 22:29:56.54 | 00:31:26.5 | QSO | 1.340 | Blue | 0.45 | 0.07 |
| 2dFGRS TGS338Z165 | 22:30:01.84 | -29:35:52.7 | Galaxy | 0.010 | Blue | 0.83 | 0.02 |
| 2dFGRS TGS338Z165 | 22:30:01.85 | -29:35:52.6 | Galaxy | 0.010 | Blue | 0.80 | 0.05 |
| NAME Kinman Dwarf | 22:30:36.83 | -00:06:35.8 | BlueCompG | 0.006 | Blue | 0.58 | 0.14 |
| LEDA 1149494 | 22:31:06.00 | -00:11:43.9 | Galaxy | – | Blue | 1.00 | 0.00 |
| 2QZ J223114.0-312005 | 22:31:13.95 | -31:20:04.4 | Star | – | Blue | 0.77 | 0.08 |
| [VV2006] J223251.7-303250 | 22:32:51.74 | -30:32:49.6 | QSO | 0.350 | Blue | 0.31 | 0.07 |
| 2QZ J223342.5-301936 | 22:33:42.56 | -30:19:35.4 | Galaxy | 0.324 | Blue | 0.80 | 0.06 |
| 2MASS J22340663+0001199 | 22:34:06.67 | 00:01:20.8 | Star | – | Red | 0.06 | 0.20 |
| FASTT 1560 | 22:34:39.93 | 00:41:27.5 | CataclyV* | 0.001 | Blue | 0.54 | 0.07 |
| 2dFGRS TGS414Z208 | 22:34:56.56 | -31:08:44.1 | Galaxy | 0.009 | Blue | 1.00 | 0.00 |
| 2dFGRS TGS414Z208 | 22:34:56.57 | -31:08:44.1 | Galaxy | 0.009 | Blue | 1.00 | 0.00 |
| SDSS J223508.41-005359.3 | 22:35:08.42 | -00:53:59.4 | Seyfert 2 | 0.328 | Red | 0.26 | 0.32 |
| SDSS J223508.41-005359.3 | 22:35:08.43 | -00:53:59.4 | Seyfert 2 | 0.328 | Red | 0.33 | 0.61 |
| 2QZ J223532.2-294634 | 22:35:32.24 | -29:46:33.0 | EmG | 0.325 | Blue | 0.82 | 0.03 |
| 2SLAQ J223543.05-005436.5 | 22:35:43.04 | -00:54:36.6 | Galaxy | – | Blue | 0.81 | 0.11 |
| 2SLAQ J223543.05-005436.5 | 22:35:43.05 | -00:54:36.6 | Galaxy | – | Blue | 0.67 | 0.02 |
| 2SLAQ J223543.05-005436.5 | 22:35:43.06 | -00:54:36.4 | Galaxy | – | Blue | 0.50 | 0.07 |
| SDSS J223543.94-003931.4 | 22:35:43.93 | -00:39:32.1 | low-mass* | 0.000 | Red | 0.15 | 0.18 |
| [EKS96] NGC 7314 28 | 22:35:44.87 | -26:02:27.4 | HII | – | Blue | 0.84 | 0.05 |
| [EKS96] NGC 7314 43 | 22:35:45.40 | -26:02:10.8 | HII | – | Blue | 0.68 | 0.02 |
| [EKS96] NGC 7314 71 | 22:35:46.29 | -26:04:29.1 | HII | – | Blue | 0.80 | 0.09 |
| [EKS96] NGC 7314 130 | 22:35:48.23 | -26:01:24.0 | HII | – | Blue | 0.91 | 0.07 |
| [VV2006] J223633.5+002652 | 22:36:33.54 | 00:26:52.8 | QSO | 1.354 | Blue | 0.69 | 0.07 |
| SDSS J223649.60+005413.5 | 22:36:49.60 | 00:54:13.8 | QSO | 3.313 | – | – | – |
| 2SLAQ J223723.84-010120.3 | 22:37:23.88 | -01:01:19.2 | Galaxy | – | Blue | 0.97 | 0.03 |
| SDSS J223729.86-010549.1 | 22:37:29.86 | -01:05:49.3 | HB* | -0.001 | – | – | – |
| PHL 354 | 22:38:23.25 | -00:57:08.2 | QSO | 0.361 | Blue | 0.34 | 0.06 |
| PHL 354 | 22:38:23.26 | -00:57:08.1 | QSO | 0.361 | Blue | 0.43 | 0.08 |
| 2SLAQ J223844.30-005655.3 | 22:38:44.29 | -00:56:55.3 | QSO | 1.357 | Blue | 0.53 | 0.08 |
| LEDA 131686 | 22:41:19.49 | -39:58:23.3 | Galaxy | – | Blue | 0.72 | 0.05 |
| 2QZ J224149.5-301945 | 22:41:49.50 | -30:19:44.5 | Galaxy | 0.322 | Blue | 0.66 | 0.08 |
| [GDB2008] 503 | 22:43:16.38 | -39:51:39.9 | Galaxy | 0.007 | Blue | 0.80 | 0.05 |
| [GDB2008] 504 | 22:43:19.40 | -39:52:44.4 | Galaxy | 0.007 | Blue | 0.49 | 0.13 |
| [GDB2008] 509 | 22:43:25.11 | -39:55:20.0 | Galaxy | 0.327 | Red | 0.11 | 0.88 |
| SDSS J224352.11-002259.7 | 22:43:52.21 | -00:22:59.9 | Galaxy | 0.010 | Blue | 0.97 | 0.03 |
| 2SLAQ J224531.20-004509.4 | 22:45:31.20 | -00:45:09.4 | QSO | 1.368 | Blue | 0.58 | 0.05 |
| 2SLAQ J224531.20-004509.4 | 22:45:31.20 | -00:45:09.3 | QSO | 1.368 | Blue | 0.31 | 0.06 |

Table B1: –continued

| Id Object | RA | Dec | Type | Redshift | Group | P(Blue) | P(Red) |
|----------------------------|-------------|-------------|-----------|----------|-------|---------|---------|
| | | | | | | HAC | HDBSCAN |
| SDSS J224539.94-002419.7 | 22:45:39.94 | -00:24:19.6 | QSO | 3.280 | Blue | 0.98 | 0.02 |
| 2MASS J22495608+0002182 | 22:49:56.08 | 00:02:18.4 | QSO | 3.307 | Blue | 0.88 | 0.07 |
| 2SLAQ J225012.91-003959.0 | 22:50:12.92 | -00:39:58.9 | Galaxy | — | Blue | 0.78 | 0.08 |
| SDSS J225149.74-002811.7 | 22:51:49.75 | -00:28:11.4 | QSO | 3.228 | Blue | 0.97 | 0.03 |
| 2QZ J225157.1-292451 | 22:51:57.10 | -29:24:50.8 | EmG | 0.318 | Blue | 0.39 | 0.06 |
| 2SLAQ J225257.45+002731.5 | 22:52:57.44 | 00:27:31.6 | Star | — | Blue | 0.59 | 0.12 |
| 2QZ J225352.9-300944 | 22:53:52.96 | -30:09:43.7 | Seyfert 1 | 0.326 | Blue | 0.26 | 0.09 |
| [VV2006] J225411.2-312712 | 22:54:11.15 | -31:27:11.3 | QSO | 1.360 | Blue | 0.71 | 0.04 |
| SDSS J225411.96-004949.5 | 22:54:11.96 | -00:49:49.4 | QSO | 3.297 | Blue | 0.50 | 0.06 |
| SDSS J225411.96-004949.5 | 22:54:11.96 | -00:49:49.3 | QSO | 3.297 | Blue | 0.99 | 0.01 |
| 2QZ J225503.9-301914 | 22:55:03.89 | -30:19:13.3 | EmG | 0.326 | Blue | 0.99 | 0.01 |
| 2QZ J225908.1-312717 | 22:59:08.12 | -31:27:16.7 | Star | — | Blue | 0.30 | 0.07 |
| 2SLAQ J230030.09-003005.9 | 23:00:30.09 | -00:30:05.8 | Galaxy | — | Blue | 0.61 | 0.07 |
| 2SLAQ J230201.20+003047.2 | 23:02:01.20 | 00:30:47.3 | QSO | 1.344 | Blue | 0.63 | 0.05 |
| [VV2006] J230235.5-285630 | 23:02:35.44 | -28:56:29.7 | QSO | 0.368 | Blue | 0.60 | 0.07 |
| 2SLAQ J230316.40-001211.5 | 23:03:16.41 | -00:12:11.4 | QSO | 1.516 | Blue | 0.60 | 0.08 |
| V* HY Psc | 23:03:51.63 | 01:06:51.4 | CataclyV* | -0.000 | Blue | 0.67 | 0.07 |
| SDSS J230428.31+005701.2 | 23:04:28.34 | 00:57:01.2 | QSO | 0.317 | Blue | 0.56 | 0.11 |
| 2SLAQ J230444.16-010251.7 | 23:04:44.16 | -01:02:51.5 | QSO | 1.377 | Blue | 0.44 | 0.08 |
| LEDA 1122038 | 23:08:10.78 | -01:17:58.5 | Galaxy | — | Blue | 0.74 | 0.06 |
| SDSS J230855.49+003705.6 | 23:08:55.49 | 00:37:05.7 | QSO | 1.784 | Blue | 1.00 | 0.00 |
| ESO 469-15 | 23:08:55.60 | -30:51:28.2 | GinGroup | 0.005 | Blue | 0.73 | 0.14 |
| [VV2006] J230914.4-305913 | 23:09:14.31 | -30:59:12.5 | QSO | 1.380 | Blue | 0.61 | 0.05 |
| 2MASS J23094616+0000496 | 23:09:46.15 | 00:00:49.1 | Seyfert 1 | 0.352 | Blue | 0.61 | 0.10 |
| 2MASS J23094616+0000496 | 23:09:46.16 | 00:00:49.0 | Seyfert 1 | 0.352 | Blue | 0.65 | 0.11 |
| [GPM2009] J2310-0109 2 | 23:10:41.99 | -01:09:48.0 | EmG | 0.012 | Blue | 0.78 | 0.07 |
| [VV2006] J231135.1-312644 | 23:11:35.12 | -31:26:44.1 | QSO | 1.350 | Blue | 0.58 | 0.04 |
| 2dFGRS TGS422Z155 | 23:12:08.96 | -31:04:13.3 | Galaxy | 0.165 | Red | 0.43 | 0.21 |
| 2SLAQ J231231.36-011137.5 | 23:12:31.36 | -01:11:37.3 | QSO | 1.360 | Blue | 0.71 | 0.05 |
| SDSS J231259.07+010805.6 | 23:12:59.06 | 01:08:05.9 | QSO | 3.295 | Blue | 0.84 | 0.04 |
| [VV2006] J231311.9-004538 | 23:13:11.91 | -00:45:38.0 | QSO | 1.364 | Blue | 0.54 | 0.04 |
| SDSS J231351.87-011031.9 | 23:13:51.86 | -01:10:30.8 | HII G | 0.012 | Blue | 0.84 | 0.08 |
| 2MASX J23145046+0123280 | 23:14:50.52 | 01:23:26.7 | LSB G | 0.016 | Blue | 1.00 | 0.00 |
| [VV2006] J231519.4-303857 | 23:15:19.39 | -30:38:57.2 | QSO | 1.356 | Blue | 0.81 | 0.05 |
| V* CC Scl | 23:15:31.78 | -30:48:48.7 | CataclyV* | — | Blue | 0.70 | 0.10 |
| [VV2006] J231652.0+005125 | 23:16:52.04 | 00:51:25.9 | QSO | 3.229 | Blue | 0.80 | 0.03 |
| 3XMM J231742.5+000535 | 23:17:42.61 | 00:05:35.3 | Seyfert 1 | 0.321 | Blue | 0.56 | 0.06 |
| [VV2006] J231942.8-302629 | 23:19:42.76 | -30:26:29.5 | QSO | 2.473 | Blue | 0.83 | 0.08 |
| LEDA 71137 | 23:20:35.21 | -00:52:50.9 | Galaxy | 0.015 | Blue | 0.64 | 0.08 |
| LEDA 71137 | 23:20:35.22 | -00:52:50.8 | Galaxy | 0.015 | Blue | 0.56 | 0.08 |
| 2QZ J232126.5-310730 | 23:21:26.51 | -31:07:29.5 | Galaxy | 0.309 | Blue | 1.00 | 0.00 |
| [SIG2010] 389821 | 23:23:31.32 | 01:08:06.0 | RRLyr | — | Blue | 0.86 | 0.02 |
| GALEX 2417063145906373262 | 23:24:20.34 | -00:06:25.0 | HII | — | Blue | 0.10 | 0.04 |
| [GPM2009] J2324-0006 | 23:24:21.37 | -00:06:29.4 | HII G | 0.009 | Blue | 0.24 | 0.08 |
| 2SLAQ J232457.75+002153.2 | 23:24:57.75 | 00:21:53.4 | QSO | 0.345 | Blue | 0.20 | 0.07 |
| 2SLAQ J232524.40+004612.0 | 23:25:24.43 | 00:46:12.2 | Galaxy | 0.016 | Blue | 0.87 | 0.06 |
| 2MASS J23255145-0140232 | 23:25:51.48 | -01:40:23.8 | CataclyV* | — | Blue | 0.33 | 0.10 |
| [VV2006c] J232555.5-003710 | 23:25:55.51 | -00:37:10.7 | Seyfert 1 | 0.332 | — | — | — |
| SDSS J232743.68-020055.8 | 23:27:43.70 | -02:00:55.7 | BlueCompG | 0.018 | Blue | 0.13 | 0.05 |
| 6dFGS gJ232744.4-020047 | 23:27:44.38 | -02:00:46.8 | Galaxy | 0.018 | Blue | 0.10 | 0.04 |
| LEDA 1127711 | 23:28:12.30 | -01:03:44.8 | HII G | 0.009 | Blue | 0.79 | 0.06 |
| GD 1662 | 23:29:00.44 | -29:46:46.0 | CataclyV* | 0.000 | Blue | 0.55 | 0.08 |
| SDSS J233104.38-004237.2 | 23:31:04.40 | -00:42:37.1 | QSO | 1.353 | Red | 0.53 | 0.09 |
| 2MASS J23315973-0048192 | 23:31:59.77 | -00:48:18.5 | Galaxy | 0.017 | Blue | 0.99 | 0.01 |
| 2QZ J233254.8-305844 | 23:32:54.78 | -30:58:43.8 | EmG | 0.329 | Blue | 0.58 | 0.07 |
| SDSS J233256.68+011122.9 | 23:32:56.68 | 01:11:23.1 | BCIG | 0.382 | — | — | — |
| SDSS J233300.21-002030.5 | 23:33:00.22 | -00:20:30.5 | QSO | 3.328 | Blue | 0.95 | 0.05 |
| [VV2006] J233438.5+002341 | 23:34:38.55 | 00:23:41.9 | QSO | 1.385 | Blue | 0.46 | 0.07 |

Table B1: –continued

| Id Object | RA | Dec | Type | Redshift | Group | | P(Blue) | P(Red) |
|---------------------------|-------------|-------------|-----------|----------|-------|---------|---------|--------|
| | | | | | HAC | HDBSCAN | | |
| 2MASX J23352102+0110271 | 23:35:20.98 | 01:10:27.4 | Galaxy | 0.085 | Red | 0.45 | 0.31 | |
| 2SLAQ J233522.69-000635.2 | 23:35:22.69 | -00:06:35.2 | QSO | 1.373 | Blue | 0.53 | 0.07 | |
| LEDA 135900 | 23:36:46.97 | 00:37:23.8 | LSB G | 0.009 | Blue | 0.99 | 0.01 | |
| [VV2006] J233722.0+002239 | 23:37:22.02 | 00:22:39.2 | QSO | 1.377 | Blue | 0.46 | 0.06 | |
| 2XMM J233731.7+002559 | 23:37:31.79 | 00:25:59.9 | AGN | 0.314 | Blue | 0.72 | 0.13 | |
| DES J233747.57+001742.6 | 23:37:47.57 | 00:17:42.8 | GinCl | – | – | – | – | |
| RESOLVE rf772 | 23:40:38.43 | -00:53:30.6 | Galaxy | 0.019 | Blue | 0.66 | 0.07 | |
| [VV2006] J234329.1-300200 | 23:43:29.16 | -30:02:00.1 | QSO | 1.358 | Blue | 0.53 | 0.07 | |
| 2SLAQ J234440.53-001205.8 | 23:44:40.53 | -00:12:06.1 | CataclyV* | – | Blue | 0.40 | 0.06 | |
| LEDA 1109937 | 23:48:23.99 | -01:47:31.1 | Galaxy | – | Blue | 1.00 | 0.00 | |
| 2dFGRS TGS356Z227 | 23:50:01.55 | -30:11:07.1 | Galaxy | 0.010 | Blue | 0.63 | 0.07 | |
| 2SLAQ J235115.66-000000.0 | 23:51:15.66 | -00:00:00.0 | Galaxy | – | Blue | 0.23 | 0.05 | |
| 2SLAQ J235115.66-000000.0 | 23:51:15.68 | -00:00:00.2 | Galaxy | – | Blue | 0.55 | 0.08 | |
| [VV2006] J235546.2-002342 | 23:55:46.14 | -00:23:42.8 | QSO | 3.245 | Blue | 0.99 | 0.01 | |
| [VV2006] J235718.4+004350 | 23:57:18.37 | 00:43:50.5 | QSO | 4.366 | Red | 0.04 | 0.10 | |
| SDSS J235805.25-012153.9 | 23:58:05.25 | -01:21:53.9 | QSO | 1.368 | Blue | 0.63 | 0.04 | |

Table B2: Espectra from SDSS DR16

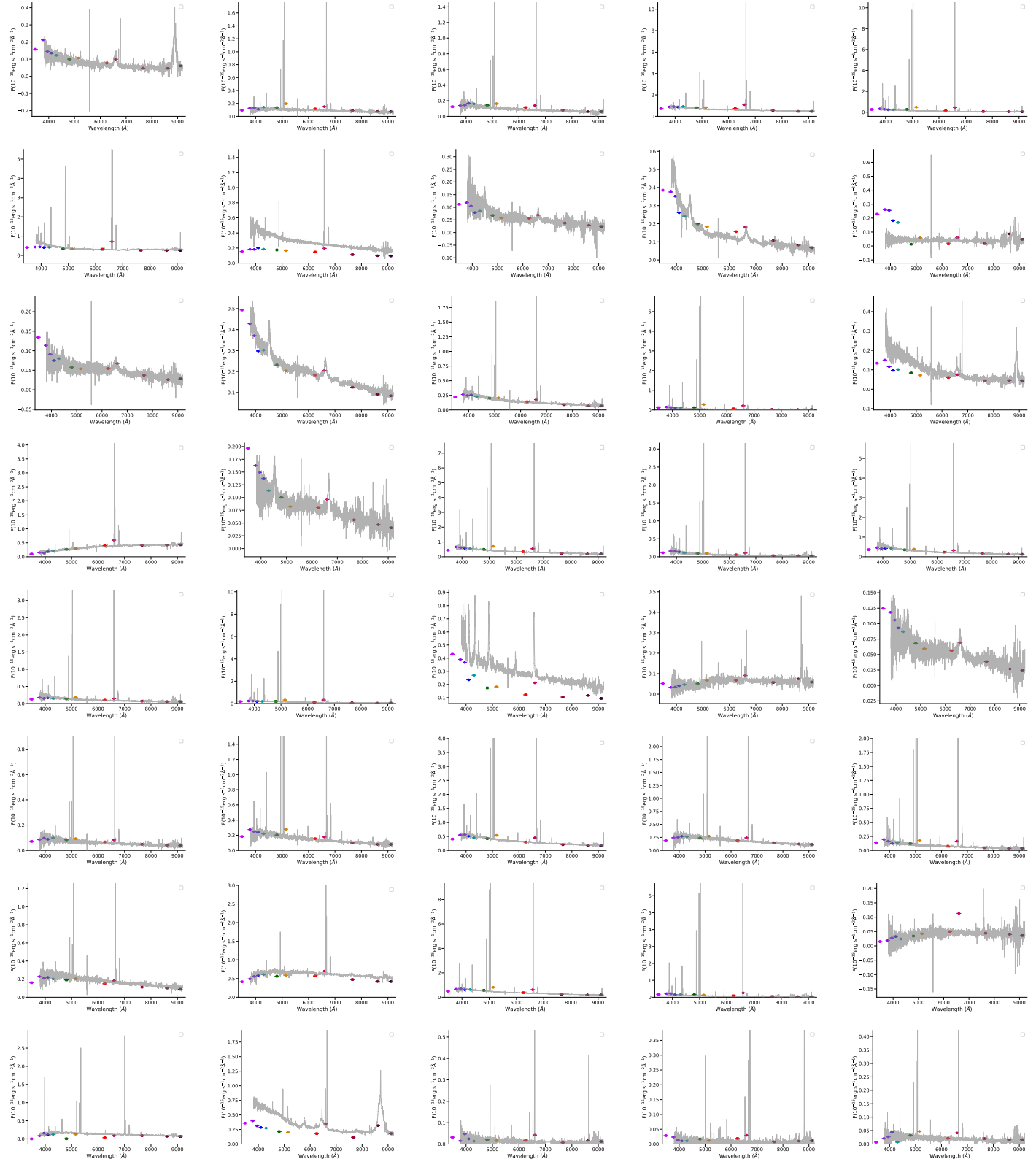


Table B2: –continued

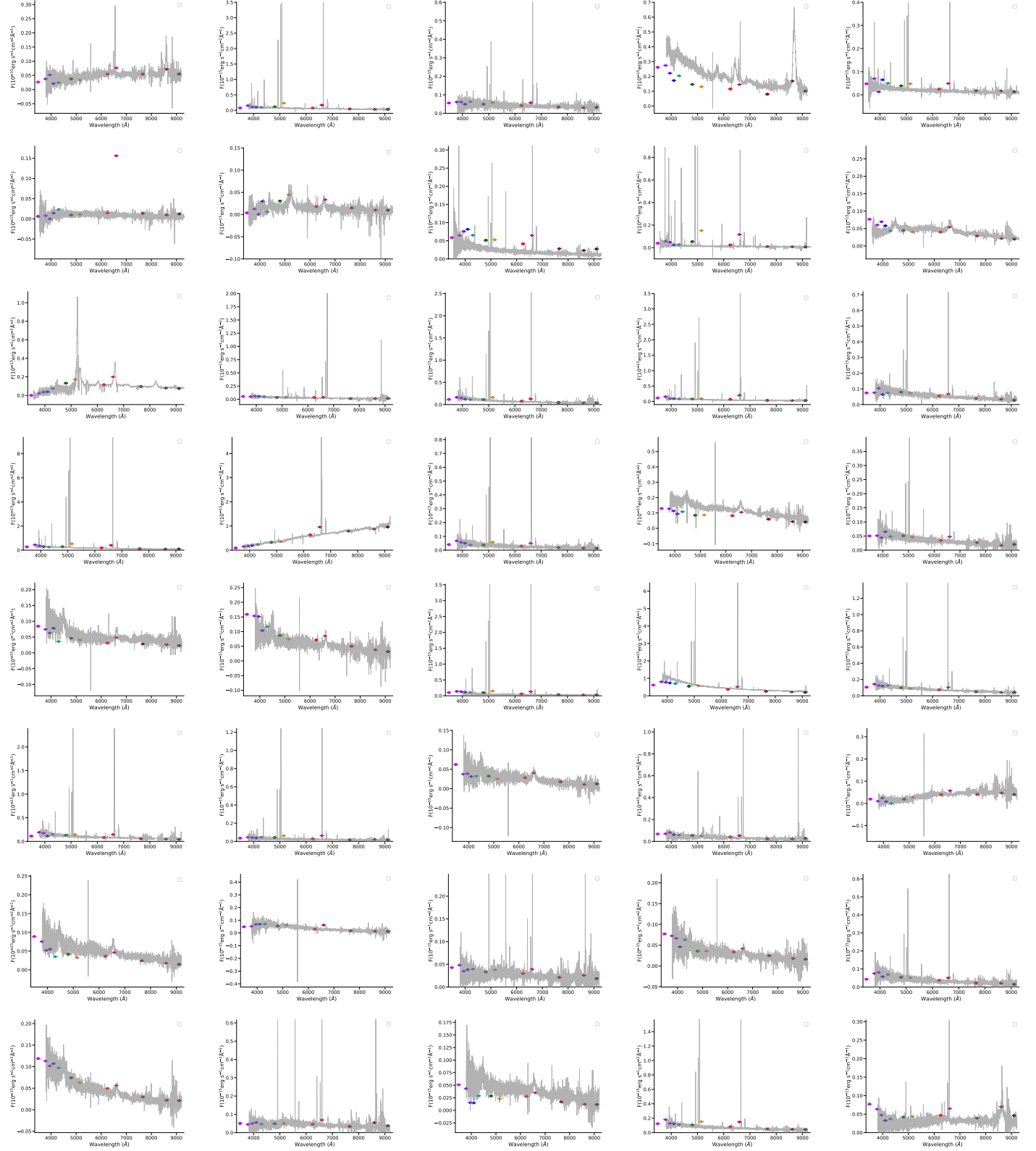


Table B2: –continued

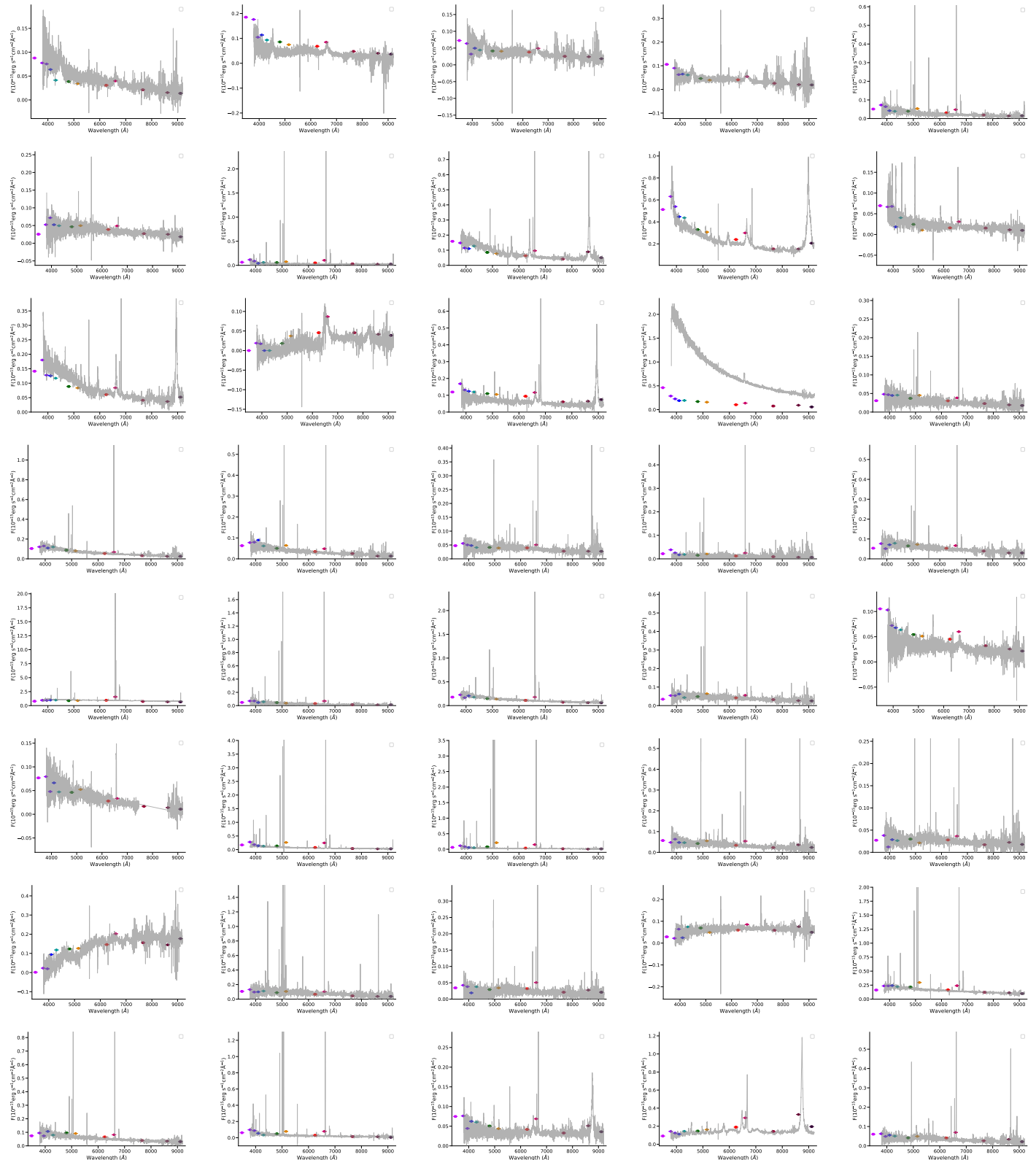


Table B2: –continued

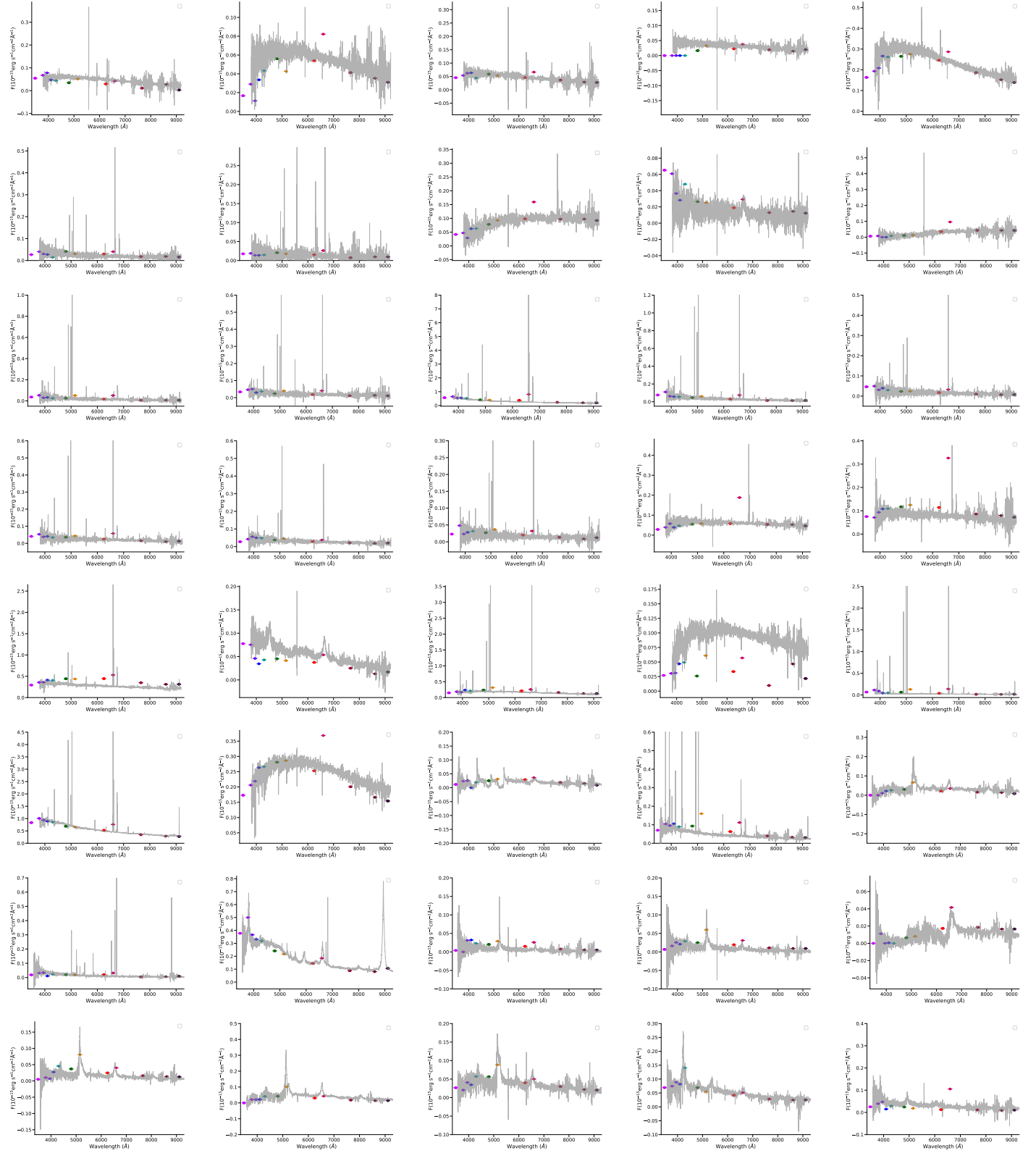


Table B2: –continued

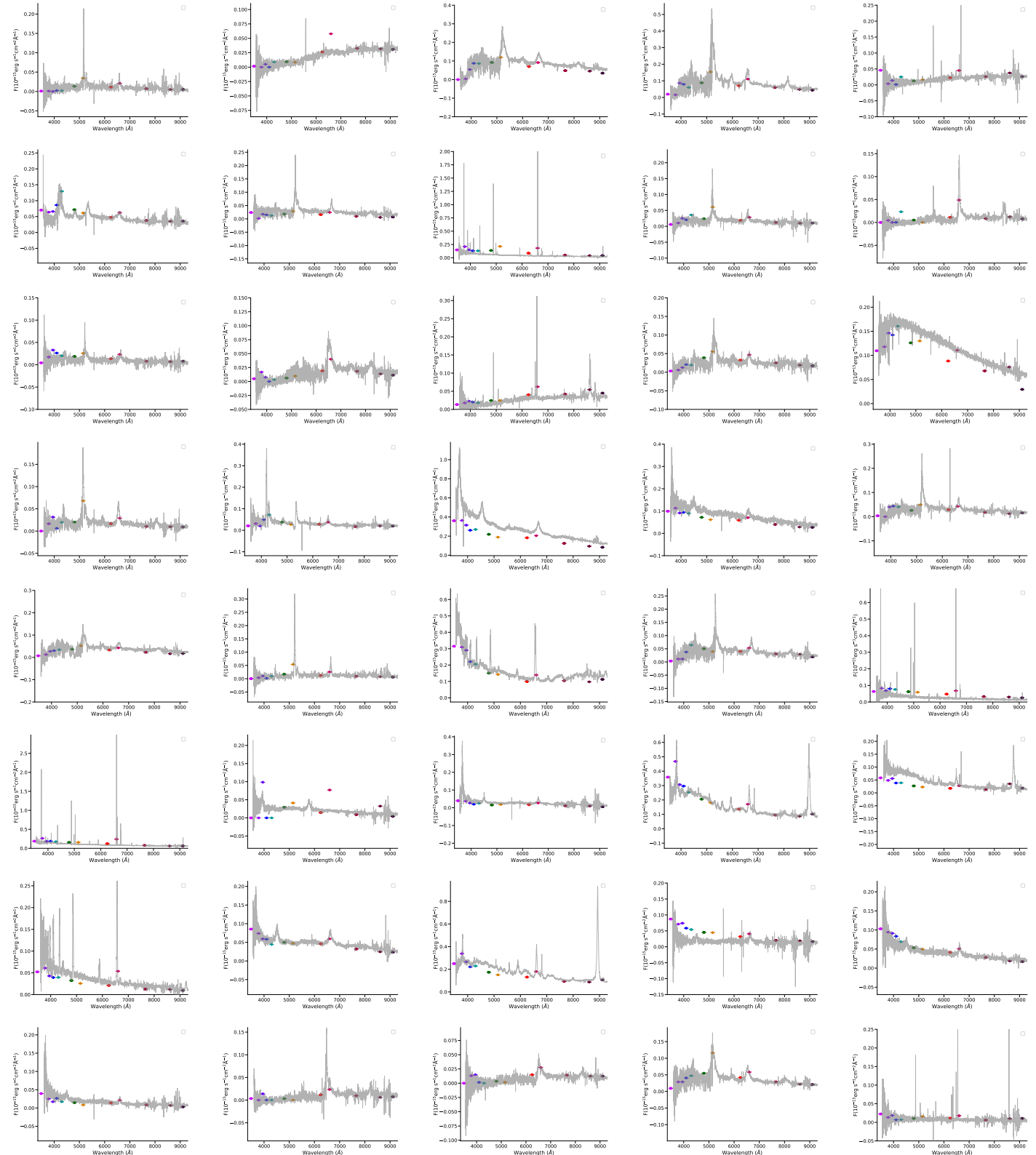


Table B2: –continued

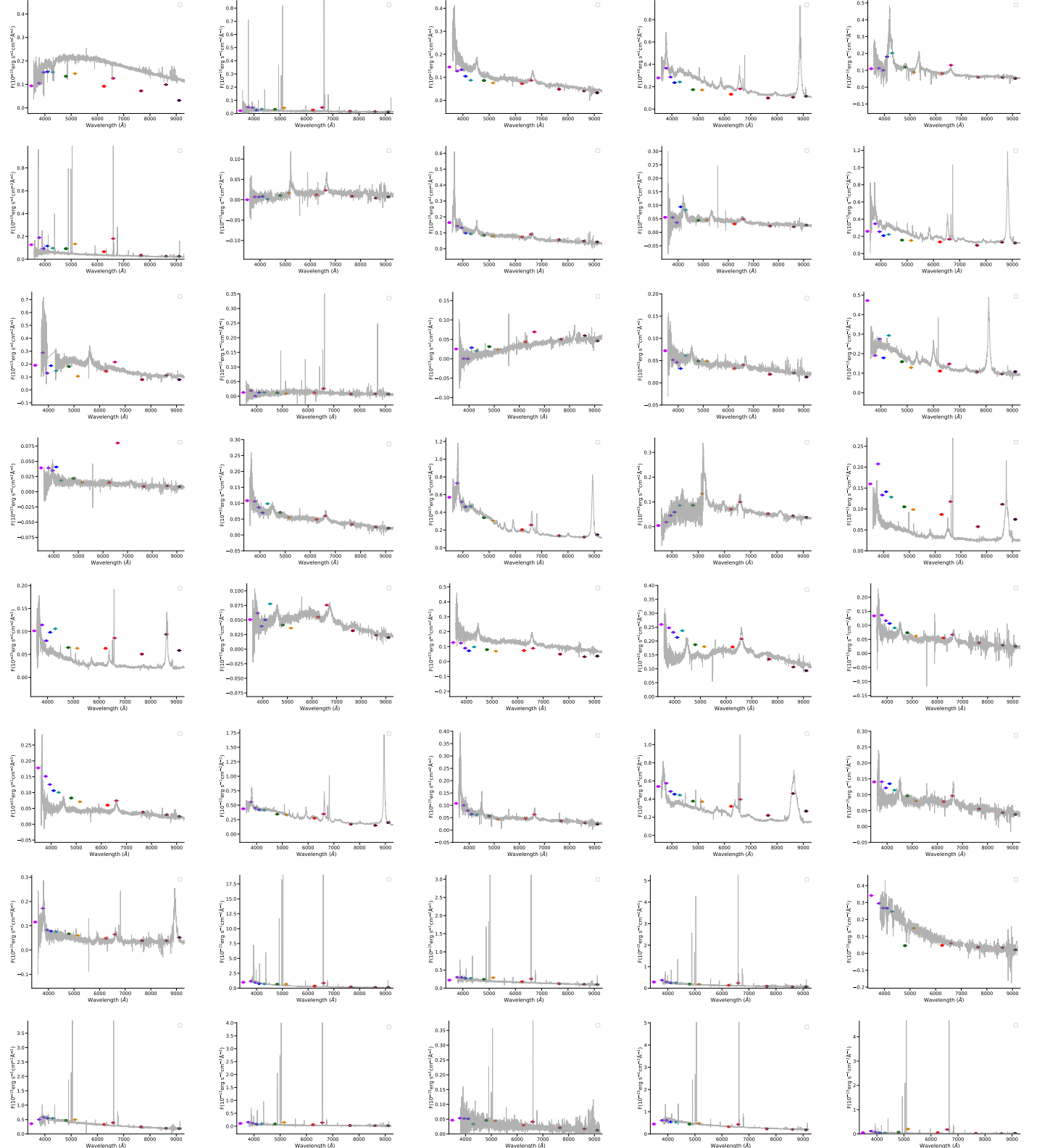


Table B2: –continued

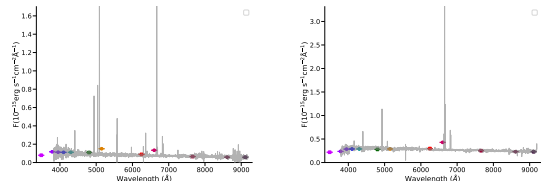


Table B3: Espectra from LAMOST DR6

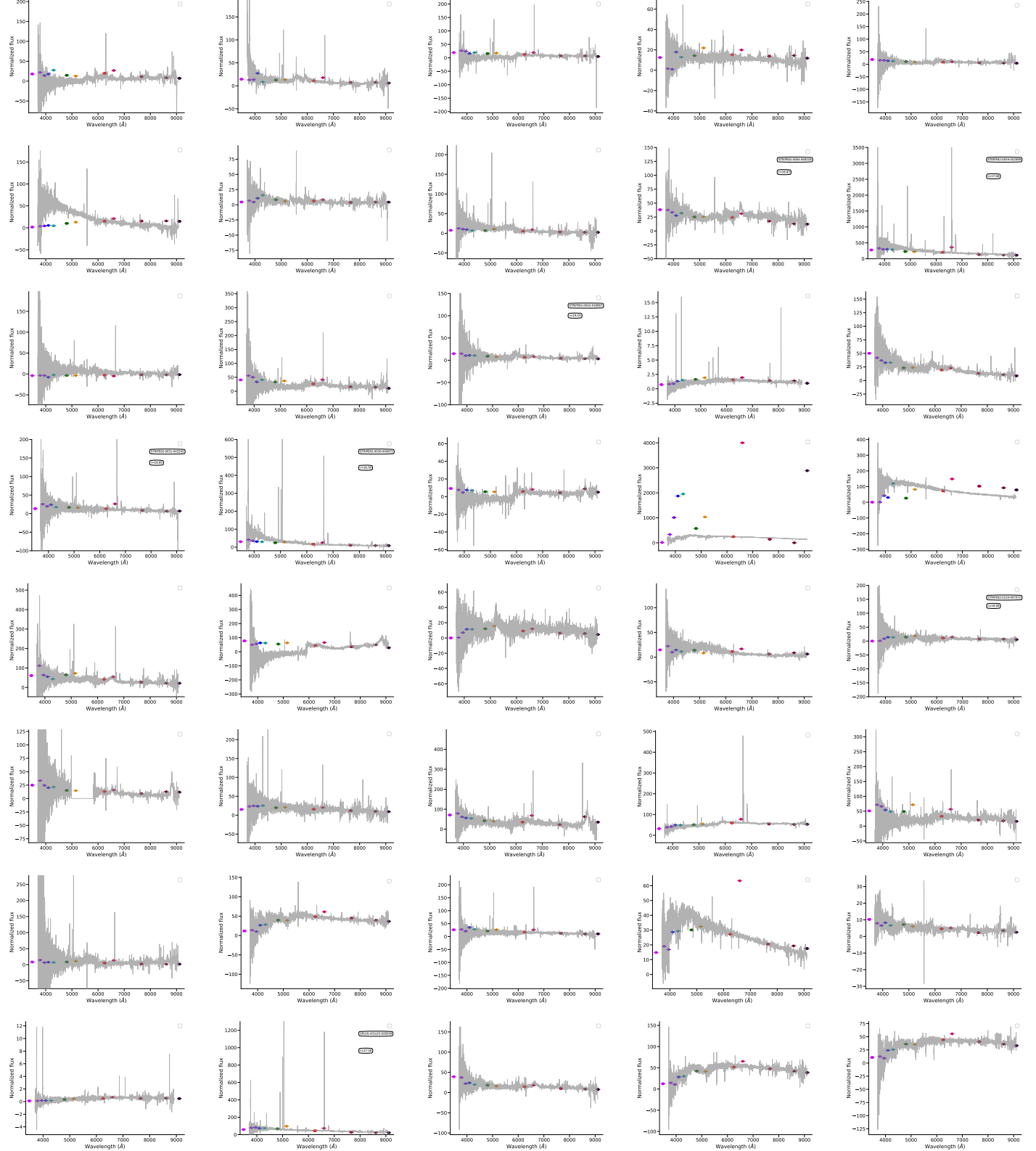


Table B3: –continued

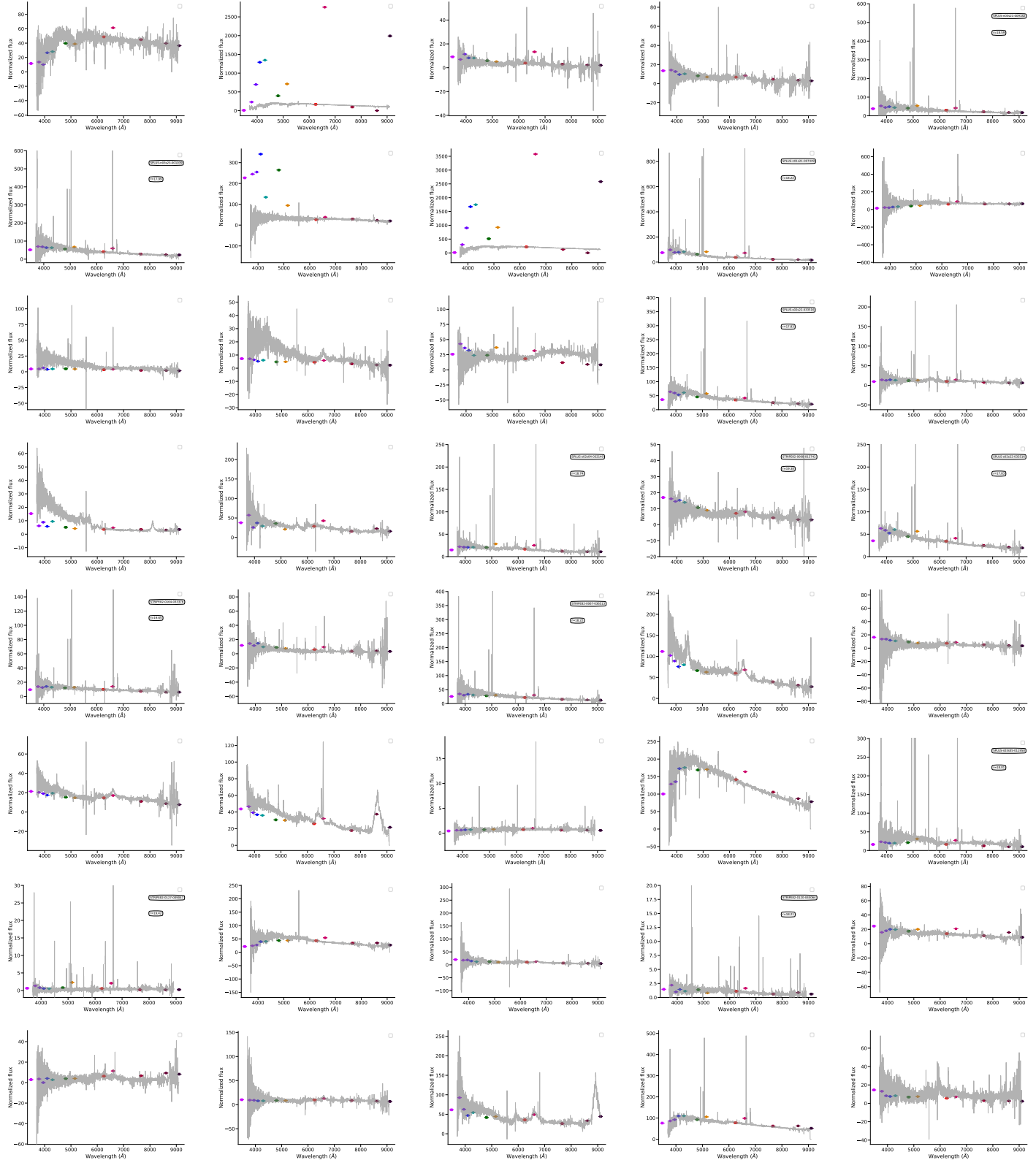
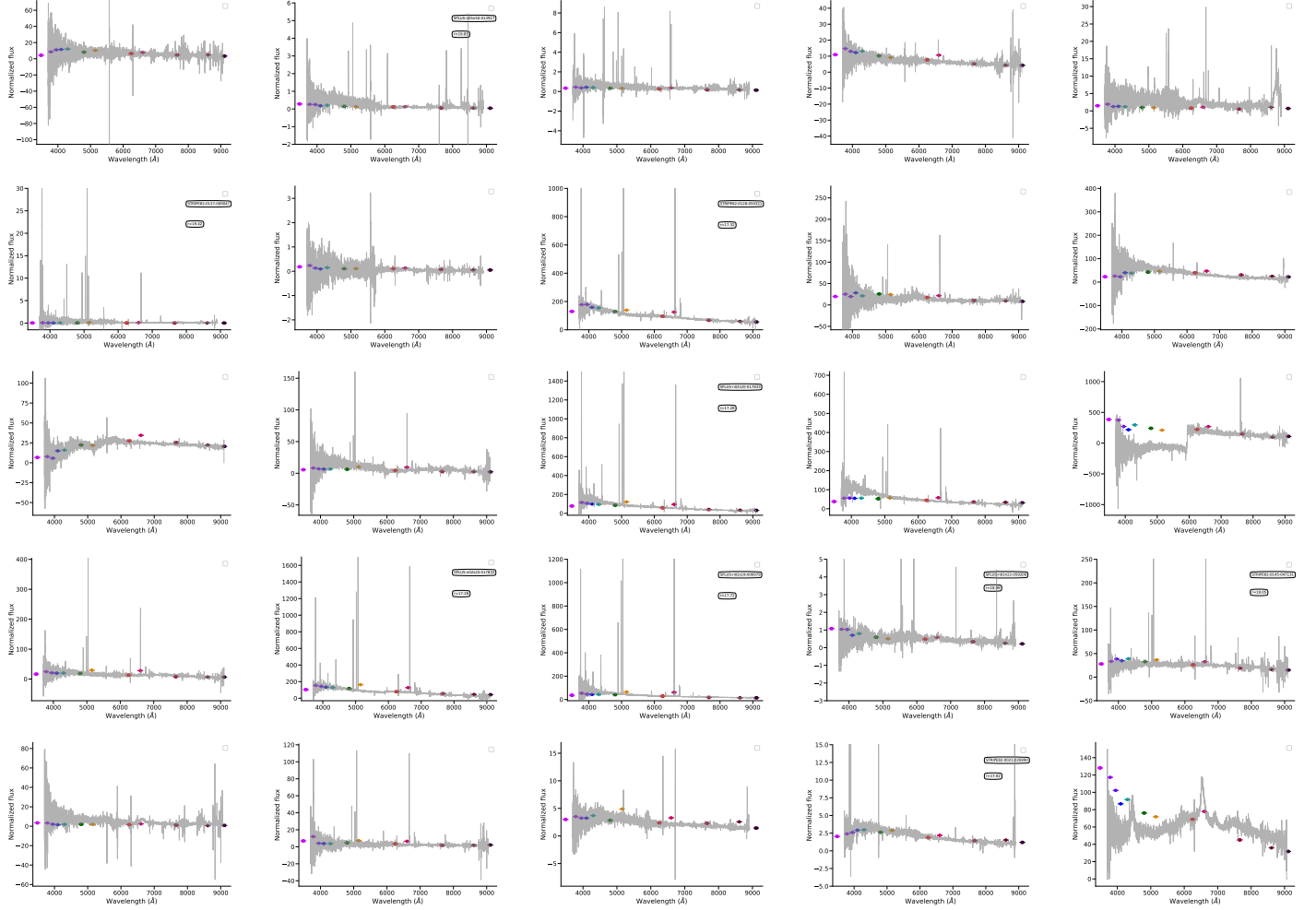


Table B3: –continued



This paper has been typeset from a TeX/LaTeX file prepared by the author.